Increased circulation time of Plasmodium falciparum underlies persistent asymptomatic infection in the dry season

Carolina Andrade, Hannah Fleckenstein, Richard Thomson-Luque, Safiatou Doumbo, Nathalia Lima, Carrie Anderson, Julia Hibbert, Christine Hopp, Tuan Tran, Shanping Li, et al.

Plasmodium falciparum increased time in circulation underlies persistent asymptomatic infection in the dry season

Carolina M. Andrade[1], Hannah Fleckenstein[1], Richard Thomson-Luque[1], Safiatou Doumbo[2], Nathalia F Lima[1], Carrie Anderson[1], Julia Hibbert[1], Christine S. Hopp[3], Tuan M. Tran[4], Shanping Li[3], Moussa Niangaly[2], Hamidou Cisse[2], Didier Doumtabe[2], Jeff Skinner[3], Dan Sturdevant[5], Stacy Ricklefs[5], Kimmo Virtaneva[5], Muhammad Asghar[6], Manijeh Vafa Homann[6], Louise Turner[7], Joana Martins[8], Erik L. Allman[9], Marie-Esther N'Dri[10], Volker Winkler[11], Manuel Llinás[9], Catherine Lavazec[10], Craig Martens[5], Anna Färnert[6], Kassoum Kayentao[2], Aissata Ongoiba[2], Thomas Lavstsen[7], Nuno S. Osório[8], Thomas D. Otto[12], Mario Recker[13], Boubacar Traore[2], Peter D. Crompton[3], Silvia Portugal[1,14*]

[1] Center for Infectious Diseases, Parasitology, Heidelberg University Hospital, Heidelberg, Germany
[2] Mali International Center of Excellence in Research, University of Sciences, Techniques and Technologies of Bamako, Mali
[3] Laboratory of Immunogenetics, National Institute of Allergy and Infectious Diseases, National Institutes of Health, Rockville, Maryland, USA
[4] Division of Infectious Diseases, Indiana University School of Medicine, Indianapolis, Indiana, USA
[5] Rocky Mountain Laboratory Research Technologies Section, Genomics Unit, National Institute of Allergy and Infectious Diseases, National Institutes of Health, Hamilton, Montana, USA
[6] Division of Infectious Diseases, Department of Medicine Solna, Karolinska Institutet, Stockholm Sweden and Department of Infectious Diseases, Karolinska University Hospital, Stockholm, Sweden
[7] Centre for Medical Parasitology, Department of Immunology and Microbiology, Faculty of Health and Medical Sciences, University of Copenhagen and Department of Infectious Diseases, Copenhagen University Hospital (Rigshospitalet), Copenhagen, Denmark
[8] Life and Health Sciences Research Institute (ICVS), School of Medicine, University of Minho, Portugal and ICVS/3B's - PT Government Associate Laboratory, Portugal.
[9] Department of Biochemistry and Molecular Biology, Huck Center for Malaria Research, The Pennsylvania State University, Pennsylvania, USA and Department of Chemistry, The Pennsylvania State University, Pennsylvania, USA
[10] Université de Paris, CNRS UMR8104, Inserm U1016, Institut Cochin, Paris, France
[11] Institute of Global Health, Heidelberg University Hospital, Heidelberg, Germany
[12] Institute of Infection, Immunity & Inflammation, MVLS, University of Glasgow, Glasgow, United Kingdom
[13] Centre for Mathematics & the Environment, University of Exeter, Penryn Campus, Penryn, United Kingdom
[14] German Center for Infection Research (DZIF), partner site Heidelberg, Heidelberg, Germany
*corresponding author: silvia.portugal@med.uni-heidelberg.de

The dry season is a major challenge for *Plasmodium falciparum* parasites in many malaria endemic regions, where water availability limits mosquitoes to only part of the year. How *P. falciparum* bridges two transmission seasons months apart, without being cleared by the host or compromising host survival is poorly understood. Here we show that low levels of *P. falciparum* parasites persist in the blood of asymptomatic Malian individuals during the 5- to 6-month dry season, rarely causing symptoms and minimally affecting the host immune response. Parasites isolated during the dry season are transcriptionally distinct from those of subjects with febrile malaria in the transmission season, reflecting longer circulation within each replicative cycle of parasitized erythrocytes without adhering to the vascular endothelium. Low parasite levels during the dry season are not due to impaired replication, but rather increased splenic clearance of longer-circulating infected erythrocytes. We propose that *P. falciparum* virulence in areas of seasonal malaria transmission is regulated so that the parasite decreases its endothelial binding capacity, allowing increased splenic clearance and enabling several months of subclinical parasite persistence.

(Introduction) The mosquito-borne *Plasmodium falciparum* parasite is responsible for over 200

million malaria cases yearly, and killed nearly 400.000 African children in 2018[1]. *P. falciparum* causes disease while multiplying asexually within red blood cells (RBCs) and exporting its variant surface antigens to the RBC surface. Variant surface antigens mediate adhesion to vascular endothelium, thereby helping the parasite avoid splenic clearance[2,3]. During each ~48h replicative cycle in RBCs, *P. falciparum* follows a regulated transcriptional pattern from the invading merozoite, through the ring- and trophozoite-stages, and to the multinucleated schizont[4,5], which yields 16-32 new merozoites. In parallel with a predictable transcriptional pattern, the parasite develops a network of membrane structures[6] in the infected RBC (iRBC) and at the trophozoite stage the host cell membrane presents knobs[7] exposing parasite-derived *P. falciparum* erythrocyte membrane protein 1 (PfEMP1)[8]. The multigene family *var* is expressed in a monoallelic fashion, coding for PfEMP1s that bind host endothelial cell receptors, with different binding phenotypes associating with varying virulence and pathological outcomes[9]. In Mali and many African regions, malaria cases are restricted to the rainy season when the mosquitoes transmitting *P. falciparum* are present[10], while subclinical *P. falciparum* infections can persist throughout the dry season, enabling the parasite to bridge transmission seasons several months apart[11-13]. We have recently shown that although *P. falciparum*-specific humoral immunity is higher in subclinical *P. falciparum* carriers in the dry season, it decreases similarly during this time in carriers and non-carriers[13], suggesting that chronic low parasitaemia in endemic settings may not maintain nor boost malaria immunity. While much is known about immune responses to clinical malaria, and to some extent to subclinical infections during the transmission season[14], the impact on immunity of subclinical *P. falciparum* persistence in the dry season has not been extensively studied. Host survival during the dry months is essential for resuming *P. falciparum* transmission in the ensuing rainy season, thus the parasite has likely evolved strategies to prevent potentially fatal host pathology, and assure persistence during mosquito-free periods. In this study we address the host and parasite features that associate with parasite persistence between two transmission seasons, and provide insights into the complex interaction between *P. falciparum*, its human hosts and the surrounding environment. By comparing parasites from the dry season to malaria-causing parasites in the transmission season, we show that despite inducing a minimal immune response and conserving its replication ability, *P. falciparum* dry season parasitaemias can be maintained low by splenic clearance of a large proportion of iRBCs that circulate longer than observed in malaria cases.

RESULTS

***P. falciparum* persists during the dry season.** In a cohort study in Kalifabougou, Mali, we followed ~600 individuals from 3 months to 45 years of age during 2017 and 2018. As reported earlier[13], clinical episodes of malaria (temperature ≥37.5ºC, ≥2500 asexual parasites/µL, and no other clinically discernible cause of fever) were largely restricted to the transmission seasons (June - December), whereas nearly all subjects remained free of symptomatic malaria during the intervening dry seasons (January - May). Specifically, there were 386 and 347 febrile malaria cases diagnosed during the 2017 and 2018 rainy seasons, respectively, while only 12 and 5 febrile malaria episodes occurred during the dry seasons (Fig.1a and Table 1). Despite the very low incidence of clinical malaria in the dry season, we consistently observed 10-20% prevalence of subclinical *P. falciparum* infections during this time. Analysing over 400 individuals with paired data at the beginning (January) and end (May) of each dry season, we found that 20% of individuals were *P. falciparum* PCR$_+$ both in January 2017 and January 2018, and 15% and 12% of individuals were *P. falciparum* PCR$_+$ at the end of the 2017 and 2018 dry seasons, respectively (Fig. 1b). Older children and young adults carried subclinical *P. falciparum* more frequently than young children at the end of the dry season (Fig. 1c and Table 1), as reported earlier for this cohort[13]. Also, as previously reported, we observed that subclinical *P. falciparum* carriers at the end of the dry season were very likely to have been infected since its beginning (January 2017 or January 2018), while uninfected subjects at the beginning of dry season remained uninfected until its end (Fig. 1b). The odds ratios (OR) of maintaining the same infection status through the entire dry seasons were OR 90.9 (95% CI (38.6 , 213.8) $P < 0.0001$) in 2017, and OR Odds ratio 43.5 (95% CI (17.5 , 107.5) $P < 0.0001$) in 2018 (Supplementary Table 1). Consistent with the continued absence of clinical malaria during the dry season, parasitaemias of subclinical carriers determined by RT-qPCR and flow cytometry were found to remain low, or in some individuals decline as the dry season progressed, while clinical cases of malaria in the wet season presented with high parasite burdens (Fig.1d). Interestingly, the very few clinical malaria cases occurring during the dry seasons had significantly lower parasitaemias than those presented by the same individuals in clinical cases during the ensuing rainy seasons (Extended Data Fig. 1).

***P. falciparum* induces a minimal immune response during the dry season.** To test the hypothesis that host immunity may contribute to the suppression of parasitaemia during the dry season, we compared the immune responses of subclinical carriers of *P. falciparum* (May$_+$) versus non-infected children (May$_-$). We profiled serological markers of inflammation and cytokines, circulating immune cells, and humoral responses to *P. falciparum* variant surface

antigens (VSAs) of age- and gender-matched children who did or did not carry *P. falciparum* during the dry season, detected retrospectively by PCR. Inflammation markers previously reported to be elevated in clinical cases of malaria, such as C-reactive protein (CRP)[15], von Willebrand factor (vWF)[16], and hepcidin[17] were quantified in plasma samples obtained at the beginning (Jan) and end (May) of the dry season. None of the three markers were significantly different in subclinical carriers compared to uninfected children at either timepoint (Fig. 2a). We complemented these serological analyses with a multiplex bead array to detect 32 cytokines and chemokines and observed no differences between children with or without *P. falciparum* at the end of the dry season (May) in all but one of the quantified analytes (Supplementary Table 2). Only CXCL1, a pro-inflammatory chemokine known to recruit neutrophils, that has thus far not been associated with malaria in the clinical setting, was significantly increased in children with *P. falciparum* persistent parasitaemias at the end of the dry season (Fig. 2b). In contrast, CCL3, IL-10, IL-6 and IL-1β, previously associated with clinical malaria[18-20] were comparable in the plasma of infected versus uninfected children at the end of the dry season (Fig. 2b and Supplementary Table 2). We next quantified the proportions of major leucocyte populations from thawed PBMCs collected at the end of the dry season from children with or without subclinical *P. falciparum* (gating strategy in Extended Data Fig. 2). We observed that monocytes, T cells, B cells and NK cell subpopulations were not significantly different between children who carried (May_{+}) or not (May_{-}) *P. falciparum* (Fig. 2c and Extended Data Fig. 3). To interrogate differences in cell function, we quantified intracellular cytokines, activation or cytotoxicity markers, transcription factors or exhaustion markers of freshly collected PBMCs from *P. falciparum* subclinical infected and non-infected children at the end of the dry season. The levels of the activation marker CD25, transcription factor T-bet or cytokine IL-2 of CD4 T cells; granzyme B of CD8 T and NK cells, and exhaustion marker FCRL5 of atypical memory B cells were comparable between children who carried or not *P. falciparum* (Fig. 2d and Supplementary Table 3). We further questioned whether memory B cells (MBCs defined as $CD19_{+}$, $CD10_{-}$, $CD21_{-}$ and $CD27_{+\text{ or }-}$, gating strategy in Extended Data Fig. 2) specific for *P. falciparum* were affected in subclinical carriers compared to non-infected individuals at the end of the dry season. Using biotinylated AMA-1 and MSP1[21], we quantified AMA-1- or MSP1-specific MBCs in children who carried *P. falciparum* parasites, and non-infected children at the end of the dry season. We found that the proportion of class-switched *P. falciparum*-specific MBCs ($AMA1_{+}$ or $MSP1_{+}$ IgG_{+} IGM_{-} MBCs) was significantly increased in subclinical carriers at the end of the dry season, while no such difference was found in non-class-switched MBC population ($AMA1_{+}$ or $MSP1_{+}$ IgG_{-} IGM_{+} MBCs) (Fig. 2e). Within the IgG_{+} MBC subpopulations, we failed to observe

differences between *P. falciparum* carriers and uninfected individuals at the end of the dry season in *P. falciparum*-specific classical and atypical MBCs, but detected increased *P. falciparum*-specific activated MBCs in subclinical carriers (Extended Data Fig. 3). Using another multiplex bead array, we quantified humoral responses of *P. falciparum* subclinical carriers and uninfected individuals at the beginning and end of the dry season, to 35 domain types of the VSA multigene family *var*, which were grouped according to their endothelial-receptor affinity (CD36, EPCR or unknown receptor) and PfEMP1 UPS type (A, B or B/A types)[22] (Supplementary Table 4). We observed that more subclinical carriers (May^{+}) than non-infected individuals (May^{-}) were reactive against PfEMP1 domains binding to CD36, EPCR or to unknown receptors at both time-points, and also that the proportion of individuals reactive to the different PfEMP1 domains decreased over the dry season independently of individual infection status (Fig. 2f and Extended Data Fig. 3), these differences parallel our previously published data on *P. falciparum*-specific humoral responses to non-VSA[13], suggesting comparable humoral dynamics for PfEMP1s and non-VSA antigens. Additionally, we observed that the magnitude of IgG reactivity to A, B or B/A types of PfEMP1 declined similarly from the beginning to end of the dry season in children who carried subclinical infection (May^{+}) or were uninfected (May^{-}) during the dry season (Fig. 2g and Extended Data Fig. 3). Antibodies against PfEMP1 domains (Fig. 2f-g), against a large set of *P. falciparum* non- VSA[13], and also particularly against RBC invasion-related proteins[23] (Extended Data Fig. 3) were consistently higher in subclinical carriers compared to non-infected children at the end of the dry season, so we questioned if the difference in humoral response at the end of the dry season could impose variance in inhibition of merozoite invasion in vitro. We tested merozoite invasion of a laboratory-adapted *P. falciparum* strain in the presence of plasma from Malian children who carried parasites or not during the dry season, and evaluated the antibodies' ability to block RBC invasion. Testing complete and antibody-depleted plasma, we observed that antibody-depleted Malian plasma allowed for ~5-fold increase in invasion of merozoites compared to complete Malian plasma, while antibody depletion had no differential effect on the control German plasma used (Fig. 2h and Extended Data Fig. 3). Notably, however, plasma from Malian children carrying subclinical infections (May^{+}) or not carrying parasites (May^{-}), had similar ability to inhibit merozoite invasion, suggesting that the antibodies remaining elevated at the end of the dry season have no significant effect on inhibiting merozoites invasion of RBCs, and are unlikely to contribute to the maintenance of low parasitaemias through this mechanism.

***P. falciparum* genetic diversity is maintained throughout the year.** Next, we asked whether *P. falciparum* parasites persisting through the dry season are genetically distinct from those causing acute malaria during the transmission season. To that end, we measured the size of the merozoite surface protein 2 gene (*msp2)*, which is highly polymorphic and discriminates different *P. falciparum* genotypes[24,25]. Through nested PCR followed by fragment analysis using capillary electrophoresis, we compared paired samples from 93 subclinical carriers at the beginning (Jan) and end (May) of the dry season, with 136 samples from clinical cases of malaria in the ensuing transmission season (MAL). The number of clones detected per individual did not significantly differ between parasites isolated during the dry season or transmission season, nor did the percentage of individuals with different numbers of clones (Fig. 3a-b). Furthermore, the size and distribution of *msp2* clones identified during the dry season were similar to those isolated from clinical malaria cases during the transmission season (Fig. 3c-d), with the most frequent clone sizes being the same at any of the time-points analysed.

Transcriptome of circulating subclinical *P. falciparum* at the end of the dry season differs from that of *P. falciparum* during clinical malaria. We performed RNA sequencing of leucocyte-depleted blood from 12 children with persistent subclinical *P. falciparum* at the end of the dry season (May), and from 12 age- and gender- matched children presenting with their first clinical malaria case in the ensuing transmission season (MAL) (Supplementary Table 5). Principal component (Fig. 4a) and unsupervised clustering (Fig. 4b) analyses showed segregation of transcription profiles based on seasonality. Differentially expressed genes (DEGs) determined at a false discovery rate threshold of 5% resulted in 1607 DEGs, 1131 transcripts up-regulated, and 476 transcripts down-regulated in the dry season compared to clinical malaria samples (Fig. 4c and Supplementary Table 6). Validation of the RNA-Seq data was performed by RT-qPCR of eight DEGs and the correlation between the two methods resulted in highly significant r_2=0.929 (Fig. 4d and Supplementary Table 7). Furthermore, samples from additional children (6 end of the dry season and 12 malaria cases during the transmission season) were used to quantify expression of three DEGs in parallel with the initial 24 samples, and revealed similar fold changes by RT-qPCR (Fig. 4e). We investigated similarities in the DEGs obtained in this study with those of previous reports comparing parasite physiological states and transcriptomes from a range of clinical malaria severities[26], or parasites causing malaria in high versus low transmission areas[27], but no enrichment was found (Extended Data Fig. 4), suggesting that singular mechanisms may be at play during the dry season. Functional and Gene Ontology analysis of the dry season DEGs revealed a significant

enrichment of transcripts involved in cellular processes related with several metabolic pathways and also *Phagosome*, *DNA replication* or *Homologous recombination* (Fig. 4f). Indeed, DEGs involved in metabolic pathways suggest that *Glycolysis*, *Glycerophospholipid*, *Purine and Pyrimidine* pathways *were* increased in parasites from the end of the dry season (May), while *Fatty acid biosynthesis* appeared downregulated compared to parasites from clinical malaria (MAL) in the wet season (Fig. 4g). Interestingly, apparent exceptions to the trend of up- or down-regulation in each of the pathways, highlight transcripts which also have exceptional patterns of expression within the 48-hour intraerythrocytic developmental cycle[4] thus promoting different relative expressions (Extended Data Fig. 5). To follow-up on possible metabolic differences between parasites persisting through the dry season and parasites causing malaria in the transmission season we used liquid chromatography–mass spectrometry to profile both hydrophilic and hydrophobic metabolites from the plasma of 12 subclinical children with *P. falciparum* infections at the end of the dry season (May), and of 12 children presenting with their first clinical malaria case (MAL) in the rainy season. We found significant separation between metabolites present in the two groups of samples (Fig. 4h and Supplementary Table 8), however the difficulty of normalization of measured metabolite levels to parasite burden, plus the strong parasitaemia differences at the time of the blood draw, hinder conclusive interpretation of what may be seasonal or parasite induced metabolic alterations (Supplementary Table 9).

***P. falciparum* replication is not impaired in the dry season.** We then tested the hypothesis that dry season parasitaemias were maintained low and subclinical due to decreased parasite replication capacity during this period. We cultured *P. falciparum* in vitro directly after blood draw for 36 to 48 h, from rapid diagnostic test positive (RDT^+) samples of asymptomatic individuals at three time points of the dry season (January, March and May), and from samples of children presenting with their first clinical malaria episode of the ensuing transmission season (MAL). By flow cytometry, we measured the increase in parasitaemia and parasite development at 0, 16, 24, 30, 36 and 48 h after in vitro culture. Parasite in vitro growth rates of samples from >40 subclinical donors during the dry season, and ~30 malaria cases in the transmission season indicated that the highest growth determined between any two time-points of the short-term culture was similar throughout the year. Parasitaemias increased in vitro between 2 and 5-fold at any point in the year, 2.8-fold in January, 95% CI (2.3 , 3.3), 4.1-fold in March, 95% CI (3.4 , 4.7), 3.6-fold in May, 95% CI (2.6 , 4.6), and 2.8-fold in malaria cases, 95% CI (2.1 , 3.5). However, the number of hours in culture needed to increase parasitaemia was shorter in the dry

season samples than in samples from malaria-causing parasites in the transmission season (Fig. 5a). In accordance with an earlier increase in parasitaemia in vitro during the dry season, we could frequently identify on Giemsa smears mature schizonts after 16 and 24 h of culture, and young ring-stages after 30 or 36 h in the dry season samples; while mature schizonts of malaria-causing parasite samples were mostly observed after 36 h in culture and young ring-stages were largely found after 48 h in vitro (Fig. 5b). When we calculated the number of hours in culture at which the highest increase of parasitaemia could be detected for each sample, we observed that it decreased from the beginning to the end of the dry season, Jan 26.4 h, 95% CI (24.5 , 28.3), Mar 24.9 h, 95% CI (23.9 , 25.9), May 22.7 h, 95% CI (20.8 , 24.6), and was maximum during malaria cases in the transmission season, MAL 44.0 h , 95% CI (41.5 , 46.6) (Fig. 5c). Nevertheless, when we measured the number of merozoites per multinucleated schizont prior to or at the time of the highest increase in parasitaemia in vitro, we obtained comparable values at the end of dry season and in clinical malaria cases in the wet season (Fig. 5d). Finding later developmental parasite stages at earlier times in this short-term in vitro experiment during the dry season could indicate a faster than 48 h intraerythrocytic replicative cycle, or alternatively, that dry season parasites circulate longer without adhering to the host vascular endothelium, and were more developed than circulating parasites in clinical malaria cases at the time of the blood draw. To test the latter, we used the RNA-seq data described in Fig. 4 to estimate, with a likelihood-based statistical method previously described[28], the age in hours post-invasion (hpi) of circulating parasites from subclinical children at the end of the dry season (May) and from clinical cases during the wet season (MAL). We determined that parasites circulating in the dry season had a transcriptional signature of ~17 hpi, 95%CI (14.05 , 20.8), while parasites circulating in malaria cases during the wet season had a transcription profile comparable to parasites with ~7 hpi, 95% CI (6.5 , 7.7) (Fig. 5e). Accordingly, imaging the thick blood films made in the field at the time of the blood draw, we confirmed that trophozoites were present on the end dry season samples, while clinical malaria samples in the transmission season had much smaller ring-stages (Fig. 5f-g).

Infected erythrocytes in circulation at the end of the dry season are at higher risk of splenic clearance. To investigate if longer circulation of iRBCs in the dry season would impact host RBC deformability and potentiate splenic clearance, we used a microsphiltration system mimicking the narrow and short inter-endothelial slits of the human spleen with different sized microspheres[29]. Using freshly collected blood samples from asymptomatically infected children at the end of the dry season and from children presenting with febrile malaria during the

transmission season, we assessed retention in the microspheres and flow-through of circulating iRBCs at time 0, and after 6, 18 and 30 h in vitro. We observed that iRBCs collected from malaria (MAL) cases were not significantly retained in the spleen-like system at 0, 6 or 18 h post-culture, and that only after 30 h was the percentage of iRBCs in the flow-through reduced, indicating splenic retention of iRBCs (Fig. 6a). Conversely, iRBCs in RDT+ blood collected at the end of the dry season (May) had significantly reduced flow-through immediately after the blood draw (~25% retention of 0 h iRBCs in the microsphere-system), and over 50% retention of iRBCs after 6 h or 18 h in culture (Fig. 6a). Accordingly, we observed that trophozoites or schizonts which fail to flow through the microsphere system were circulating (at 0 h) only in the dry season samples (Fig. 6b).

We then investigated whether differences in cytoadhesion, affecting the length of time that parasitized cells remain in circulation, could explain the observed age distributions and microsphiltration results. For this we used a mathematical model to describe the within-host growth and removal of iRBCs from circulation through cytoadhesion in the vasculature and through splenic retention (see Methods). Both processes were assumed to be dependent on the parasite's developmental stage, increasing as the parasite starts to express adherence-mediating surface antigens and RBC modification leads to cell rigidity. Whereas cytoadhering parasites still replicate, those filtered out by the spleen were assumed to be removed. As shown in Fig. 6c, effective growth rates and population sizes of low-cytoadhering parasites are significantly lower than those of high-cytoadhering parasites, which can avoid splenic clearance before parasitized cells become too rigid to pass through the spleen. We then obtained estimated parasite age distributions for both scenarios (Fig. 6d) by sampling from the modelled parasite population at random points over the simulated infection time course, akin to blood sampling from a population. As low-adhesion parasites are predominantly removed by the spleen towards the end of their life-cycle, they show a much broader age-range than high-cytoadhesion parasites, which are removed from circulation earlier through cytoadhesion and therefore show a narrower and younger age range, in agreement with the observed age distribution from thick blood smears (Fig. 5e-f). Next, we simulated a microsphiltration experiment by "growing" our sampled model parasites older and evaluating their projected average flow-through based on our assumed, age-dependent splenic retention function (see Methods and Extended Data Fig. 6.). The throughput of high-cytoadhering parasites is high for the first 6-10h before dropping off gradually as parasites grow older (Fig. 6e). In contrast, samples from low-cytoadhering parasites with their more uniformly distributed age range already have a much-reduced flow-through at 0 h, which, however, remained more stable as

parasites mature over the next 30h; again in line with the empirical observations (Fig. 6a). These mathematical results suggest that cytoadhesion alone can explain the differences between parasites sampled during the dry season (low-adhesion) and parasites sampled from malaria cases (high-adhesion).

To investigate if the expression of cytoadhesion-mediating PfEMP1 proteins differed in abundance or quality in parasites found subclinical in the dry season and parasites found in malaria cases during the wet season, we assembled the *var* genes from the RNA-Seq reads of the 24 samples from end of the dry season and malaria cases (see Methods). Expression of several *var* genes has been shown to remain fairly stable between ~10 and 20h post invasion[30] which should be close to the average ages estimated for parasites in malaria cases and dry season samples respectively. Using a recently developed analytical pipeline[31], we could detect LARSFADIG motifs identifying PfEMP1 coding genes[32] in 8 out of 12 samples from the dry season, and in 10 out of 12 malaria cases (Table 2). We were able to annotate full length *var* genes, including both the start N-terminal sequence (NTS) and the acidic terminal sequence (ATS) domains, and also many isolated fragments, and we observed more contigs with LARSFADIG motifs and *var* gene fragments in the wet season samples (Supplementary Table 10). We used different methods to access enrichment of higher expressed *var* genes in the wet versus the dry season samples. Although we did not see statistically significant enrichment, we observed a trend that the top expressed *var* genes in each individual in the wet season are higher expressed (Fig. 6f), and anticipate that further studies with larger samples size will confirm this trend. Furthermore, we identified known *var* gene domains such as Duffy Binding Like (DBL) and Cysteine Rich Interdomain Regions (CIDR) as well as the NTS and ATS, and searched for typical 5′ upstream (UPS) sequences associating with different pathological outcomes[22] in the dry season and malaria cases' assembled *vars.* Although we were unable to determine the UPS type of expressed *vars* due to the short assembly of the 5' UTR region, we did find more *var* genes with a DBLz domains in the malaria samples (13 out of 61 in *var* fragments longer than 3.5 kb) compared to the dry season (1 out of 11 in *var* fragments longer than 3.5 kb) (Supplementary Table 10).

Discussion

Asymptomatic individuals carrying *P. falciparum* at the end of the dry season in areas of seasonal malaria have been broadly described[13,33-37], but how the parasite bridges two rainy seasons without promoting malaria symptoms or being cleared remained elusive. In this study, with samples from Malians exposed to alternating six-month dry and transmission seasons, we

show that within each 48h replicative cycle, *P. falciparum* iRBCs circulate longer in the bloodstream during the dry season, allowing increased clearance in the spleen, and thus preventing high parasitaemias which could lead to immune activation or malaria symptoms[38,39]. Although asymptomatic parasitaemia at the end of the dry season associates with a lower risk of clinical malaria in the ensuing wet season[13,33-35], clearance of parasitaemia with anti-malarials prior to the transmission season does not increase subsequent malaria risk, and the persistence of infection during the dry season does not prevent nor slow the decline of *P. falciparum*-specific antibodies[13] (Fig. 2f-g). Consistent with these observations, low parasitaemia during the dry season did not elicit detectable inflammation, nor affect immune cell function (Fig. 2), indicating that chronic low parasitaemia in seasonal endemic settings might differ from Controlled Human Malaria Infections (CHMI) in naïve individuals, where low parasitaemias appear to induce immunity[40]; and also pointing that slow and continuous stimulation of the immune system is less effective than sudden changes in antigenic stimulation[41]. Nevertheless, cumulative immunity may be determinant to sustain the dry season reservoir of *P. falciparum*. Dry season subclinical carriers have higher anti-*P. falciparum* humoral immunity ([13] and Fig. 2f-g), and higher *P. falciparum*-specific MBCs (Fig. 2e) than non-infected individuals, suggesting that a certain cumulative exposure is necessary to carry dry season subclinical infections. Additionally, we and others have shown that end of dry season parasitaemias are more frequent in older than younger children[13,42], which is consistent with an age-dependent decrease in parasitaemia and increase in anti-parasitic immunity[43,44]. It is possible that within each *P. falciparum* infection, sequential presentation of different VSAs on the surface of iRBCs, and its corresponding ordered acquisition of antibodies[45,46] favours progressively less virulent parasites. Accordingly, a recent study of CHMI including naïve and semi-immune individuals observed clinical cases in naïve individuals, while chronic infections appeared in semi-immune with intermediate antibody levels[47].

Reports from the transmission season show that increasing malaria severity associates with different parasite transcriptional profiles[26,48-50], but the persisting dry season reservoir had not been investigated. Our data shows that, while *P. falciparum* causing malaria in the transmission season has a ring-stage transcriptional signature, parasites persisting at the end of the dry season resemble more developed intraerythrocytic stages, which we confirmed both visually and through differential growth kinetics in vitro (Fig. 5). Future single-cell transcript analysis of iRBCs[5] will allow comparing stage-matched pools of parasites to better understand how *P. falciparum* achieves low cytoadhesion in the dry season. Also of interest will be to revisit earlier reports of transcriptional differences between parasites inducing varying degrees of malaria

severity[26,48,49], and question if these could be partially imposed by the hpi of circulating parasites. In fact, Tonkin-Hill and colleagues found a bias towards early trophozoite transcription in the non-severe malaria samples compared to the ring-stage transcriptional profile of the severe malaria cases[48], which could be due to differing adhesion efficiencies in vivo. Interestingly, in vitro replication rates of severe and uncomplicated malaria causing parasites[51,52] have not consistently explained the higher parasitaemias observed in severe malaria cases, suggesting that adhesion efficiency differences may also contribute. Continued asexual replication (independently or coupled with immunity) may lead to progressively less adhesive iRBCs, as observed in parasites collected during the dry season. In a rodent-malaria model, uninterrupted asexual-stage growth led to bias in gene expression of VSA and parasite virulence[53]; and the transition between acute and chronic phases is suggested to be independent of adaptive immunity[54]. Also, in humans it has been suggested that continued asexual replication can skew the PfEMP1 expression profile[47,55], which is consistent with our *var* genes RNA-Seq data (Fig. 6f and Table 2). The mechanisms by which the parasite adapts to the dry season, and how transmission is assured as the rainy season ensues remain to be investigated. In a varying or unpredictable environment, organisms can overcome unfavourable conditions by sensing environmental changes and adapting their individual developmental program to increase survival; or alternatively, stochastic population heterogeneity increases the probability of survival under changing conditions[56]. *P. falciparum* may sense and respond to environmental cues of transmissibility opportunity, as has been described for detection of nutrient availability[57], sexual commitment[58], or appropriate environment for gametogenesis[59]. Such a mechanism could act through epigenetic modulation of VSAs, or be seasonally imposed by different metabolic states of the host, driving a shift on the parasite from a fast- to a slow-growing program as the transmission season ends and persistence is required, and return to fast growth as transmission resumes. In an avian-malaria model, chronic *P. relictum* has been shown to respond to bites from uninfected mosquitoes and increase its replication promoting transmission[60]. Parasite survival during the dry season is imperative, but will only be efficient in resuming transmission if these retain the ability to produce gametocytes that mosquitoes can uptake, thus investigating potential adaptive changes in the sexual stages of *P. falciparum* during the dry season will likely also reveal seasonal adjustments. Also, investigating the transcriptional profile of the few malaria cases diagnosed in the dry season (Fig. 1a, Extended Data Fig. 1) should be the focus of future studies, which we could not do because study protocol did not include venipuncture blood draws from clinical cases during the dry season.

The survival of *P. falciparum*-infected individuals during the dry season is advantageous for the parasite, and low adhesion of infected erythrocytes is likely a central feature to the subclinical carriage of *P. falciparum* demonstrating the adaptability of *P. falciparum* parasites to the vector-free period.

Acknowledgments

We thank the residents of Kalifabougou, Mali for participating in this study. We acknowledge the support of the Flow Cytometry Core Facility of DKFZ in Heidelberg, Germany, and the Immunology Core Lab of the UCRC in Bamako, Mali. We thank the Metabolomics Core Facility at Penn State University, and A. Patterson and P. Smith from the Penn State Metabolomics Core. We thank Zbynek Bozdech and lab at Nanyang Technological University, Singapore for help and expertise with RNA extraction. This work was supported by the German Center for Infection research (DZIF), the European Research Council (ERC) under the European Union's Horizon 2020 research and innovation programme (grant agreement No 759534), the SFB 1129 of the German Research Foundation (DFG) and the Division of Intramural Research, National Institute of Allergy and Infectious Diseases, of NIH. RTL was funded by the European Union's Horizon 2020 research and innovation programme under the Marie Skłodowska-Curie Grant Agreement No. DLV-839998.

Author contributions

CMA, HF, RTL, NFL, CA, JH, CSH, SL, MN, HC, DS, CM, SR, KM, MVH, ELA and SP performed experiments and analysed data; SD, DD, KK, AO, BB and PDC designed, conducted and supervised field work generating the clinical data and samples; JM, NOS and TDO performed bioinformatic analysis; MEN, CL, TL, AM, and AF, ML provided technical expertise and TL and LT provided essential reagents; MR performed mathematical models; TMT, JS and VW provided statistics expertise; CMA prepared figures and CMA, HF, RTL, TMT, NSO and TDO and helped prepare the manuscript; TMT, AF, ML, TL, TDO, MR and PDC provided insightful comments to the manuscript. PDC discussed initial field and study designs. SP designed the study and wrote the manuscript. All authors read and approved the final manuscript.

Competing interests

The authors declare no competing interests.

452

References

1 WHO. World malaria report 2019. Report No. 978 92 4 156565 3, volumes (World Health Organization, Geneva, Switzerland, 2019).

2 Hommel, M., David, P. H. & Oligino, L. D. Surface alterations of erythrocytes in Plasmodium falciparum malaria. Antigenic variation, antigenic diversity, and the role of the spleen. *J Exp Med* **157**, 1137-1148, doi:10.1084/jem.157.4.1137 (1983).

3 Roberts, D. J. *et al.* Rapid switching to multiple antigenic and adhesive phenotypes in malaria. *Nature* **357**, 689-692, doi:10.1038/357689a0 (1992).

4 Bozdech, Z. *et al.* The transcriptome of the intraerythrocytic developmental cycle of Plasmodium falciparum. *PLoS Biol* **1**, E5, doi:10.1371/journal.pbio.0000005 (2003).

5 Howick, V. M. *et al.* The Malaria Cell Atlas: Single parasite transcriptomes across the complete Plasmodium life cycle. *Science* **365**, doi:10.1126/science.aaw2619 (2019).

6 Marti, M., Good, R. T., Rug, M., Knuepfer, E. & Cowman, A. F. Targeting malaria virulence and remodeling proteins to the host erythrocyte. *Science* **306**, 1930-1933, doi:10.1126/science.1102452 (2004).

7 Crabb, B. S. *et al.* Targeted gene disruption shows that knobs enable malaria-infected red cells to cytoadhere under physiological shear stress. *Cell* **89**, 287-296, doi:10.1016/s0092-8674(00)80207-x (1997).

8 Oh, S. S. *et al.* Plasmodium falciparum erythrocyte membrane protein 1 is anchored to the actin-spectrin junction and knob-associated histidine-rich protein in the erythrocyte skeleton. *Mol Biochem Parasitol* **108**, 237-247, doi:10.1016/s0166-6851(00)00227-9 (2000).

9 Lavstsen, T. *et al.* Plasmodium falciparum erythrocyte membrane protein 1 domain cassettes 8 and 13 are associated with severe malaria in children. *Proc Natl Acad Sci U S A* **109**, E1791-1800, doi:10.1073/pnas.1120455109 (2012).

10 Lehmann, T. *et al.* Aestivation of the African malaria mosquito, Anopheles gambiae in the Sahel. *Am J Trop Med Hyg* **83**, 601-606, doi:10.4269/ajtmh.2010.09-0779 (2010).

11 Babiker, H. A., Abdel-Muhsin, A. M., Ranford-Cartwright, L. C., Satti, G. & Walliker, D. Characteristics of Plasmodium falciparum parasites that survive the lengthy dry season in eastern Sudan where malaria transmission is markedly seasonal. *Am J Trop Med Hyg* **59**, 582-590 (1998).

12 Ouedraogo, A. L. *et al.* Dynamics of the Human Infectious Reservoir for Malaria Determined by Mosquito Feeding Assays and Ultrasensitive Malaria Diagnosis in Burkina Faso. *J Infect Dis* **213**, 90-99, doi:10.1093/infdis/jiv370 (2016).

13 Portugal, S. *et al.* Treatment of Chronic Asymptomatic Plasmodium falciparum Infection Does Not Increase the Risk of Clinical Malaria Upon Reinfection. *Clin Infect Dis* **64**, 645-653, doi:10.1093/cid/ciw849 (2017).

14 Kimenyi, K. M., Wamae, K. & Ochola-Oyier, L. I. Understanding P. falciparum Asymptomatic Infections: A Proposition for a Transcriptomic Approach. *Front Immunol* **10**, 2398, doi:10.3389/fimmu.2019.02398 (2019).

15 O'Donnell, A. *et al.* The acute phase response in children with mild and severe malaria in Papua New Guinea. *Trans R Soc Trop Med Hyg* **103**, 679-686, doi:10.1016/j.trstmh.2009.03.023 (2009).

16 Park, G. S., Ireland, K. F., Opoka, R. O. & John, C. C. Evidence of Endothelial Activation in Asymptomatic Plasmodium falciparum Parasitemia and Effect of Blood Group on Levels of von Willebrand Factor in Malaria. *J Pediatric Infect Dis Soc* **1**, 16-25, doi:10.1093/jpids/pis010 (2012).

17 Burte, F. *et al.* Circulatory hepcidin is associated with the anti-inflammatory response but not with iron or anemic status in childhood malaria. *Blood* **121**, 3016-3022, doi:10.1182/blood-2012-10-461418 (2013).

18 Weinberg, J. B. *et al.* Monocyte polarization in children with falciparum malaria: relationship to nitric oxide insufficiency and disease severity. *Sci Rep* **6**, 29151, doi:10.1038/srep29151 (2016).

19 Oyegue-Liabagui, S. L. *et al.* Pro- and anti-inflammatory cytokines in children with malaria in Franceville, Gabon. *Am J Clin Exp Immunol* **6**, 9-20 (2017).

20 Lyke, K. E. *et al.* Serum levels of the proinflammatory cytokines interleukin-1 beta (IL-1beta), IL-6, IL-8, IL-10, tumor necrosis factor alpha, and IL-12(p70) in Malian children with severe Plasmodium falciparum malaria and matched uncomplicated malaria or healthy controls. *Infect Immun* **72**, 5630-5637, doi:10.1128/IAI.72.10.5630-5637.2004 (2004).

21 Hopp, C. S. *et al.* Plasmodium falciparum-specific IgM B cells dominate in children, expand with malaria and produce parasite inhibitory IgM. *bioRxiv*, 2020.2004.2012.030049, doi:10.1101/2020.04.12.030049 (2020).
22 Lavstsen, T., Salanti, A., Jensen, A. T., Arnot, D. E. & Theander, T. G. Sub-grouping of Plasmodium falciparum 3D7 var genes based on sequence analysis of coding and non-coding regions. *Malar J* **2**, 27, doi:10.1186/1475-2875-2-27 (2003).
23 Cowman, A. F., Berry, D. & Baum, J. The cellular and molecular basis for malaria parasite invasion of the human red blood cell. *J Cell Biol* **198**, 961-971, doi:10.1083/jcb.201206112 (2012).
24 Snounou, G. *et al.* Biased distribution of msp1 and msp2 allelic variants in Plasmodium falciparum populations in Thailand. *Trans R Soc Trop Med Hyg* **93**, 369-374, doi:10.1016/s0035-9203(99)90120-7 (1999).
25 Liljander, A. *et al.* Optimization and validation of multi-coloured capillary electrophoresis for genotyping of Plasmodium falciparum merozoite surface proteins (msp1 and 2). *Malar J* **8**, 78, doi:10.1186/1475-2875-8-78 (2009).
26 Daily, J. P. *et al.* Distinct physiological states of Plasmodium falciparum in malaria-infected patients. *Nature* **450**, 1091-1095, doi:10.1038/nature06311 (2007).
27 Rono, M. K. *et al.* Adaptation of Plasmodium falciparum to its transmission environment. *Nat Ecol Evol* **2**, 377-387, doi:10.1038/s41559-017-0419-9 (2018).
28 Lemieux, J. E. *et al.* Statistical estimation of cell-cycle progression and lineage commitment in Plasmodium falciparum reveals a homogeneous pattern of transcription in ex vivo culture. *Proc Natl Acad Sci U S A* **106**, 7559-7564, doi:10.1073/pnas.0811829106 (2009).
29 Deplaine, G. *et al.* The sensing of poorly deformable red blood cells by the human spleen can be mimicked in vitro. *Blood* **117**, e88-95, doi:10.1182/blood-2010-10-312801 (2011).
30 Dahlback, M. *et al.* Changes in var gene mRNA levels during erythrocytic development in two phenotypically distinct Plasmodium falciparum parasites. *Malar J* **6**, 78, doi:10.1186/1475-2875-6-78 (2007).
31 Otto, T. D. *et al.* Evolutionary analysis of the most polymorphic gene family in falciparum malaria. *Wellcome Open Res* **4** (2019).
32 Otto, T. D. *et al.* Genome sequencing of chimpanzee malaria parasites reveals possible pathways of adaptation to human hosts. *Nat Commun* **5**, 4754, doi:10.1038/ncomms5754 (2014).
33 Sonden, K. *et al.* Asymptomatic Multiclonal Plasmodium falciparum Infections Carried Through the Dry Season Predict Protection Against Subsequent Clinical Malaria. *J Infect Dis* **212**, 608-616, doi:10.1093/infdis/jiv088 (2015).
34 Males, S., Gaye, O. & Garcia, A. Long-term asymptomatic carriage of Plasmodium falciparum protects from malaria attacks: a prospective study among Senegalese children. *Clin Infect Dis* **46**, 516-522, doi:10.1086/526529 (2008).
35 Crompton, P. D. *et al.* Sickle Cell Trait Is Associated with a Delayed Onset of Malaria: Implications for Time-to-Event Analysis in Clinical Studies of Malaria. *J Infect Dis* **198**, 1265-1275, doi:10.1086/592224 (2008).
36 Drakeley, C., Sutherland, C., Bousema, J. T., Sauerwein, R. W. & Targett, G. A. The epidemiology of Plasmodium falciparum gametocytes: weapons of mass dispersion. *Trends Parasitol* **22**, 424-430, doi:S1471-4922(06)00176-0 [pii]
10.1016/j.pt.2006.07.001 (2006).
37 Bousema, T. *et al.* Mosquito feeding assays to determine the infectiousness of naturally infected Plasmodium falciparum gametocyte carriers. *PLoS One* **7**, e42821, doi:10.1371/journal.pone.0042821 (2012).
38 Dicko, A. *et al.* Season, fever prevalence and pyrogenic threshold for malaria disease definition in an endemic area of Mali. *Trop Med Int Health* **10**, 550-556, doi:TMI1418 [pii]
10.1111/j.1365-3156.2005.01418.x (2005).
39 Smith, T., Schellenberg, J. A. & Hayes, R. Attributable fraction estimates and case definitions for malaria in endemic areas. *Stat Med* **13**, 2345-2358, doi:10.1002/sim.4780132206 (1994).
40 Stanisic, D. I., McCarthy, J. S. & Good, M. F. Controlled Human Malaria Infection: Applications, Advances, and Challenges. *Infect Immun* **86**, doi:10.1128/IAI.00479-17 (2018).
41 Pradeu, T. & Vivier, E. The discontinuity theory of immunity. *Sci Immunol* **1**, doi:10.1126/sciimmunol.aag0479 (2016).

42 Goncalves, B. P. *et al.* Examining the human infectious reservoir for Plasmodium falciparum malaria in areas of differing transmission intensity. *Nat Commun* **8**, 1133, doi:10.1038/s41467-017-01270-4 (2017).
43 Tran, T. M. *et al.* An intensive longitudinal cohort study of Malian children and adults reveals no evidence of acquired immunity to Plasmodium falciparum infection. *Clin Infect Dis* **57**, 40-47, doi:10.1093/cid/cit174 (2013).
44 Crompton, P. D. *et al.* A prospective analysis of the Ab response to Plasmodium falciparum before and after a malaria season by protein microarray. *Proc Natl Acad Sci U S A* **107**, 6958-6963, doi:1001323107 [pii]
10.1073/pnas.1001323107 (2010).
45 Cham, G. K. *et al.* Hierarchical, domain type-specific acquisition of antibodies to Plasmodium falciparum erythrocyte membrane protein 1 in Tanzanian children. *Infect Immun* **78**, 4653-4659, doi:IAI.00593-10 [pii]
10.1128/IAI.00593-10.
46 Obeng-Adjei, N. *et al.* Longitudinal analysis of naturally acquired PfEMP1 CIDR domain variant antibodies identifies associations with malaria protection. *JCI Insight*, doi:10.1172/jci.insight.137262 (2020).
47 Bachmann, A. *et al.* Controlled human malaria infection with Plasmodium falciparum demonstrates impact of naturally acquired immunity on virulence gene expression. *PLoS Pathog* **15**, e1007906, doi:10.1371/journal.ppat.1007906 (2019).
48 Tonkin-Hill, G. Q. *et al.* The Plasmodium falciparum transcriptome in severe malaria reveals altered expression of genes involved in important processes including surface antigen-encoding var genes. *PLoS Biol* **16**, e2004328, doi:10.1371/journal.pbio.2004328 (2018).
49 Almelli, T. *et al.* Differences in gene transcriptomic pattern of Plasmodium falciparum in children with cerebral malaria and asymptomatic carriers. *PLoS One* **9**, e114401, doi:10.1371/journal.pone.0114401 (2014).
50 Lee, H. J. *et al.* Integrated pathogen load and dual transcriptome analysis of systemic host-pathogen interactions in severe malaria. *Sci Transl Med* **10**, doi:10.1126/scitranslmed.aar3619 (2018).
51 Deans, A. M. *et al.* Low multiplication rates of African Plasmodium falciparum isolates and lack of association of multiplication rate and red blood cell selectivity with malaria virulence. *Am J Trop Med Hyg* **74**, 554-563 (2006).
52 Chotivanich, K. *et al.* Parasite multiplication potential and the severity of Falciparum malaria. *J Infect Dis* **181**, 1206-1209, doi:10.1086/315353 (2000).
53 Spence, P. J. *et al.* Vector transmission regulates immune control of Plasmodium virulence. *Nature* **498**, 228-231, doi:10.1038/nature12231 (2013).
54 Brugat, T. *et al.* Antibody-independent mechanisms regulate the establishment of chronic Plasmodium infection. *Nat Microbiol* **2**, 16276, doi:10.1038/nmicrobiol.2016.276 (2017).
55 Abdi, A. I. *et al.* Global selection of Plasmodium falciparum virulence antigen expression by host antibodies. *Sci Rep* **6**, 19882, doi:10.1038/srep19882 (2016).
56 Weinberger, L. S. A minimal fate-selection switch. *Curr Opin Cell Biol* **37**, 111-118, doi:10.1016/j.ceb.2015.10.005 (2015).
57 Mancio-Silva, L. *et al.* Nutrient sensing modulates malaria parasite virulence. *Nature* **547**, 213-216, doi:10.1038/nature23009 (2017).
58 Brancucci, N. M. B. *et al.* Lysophosphatidylcholine Regulates Sexual Stage Differentiation in the Human Malaria Parasite Plasmodium falciparum. *Cell* **171**, 1532-1544 e1515, doi:10.1016/j.cell.2017.10.020 (2017).
59 Billker, O. *et al.* Identification of xanthurenic acid as the putative inducer of malaria development in the mosquito. *Nature* **392**, 289-292, doi:10.1038/32667 (1998).
60 Cornet, S., Nicot, A., Rivero, A. & Gandon, S. Evolution of plastic transmission strategies in avian malaria. *PLoS pathogens* **10**, e1004308, doi:10.1371/journal.ppat.1004308 (2014).
61 Auburn, S. *et al.* An effective method to purify Plasmodium falciparum DNA directly from clinical blood samples for whole genome high-throughput sequencing. *PLoS One* **6**, e22213, doi:10.1371/journal.pone.0022213 (2011).
62 Ratsimbasoa, A. *et al.* Evaluation of two new immunochromatographic assays for diagnosis of malaria. *Am J Trop Med Hyg* **79**, 670-672 (2008).

63 Radfar, A. *et al.* Synchronous culture of Plasmodium falciparum at high parasitemia levels. *Nat Protoc* **4**, 1899-1915, doi:10.1038/nprot.2009.198 (2009).
64 Boyle, M. J. *et al.* Isolation of viable Plasmodium falciparum merozoites to define erythrocyte invasion events and advance vaccine and drug development. *Proc Natl Acad Sci U S A* **107**, 14378-14383, doi:10.1073/pnas.1009198107 (2010).
65 Tonkin, C. J. *et al.* Localization of organellar proteins in Plasmodium falciparum using a novel set of transfection vectors and a new immunofluorescence fixation method. *Mol Biochem Parasitol* **137**, 13-21, doi:10.1016/j.molbiopara.2004.05.009 (2004).
66 Broadbent, K. M. *et al.* Strand-specific RNA sequencing in Plasmodium falciparum malaria identifies developmentally regulated long non-coding RNA and circular RNA. *BMC Genomics* **16**, 454, doi:10.1186/s12864-015-1603-4 (2015).
67 Kim, D., Langmead, B. & Salzberg, S. L. HISAT: a fast spliced aligner with low memory requirements. *Nat Methods* **12**, 357-360, doi:10.1038/nmeth.3317 (2015).
68 Anders, S., Pyl, P. T. & Huber, W. HTSeq--a Python framework to work with high-throughput sequencing data. *Bioinformatics* **31**, 166-169, doi:10.1093/bioinformatics/btu638 (2015).
69 Love, M. I., Huber, W. & Anders, S. Moderated estimation of fold change and dispersion for RNA-seq data with DESeq2. *Genome Biol* **15**, 550, doi:10.1186/s13059-014-0550-8 (2014).
70 Huang da, W., Sherman, B. T. & Lempicki, R. A. Systematic and integrative analysis of large gene lists using DAVID bioinformatics resources. *Nat Protoc* **4**, 44-57, doi:10.1038/nprot.2008.211 (2009).
71 Virtaneva, K. *et al.* Longitudinal analysis of the group A Streptococcus transcriptome in experimental pharyngitis in cynomolgus macaques. *Proc Natl Acad Sci U S A* **102**, 9014-9019, doi:10.1073/pnas.0503671102 (2005).
72 Schalkwijk, J. *et al.* Antimalarial pantothenamide metabolites target acetyl-coenzyme A biosynthesis in Plasmodium falciparum. *Sci Transl Med* **11**, doi:10.1126/scitranslmed.aas9917 (2019).
73 Cajka, T. & Fiehn, O. Increasing lipidomic coverage by selecting optimal mobile-phase modifiers in LC–MS of blood plasma. *Metabolomics* **12**, doi:10.1007/s11306-015-0929-x (2016).
74 Allman, E. L., Painter, H. J., Samra, J., Carrasquilla, M. & Llinas, M. Metabolomic Profiling of the Malaria Box Reveals Antimalarial Target Pathways. *Antimicrob Agents Chemother* **60**, 6635-6649, doi:10.1128/AAC.01224-16 (2016).
75 Tsugawa, H. *et al.* MS-DIAL: data-independent MS/MS deconvolution for comprehensive metabolome analysis. *Nat Methods* **12**, 523-526, doi:10.1038/nmeth.3393 (2015).
76 Li, H. Aligning sequence reads, clone sequences and assembly contigs with BWA-MEM. *arXiv* **1303.3997v1** (2013).
77 Marcais, G., Yorke, J. A. & Zimin, A. QuorUM: An Error Corrector for Illumina Reads. *PLoS One* **10**, e0130821, doi:10.1371/journal.pone.0130821 (2015).
78 Martin, M. Cutadapt removes adapter sequences from high-throughput sequencing reads. *EMBnet.journal* **17**, 10-12, doi:http://journal.embnet.org/index.php/embnetjournal/article/view/200 (2011).
79 Zerbino, D. R. in *Current Protocols in Bioinformatics* (ed A. D. Baxevanis) (John Wiley and Sons Ltd, 2010).
80 Rask, T. S., Hansen, D. A., Theander, T. G., Gorm Pedersen, A. & Lavstsen, T. Plasmodium falciparum erythrocyte membrane protein 1 diversity in seven genomes--divide and conquer. *PLoS Comput Biol* **6**, doi:10.1371/journal.pcbi.1000933 (2010).
81 Otto, T. D. *et al.* Evolutionary analysis of the most polymorphic gene family in falciparum malaria. *Wellcome Open Res* **4**, 193, doi:10.12688/wellcomeopenres.15590.1 (2019).
82 Otto, T. D. *et al.* Long read assemblies of geographically dispersed Plasmodium falciparum isolates reveal highly structured subtelomeres. *Wellcome Open Res* **3**, 52, doi:10.12688/wellcomeopenres.14571.1 (2018).

Figure Legends

Fig. 1 | *P. falciparum* persists during the dry season. a, Frequency of clinical malaria episodes every 2 days over 2 years in a cohort of ~600 subjects aged 3 months-45 years. Clinical malaria defined as axillary temperature ≥37.5°C, ≥2500 asexual parasites/μL of blood, and no other discernible cause of fever. **b**, Prevalence of subclinical *P. falciparum* detected by PCR in paired individuals (rows) at the beginning (Jan), middle (Mar), and end (May) of two consecutive dry seasons (2017 left, 2018 right). Columns are sorted such that the same individual is represented by each row at the three timepoints in each dry season. **c**, Age-stratified point prevalence of subclinical *P. falciparum* infection detected by PCR at the end of the dry season in May 2017 (left) and May 2018 (right). **d**, Parasite load detected by qRT-PCR (left) and flow cytometry (right) of RDT^+ subclinical children at the beginning (Jan), mid (Mar) and end (May) of the dry season and children with their first clinical malaria episode (MAL) in the wet season. Parasitaemia data represented as median ± IQR; Kruskal-Wallis test with multiple comparisons.

Fig. 2 | *P. falciparum* induces a minimal immune response during the dry season. a, C-reactive protein (CRP) (n=71May^-, 117 May^+), von Willebrand factor (vWF) (n=33 May^-, 51 May^+) and Hepcidin (n=41 May^-, 37 May^+) of paired plasma samples at the beginning (Jan) and end (May) of the dry season carrying *P. falciparum* (May+) or not (May^-). **b**, Plasma cytokines from children carrying or not (n= 21 May^+, 12 May^-) *P. falciparum* at the end of the dry season. **c**, Surface markers of frozen PBMCs from children that carried (May^+) or not (May^-) *P. falciparum* at the end of the dry season. **d**, Intracellular markers of fresh PBMCs from children carrying (May^+) or not (May^-) *P. falciparum* at the end of the dry season, (Supplementary Table 3). **e**, *P. falciparum*-specific $AMA1^+$ or $MSP1^+$ memory B cells (MBCs) in *P. falciparum* carriers or non-carriers (n=23 May^+, 28May^-) at the end of the dry season for class-switched (IgG^+ IGM^-) or non-class switched (IgG^- IGM^+) MBCs. **f**, Proportion of children with antibodies specific to PfEMP1 domains at the beginning and end of the dry season (n=106 Jan and May^-, 112 Jan and May^+). **g**, Magnitude of anti-PfEMP1 domains between the beginning and end of the dry season in children carrying or not subclinical *P. falciparum* (n=112 Jan and May^+, 106 Jan and May^-). **h**, Parasitaemia after invasion in complete or antibody-depleted plasma from children who carried or not (n= 29 May^+, 24 May^-) *P. falciparum* subclinical infections during the dry season. All data indicate median ± IQR; a, and f, One-way ANOVA with multiple comparisons correction b, ANOVA with Sidak multiple comparisons test. c, d, and h, Kruskal-Wallis test with multiple comparisons. e, Mann-Whitney test. g, slopes compared with a linear non-interaction model.

Fig. 3 | *P. falciparum* genetic diversity is maintained throughout the year. a, Number of *P. falciparum* clones in subclinical PCR+ children in beginning (Jan) and end (May) of the dry season, and first clinical malaria case (MAL) during the transmission season, determined by size differences in the polymorphic region of *msp2*. **b**, Proportion of individuals with different number of *P. falciparum* clones in the beginning (Jan) and end (May) of the dry season and clinical malaria cases (MAL). **c**, Size of the *msp2* alleles FC27 (left) and IC/3D7 (right) in beginning (Jan) and end (May) of the dry season, and clinical malaria cases (MAL). **d**, Prevalence of different *msp2* clone sizes of FC27 (left) and IC/3D7 (right) allelic families in Jan (n= 93), May (n= 93) and clinical malaria (MAL, n= 136); Mood's median test.

Fig. 4 | Transcriptome of circulating *P. falciparum* at the end of the dry season differs from malaria-causing *P. falciparum* during the transmission season. a, Principal components analysis and **b**, Unsupervised clustering analyses of RNA-Seq data of *P. falciparum* parasites collected at the end of the dry season and from clinical malaria cases (n= 12 May, 12MAL). **c**, Heatmap showing normalized reads of differentially expressed genes (DEGs) (rows) for each subject (columns) from *P. falciparum* collected at the end of the dry season (May) and at the first clinical malaria case (MAL) in the ensuing transmission season. **d**, RT-qPCR validation of RNA-Seq data for eight labelled DEGs (n= 24). *P* and r_2 determined by Pearson correlation. **e**, RT-qPCR validation of initial 24 RNA-Seq samples (left) and 18 additional samples (right) for three DEGs. Data indicate mean ± SD, Mann-Whitney test. **f**, Summary of KEGG pathways significantly enriched with DEGs. Blue bars indicate *P*adj for enrichment of each pathway. Grey dashed line indicates the threshold $P = 0.05$. Orange line indicates the percentage of genes in each pathway present in the DEG list. **g**, Heatmap showing normalized reads of DEGs involved in different metabolic pathways (rows) for each subject (columns) from *P. falciparum* at the end of the dry season and at the first clinical malaria (n= 12 May, 12MAL). **h**, Principal components analysis of target metabolites' data of plasmas from subclinical *P. falciparum* carriers at the end of the dry season and from clinical malaria cases (n= 12 May, 12MAL).

Fig. 5. | Replication of persistent dry season *P. falciparum* is not impaired. a, Parasitaemia fold change at 16, 24, 30 and 36 h post-culture of parasites collected from children at different times during the dry season (Jan, Mar and May) and clinical malaria case (MAL). Fold change is defined as %iRBC t(n)/ %iRBC t(n−1). Data indicate median ± IQR. Dashed line at fold change of 1. **b,** Giemsa-stained thin blood smears 16, 24, 36 or 48 h post-culture of *P. falciparum* parasites collected from children during the dry season (Jan, Mar and May) and clinical malaria case (MAL). Scale bar= 2 μm **c**, Time of highest increase in parasitaemia detected during in vitro culture of *P.*

falciparum parasites from children in Jan, Mar and May during the dry season, and clinical malaria case (MAL). Data indicate mean ± SD. Kruskal-Wallis with multiple comparisons test. **d**, Number of merozoites inside multinucleated schizonts determined by flow cytometry at the end of the dry season (May) and clinical malaria (MAL) samples. **e**, Maximum likelihood estimation (MLE) of the hours post-invasion of dry season (May) and clinical malaria (MAL) parasites. Data indicate mean ± SD; Mann-Whitney test. **f**, Giemsa-stained thick blood films of *P. falciparum* parasites collected straight from the arm of children, at the end of the dry season (May) and at their first clinical malaria (MAL). Scale bar= 5 µm. **g**, *P. falciparum* area measured from Giemsa-stained thick smears in subclinical infections at the end of the dry season (May) and in malaria cases (MAL) in the wet season. Data indicate median ± IQR; Mann-Whitney test.

Fig. 6 | Infected erythrocytes in circulation at the end of the dry season are at higher risk of splenic clearance. a, *P. falciparum* iRBCs filtration through beads mimicking the human spleen at 0, 18 and 30 h post culture at the end of the dry season and during clinical malaria (n= 8 May. 8 MAL) relative to the non-filtered same-time control. Flow-through % is defined as downstream %iRBCs / upstream %iRBCs) x 100. Data indicate mean ± SD. Dunn's multiple comparison test of the mean rank of each condition to 0h MAL, * shows $P < 0.001$. **b**, Percentage of circulating non-ring stage iRBCs at the end of the dry season and during malaria cases (n= 50 May, 39 MAL) determined by flow cytometry. Mean ± SD; Mann-Whitney test. **c**, Within-host dynamics simulation of growth rates and population sizes over five replication cycles of low-cytoadhering (left), and high-cytoadhering (right) parasites, stratified as circulating (red lines), cytoadhering (orange dashed lines) and total biomass (black lines). **d**, Simulation of circulating parasites' age distribution over two replication cycles after repeated sampling of low-cytoadhering parasites (Low), and high-cytoadhering parasites (High). **e**, Simulation of circulation and passage through the spleen of parasites aging over time, with low-cytoadhering (Low), and high-cytoadhering (High) parasites. **f**, Expression level of the highest expressed *var* gene at the end of the dry season and during a clinical malaria case (n= 8May, 10 MAL).

Extended Data Figure Legends

Extended Data Fig. 1 | Parasite density detected by thick blood smear of 17 individuals that presented malaria cases both in the dry season (January to May, MALdry) and in the ensuing

wet or malaria transmission season (June to December, MALwet) in the years on 2017 and 2018. Parasitaemia data indicates median ± IQR, Mann-Whitney test.

Extended Data Fig. 2 | Flow cytometry gating strategy to identify **a**, major leucocyte populations from frozen and fresh PBMCs (Surface staining) and fresh PBMCs intracellular content (Intracellular staining). **b**, *P. falciparum*-specific memory B cells in frozen PBMCs at the end of the dry season of children with or without subclinical *P. falciparum* infection.

Extended Data Fig. 3 | a, Proportions of NK subpopulations defined by CD56 and CD16 in children carrying (May$_+$) or not (May$_-$) *P. falciparum* at the end of the dry season. **b**, Proportion of *P. falciparum*-specific IgG$_+$ MBCs in classical, activated or atypical MBCs of *P. falciparum* carriers (May$_+$) or uninfected individuals (May$_-$) at the end of the dry season. **c**, Proportion of children with antibodies specific to PfEMP1 domains binding to unknown receptors at the beginning (Jan) and end (May) of the dry season (n=106 Jan and May$_-$, 112 Jan and May$_+$). **d**, Magnitude of IgG antibodies against PfEMP1 domains of B/A subtype between the beginning and end of the dry season in children carrying (May$_+$) or not (May$_-$) subclinical *P. falciparum* infection at the end of the dry season (n=106 Jan and May$_-$, 112 Jan and May$_+$) **e**, Breadth (left) and magnitude (right) of IgG reactivity to invasion-related antigens (Supplementary Table 11) at the end of the dry season in non-infected and subclinical children carrying *P. falciparum* (n=143 May$_-$, 139 May$_+$). Individual antigen reactivity (detailed in Portugal et al.[13]) of invasion-related antigens based on Cowman et al.[23]. Breadth is the number of antigens to which the level of IgG reactivity exceeds 2 SDs above the no DNA control. Magnitude is the sum of log2 -IgG intensity values for all antigens per sample. Boxes indicate median IQR, Tukey method. Mann-Whitney test. **f**, *P. falciparum* invasion ratio between merozoite invasion in antibody depleted plasma and merozoite invasion in paired complete plasma from subclinical carriers and non-infected children (n=28 May$_+$, 23 May$_-$), and malaria-naïve control (German adults' plasma, n=9).

Extended Data Fig. 4 | Volcano plots comparing the DEGs found in this study with the DEGs reported in two other studies [26,27] highlighted in yellow in the figure. Dots in blue represent the transcripts up-regulated (1131) and in red the transcripts down-regulated (476) in the dry season compared to clinical malaria samples. **a**, 141 DEGs previous reported in the comparison of transcriptomes of severe vs moderate malaria parasite physiological states were matched to the present study. 69 were not DEG in the dry season, 67 were upregulated and 5 were downregulated. **b**, 306 DEGs previous reported in the comparison of high vs low transmission

clinical malaria causing parasites were matched to the present study. 182 were not DEGs in the dry season, 103 were upregulated and 21 were downregulated.

Extended Data Fig. 5 | Expression patterns in 3D7 parasites along the ~48h intraerythrocytic developmental cycle (defined by Bozdech et al. PLoS Biology, 2003) of DEGs between *P. falciparum* of asymptomatic carriers at the end of the dry season (May) and at the first clinical malaria case (MAL) in the ensuing transmission season, assigned to **a.** Glycerophospholipid metabolism and **b.** Purine and Pyrimidine metabolism pathways by KEGG enrichment analysis using the DAVID tool.

Extended Data Fig. 6 | Modelled removal of infected RBCs from circulation by means of cytoadhesion and splenic clearance over the 48h replicative cycle, assuming the rate of removal increases with increasing expression of cytoadhering variant surface antigens, and where RBC modification by the parasite gradually increases the cell's rigidity and hence splenic retention.

Tables

Table 1 | Characteristics of study participants, clinical cases, and dry season asymptomatic infections stratified by year.

	all			MAL		May	
	n	female %	Age, y, mean (95% CI)	Malaria cases n	Age malaria case (y, 95% CI)	% Pf+ in May n	Age %Pf+ in May (y, 95% CI)
2017	604	46.7	11.2 (10.5 - 11.8)	398	9.4 (8.8 - 10.1)	13.4	13.3 (11.8 - 14.9)
2018	603	46.3	10.8 (10.1 - 11.5)	352	9.2 (8.5 - 10.0)	10.9	11.8 (10.0 - 13.6)

Table 2 | LARSFADIG motifs that identify PfEMP1 coding genes of 12 subclinical individuals at the end of the dry season (May) and 12 first clinical malaria episodes in the ensuing wet season (MAL).

	de novo assembly					Mapp		
SampleID	**total length in bp**	**# contigs**	**#LARSFADIG**	**Max expression**	**longest contig in bp**	**# varDB hits**	**Id of var gene with highest hit**	
May 9307	18,920	10	1	50	6,763	2,693	PF0159-C.g637	NTS-D
May 9308	9,624	5	1	37	5,348	14	PF0145-C.g513	NTS-D

May 9309	1,296	2	0	NA	670	13	PF0084-C.g173	NTS-D
May 9310	18,769	10	3	87	6,227	216	PF0043-C.g402	DBLd-C
May 9311	2,292	1	0	NA	2,292	14	PT0294-C.g1327	DBLa-C
May 9312	20,556	18	1	30	3,170	64	PF0051-C.g887	DBLa-C
May 9313	4,721	8	0	NA	2,292	6	PT0122-C.g1412	NTS-D
May 9314	39,049	28	2	66	9,011	248	PF0262-C.g611	DBLb-D
May 9315	5,824	3	1	307	4,176	193	PF0062-C.g430	NTS-D
May 9316	9,185	13	0	NA	3,400	121	PA0182-C.g826	NTS-D
May 9317	19,689	20	2	176	5,234	915	PM0098-C.g1086	NTS-D
May 9318	10,131	10	1	55	6,004	51	PF0417-C.g422	NTS-D
MAL 9319	173,674	133	24	159	10,423	1,299	PA0146-C.g1029	DBLd-C
MAL 9320	8,666	20	0	NA	2,208	66	PA0224-C.g312	DBLa-C
MAL 9321	23,668	12	2	1,263	9,564	1,149	PF0097-C.g294	NTS-D
MAL 9322	138,491	170	16	104	10,046	846	PA0092-C.g461	DBLd-C
MAL 9323	35,909	43	5	48	3,571	103	PA0253-C.g804	NTS-D
MAL 9324	43,517	56	5	27	4,626	136	PF0189-C.g397	DBLd-C
MAL 9325	3,849	1	0	NA	3,849	391	PF0801-C.g1202	DBLg-D
MAL 9326	113,437	87	17	71	8,812	785	QG0212-C.g1592	NTS-D
MAL 9327	11,330	14	2	109	4,225	82	PA0237-C.g706	NTS-D
MAL 9328	12,501	16	1	163	2,688	63	PF0228-C.g1045	CIDRa
MAL 9329	122,076	120	17	1,140	9,161	1,288	PA0167-C.g886	NTS-D
MAL 9330	106,347	87	13	85	11,752	420	PT0211-C.g738	NTS-D

818

819

Methods

Study subjects and Ethical approval

The Ethics Committee of Heidelberg University Hospital, the Faculty of Medicine, Pharmacy and Odontostomatology (FMPOS) at the University of Bamako, and the National Institute of Allergy and Infectious Diseases of the National Institutes of Health Institutional Review Board approved this study. Samples and clinical data were obtained in a cohort study conducted between 2011 and 2019 in Kalifabougou, Mali, a rural village where malaria transmission occurs from June through December. A single clinic and pharmacy provided the only access to antimalarial drugs. A detailed description of the study site and cohort design has been published elsewhere[43]. From an age-stratified, random sample of the village population, individuals aged 3 months to 45 years were enrolled. Written informed consent was obtained from all subjects and the parents/guardians of participating children. Exclusion criteria at enrolment consisted of haemoglobin concentration <7 g/dL, axillary temperature ≥37.5°C, acute systemic illness, or use of antimalarial or immunosuppressive medications in the preceding 30 days. Clinical malaria episodes were detected prospectively by passive surveillance and were defined by axillary temperature ≥37.5°C, ≥2500 asexual parasites/μL of blood, and no other cause of fever upon physical examination. Malaria episodes were treated with a standard 3-day course of artemether/lumefantrine according to national guidelines. Cross-sectional clinical visits and blood draws were performed at the beginning (January), mid (March) and end (May) of each dry season. The study is registered at ClinicalTrials.gov (identifier NCT01322581).

Sample collection

Dried blood spots on filter paper (Protein Saver 903, Whatman), thick blood smear and venous blood (4 or 8 mL depending if donor age was below or above 4 years old) were collected on dry season cross-sectional visits, and at their first malaria episode of the transmission season. Blood samples drawn by venepuncture were collected in sodium citrate-containing cell preparation tubes (Vacutainer CPT Tubes, BD) and transported to the laboratory where PBMCs, plasma and RBC pellet were separated by centrifugation and used freshly or stored at −80°C within three hours. Additional 2 mL of venous blood from RDT^+ individuals who tested at the end of the dry season (May 2012) cross-sectional[13], and from individuals at their first malaria episode of the ensuing transmission season, was collected into EDTA tubes (Vacutainer K3EDTA Tubes, BD) and processed directly at the field site. Plasma (used for metabolomic analysis) was separated by centrifugation and immediately frozen in liquid N_2. The buffy coat was discarded and leucocytes were removed from the RBC pellet in a two-step procedure; first

by density gradient on Lymphoprep solution (Fresenius Kabi), followed by Plasmodipur (EuroProxima) filtration, all according to the manufacturer instructions and as previously described[61]. RBCs pellets were then frozen in liquid N_2 and were later used for the RNA-Seq and RT-qPCR validation.

Detection of clinical malaria and subclinical *P. falciparum* infection

Thick blood smears were stained with Giemsa and *Plasmodium* parasites were counted against 300 leukocytes of all symptomatic participants presenting to the study clinic; parasite densities were recorded as the number of parasites/µL of whole blood based on a mean leukocyte count of 7500 cells/µL. Two expert microscopists evaluated each smear separately, and a third resolved discrepancies Subclinical infections during the dry season were detected at cross-sectional timepoints by RDT (SD BIOLINE Malaria Ag P.f test of histidine-rich protein II) with a sensitivity of ~100 parasites/µL[62]) once the blood was in the laboratory, and by Giemsa stained smear, and nested PCR amplification of *P. falciparum* DNA retrospectively as previously described[43] from filter papers (2017) and frozen red blood cell pellets (2018). The sensitivity of the nested PCR is ~0.5 - 1 parasites/µL[43].

***P. falciparum* quantification**

By flow cytometry, RBC pellets removed from CPT tubes after leucocyte isolation were washed and stained with 5x SYBR Green II (Invitrogen) and 7,5µM MitoTracker (Applied Biosystems) for 30 min at 37 °C. Cells were acquired using an LSR II and analysed using FlowJo software (Tree Star). By RT-qPCR, RNA was extracted immediately after thawing RBC pellets using TRIzol LS (Ambion) according to manufacturer instructions, and cDNA was synthesized using SuperScript IV VILO Master Mix with ezDNase (Invitrogen). RT-qPCR was run on a qTower (Analytik Jena) using Power SYBR Green PCR Master Mix (Applied Biosystems) with primers for the *P. falciparum* reference gene glycine-tRNA ligase (PF14_ 0198) (F: 5'TGAGTGATATGGATAATATAAAGGAACAAA3'; R: 5'GGATGATATTTCACAAAC GTATCT TTCT3') and for human GAPDH (F: 5'ACAACTTTGGTATCGTGGAAGG3'; R:5'GCCATCACGCCA CAGTTTC3').

Serologic analyses

C reactive protein, vWF and Hepcidin in human plasmas were detected through CRP human ELISA kit (Invitrogen), human vWF A2 Domain Sandwich ELISA (R&D Systems) and Hepcidin 25 ELISA kit (DRG Diagnostics) respectively, all according to the manufacturer instructions.

Results were measured using Cytation3 plate reader (BioTek). Milliplex Human Cytokine/Chemokine Magnetic Bead Panel 41-Plex kit (Merck) was used to measure circulating analytes in human plasma according to the manufacturer instructions, and read on a Bio-Plex 200 System (Bio-Rad). PfEMP1 domain antibody reactivity was measured using PfEMP1 domains covalently coupled beads following the method described by Cham *et al.,* 2008. PfEMP1 coupled beads were incubated with diluted plasma samples for 30 min, followed by incubation with human secondary F(ab')2 Goat Anti-Human IgG detection antibody for 30 min. The results were read on a Bio-Plex 200 System (Bio-Rad). The threshold for reactivity of each PfEMP1 domain was calculated with the average value of 21 German controls plus 3 standard deviations. Reactivity to PfEMP1 A, B and B/A subtypes was by determined by the fluorescence intensity of reactive individuals in the beginning (Jan) and end (May) of the dry season of subclinical carriers and non-infected individuals. Slopes of subclinical carriers and non-infected individuals were compared using a linear no interaction model.

Processing of PBMCs

PBMCs were isolated from the Vacutainer CPT Tubes (DB) according to the manufacturer instructions, and were either stained and analysed immediately, or frozen within 3 hours of the blood draw in FBS containing 7.5% DMSO (FBS: Gibco, DMSO: Sigma-Aldrich) The cells were first frozen at −80°C for 24 h, and then subsequently transferred to liquid N_2 for long term storage. For experiments where PBMCs were used from frozen vials, PBMCs were rapidly thawed in a 37°C water bath, washed with 10% heat-inactivated FBS in PBS followed by complete RPMI (RPMI 1640 supplemented with 10% heat-inactivated FBS, 1% penicillin/ streptomycin and 0,5% β-Mercaptoethanol). For each experiment, PBMCs from all individuals were thawed and assayed at the same time. The trypan blue dye exclusion assay consistently demonstrated >80% viability of PBMCs after thawing. Immediately after thawing or after washing if used fresh, 1 - $2x10_6$ PBMCs were incubated for 30 min at 4 °C with different combinations of the following fluorescently labelled surface antibodies: CD14-PE/BV71, CD16-BV421/BV605/BV711, CD19-PETexasRed/ BV421/PerCPcy5.5, CD21-FITC/PETexasRed/BV421/APC, CD27- FITC/PEcy7/AlexaFluor 700/BV421/BV650/APCcy7, CD3-BV510/BV711/PerCPcy5.5, CD4-FITC/PEcy5/APC, CD8-PEcy7/APCcy7, TCRγδ-PE, CD56-BV510/BV605. After fixing and permeabilizing the cells with FoxP3 Staining Buffer Set (eBioscience) according to the manufacturer instructions, PBMCs were stained for 30 min with fluorescently labelled intracellular antibodies: CD25-PEcy7, T-bet-PE Texas Red, IL-2-FITC,

Granzyme B-PE Texas Red, FCRL5-PE, Granzyme A-APC. Cells were acquired using a BD LSR II or LSR Fortessa flow cytometers (BD) and analysed using FlowJo software (Tree Star).

Flow cytometry with *P. falciparum*-specific B cell probes

Recently thawed PBMCs were stained with biotinylated recombinant *Pf*MSP1 and *Pf*AMA1 and then coupled to fluorescently labelled streptavidin (Hopp *et al*. *in preparation*), together with the following labelled monoclonal antibodies: CD3-BV510 (clone UCHT1), CD4-BV510 (clone SK3), CD8-BV510 (RPA-T8), CD14-BV510 (clone M5E2), CD16-BV510 (clone 3G8), CD56-BV510 (clone HCD56), CD10-BUV737 (clone Hi10a), IgD-BUV737 (clone IA-2), CD19-ECD (clone J3-119), CD21-PE-Cy7 (clone B-ly4), CD27-BV605 (clone M-T271), IgM-PerCP-Cy5.5 (clone G20-127) and IgG-AlexaFluor700 (clone G18-145). Aqua dead cell stain was added for live/dead discrimination (Thermo Fisher Scientific). Stained samples were run on a LSR Fortessa X20 (BD) and data were analysed using FlowJo (TreeStar). *Pf*MSP1 or *Pf*AMA1-specific MBCs were identified after exclusion of $CD3^+$ $CD4^+$ $CD8^+$ $CD14^+$ $CD16^+$ $CD56^+$ non-B cells, $CD10^+$ immature and IgD^- B cells. In order to increase the frequency of specific B cells detected in any given sample, PBMCs were stained simultaneously with *Pf*AMA1 and *Pf*MSP1 probes. Therefore, *Pf*AMA1 and *Pf*MSP1 probe-binding cells are indistinguishable by flow cytometry analysis and are referred to together as “Pf-specific” cells. Influenza hemagglutinin (HA) antigen was used as a non Pf-specific cells control.

***P. falciparum* culture**

3D7 *P. falciparum* parasites were maintained in fresh human O_{Rh+} erythrocytes at 5% haematocrit in RPMI 1640 complete medium (with L-glutamine and HEPES 7.4% Sodium Bicarbonate, 100µM Hypoxhantine (cc pro) and 25 mg/mL gentamycin (all Gibco)) added with 0.25% Albumax II (Gibco), at 37°C either in the presence of a gas mixture containing 5% O_2, 5% CO_2 and 90% N_2 or using the candle jar system described by Trager and Jensen 1976 method.

***P. falciparum* invasion assay**

3D7 *P. falciparum* parasites were cultured and regularly synchronized by the use of 5% sorbitol[63], and heparin to prevent re-invasion. At early schizont stage E64 compound (Sigma-Aldrich) was use to prevent merozoites egress, and later merozoites were purified through filtration as previously described[64]. Merozoites were cultured with non-infected RBCs and RPMI medium supplemented with 25% human plasma from different donors for 30 min to allow

955 invasion, and then RPMI medium supplemented with Albumax-II was provided to all parasites
956 for 30 h. iRBCs were fixed as previously described[65], stained with 5% SybrGreen and
957 successful invasion by merozoites was measured 30 h after invasion using FACS Canto II (BD)
958 and analysed using FlowJo software (Tree Star). Antibody depletion from human plasma was
959 achieved using Protein G and Protein L Plus Agarose beads (Pierce, Thermo Fisher Scientific).
960 Successful depletion was obtained after 3 incubations of plasma with the beads, and was
961 verified with a Ready-SET-Go! Elisa kit (eBioscience) measuring total IgG and IgM quantities in
962 the plasma before and after depletion read. Results were read on a Cytation3 plate reader
963 (BioTek).
964
965 ***Msp2* fragment analysis by capillary electrophoresis**
966 DNA was extracted from two 3-mm circular punches of blood spots on filter papers (Whatman
967 3M), using the DNeasy blood & tissue kit (Qiagen). Genotyping of *msp2* was performed using a
968 previously described nested PCR reaction[25]. The first PCR amplified the outer *msp2* domain (F:
969 5'ATGAAGGTAATTAAAACATTGTCTATTATA3' R: 5'CTTGTACACG GTACATTCTT3',,and the
970 second PCR used fluorescently labelled primers to identify two *msp2* allelic families: IC/3D7
971 (F: 5'AGAAGATGCAGAAAGAAKCCTYCTACT3' and R:5'GA
972 TGTAATCGGGGGATCAGTTTGTTCG 3'VIC) and FC27 (FC27 F: 5'AATACAAGAGGTGGG
973 CRATGC TCCA3' and R: 5'TTTTATTTGGTGCATTGCCAGAACTTGAAC3' 6-FAM). Fragment
974 analysis was performed by capillary electrophoresis using a DNA sequencer (3730, Applied
975 Biosystems) and analysed using GeneMapper 5 software (Thermo Fisher Scientific), where a
976 cut-off of 300 relative fluorescent units was set. Fragments were considered to be the same
977 allele within each allelic type if the size difference between them was less than 3 base pairs.
978
979 **Transcriptome analysis**
980 RNA was extracted from frozen RBC pellets using TRIzol (Ambion) as previously described[4]
981 was performed from RBC pellets that were frozen in liquid N_2 immediately after blood draw.
982 RNA quality was tested using a Bioanalyzer (Agilent). The average RIN value was 5.4 for the
983 dry season samples and 5.3 for the clinical malaria cases. The average Bioanalyzer yield was
984 27.4 ng on the dry season samples, while the clinical malaria cases average Bioanalyzer yield
985 was 25.0 ng. Twenty-four samples were selected based on parasitaemia, the highest 12 titres
986 for the wet and dry seasons. The RNA input going into NGS sample preparation ranged from
987 100 pg up to 100 ng. The samples were prepared for transcriptome analysis following a
988 previously described protocol[66] with minor modifications. Initially, samples were treated with

TURBO DNase as described. Following DNase treatment, the Agencourt RNAclean SPRI beads (Beckman Coulter) were resuspended in 19 µL to modify the protocol for a low input ribosomal RNA depletion step. Ribosomal RNA was depleted following the Clontech Modified Protocol for Removal of rRNA from Small Amounts of Total RNA (100 ng) using Human/Mouse/Rat Ribo-Zero Magnetic Kit (Epicentre). The purification beads were resuspended in 21 µL to proceed with the fragmentation step as described[66]. The first and second strand cDNA synthesis steps were followed without modification except for the final bead purification was eluted in 55 µL. Aliquots from the DNase, Ribo-zero treatment, and fragmentation were analysed on Agilent BioAnalyzer Pico RNA chips, along with the final cDNA constructs. The purified cDNA was below detectable levels of the BioAnalyzer Pico chips. 50 µL of purified cDNA were prepared for NGS sequencing using the KAPA Hyper Prep Kit (KAPA Biosystems). The adaptor stock concentration was 300 nM for the ligation with 4 h incubation at 20°C. The USER digestion step was omitted as the Hi-Fi polymerase does not amplify uracil containing products. The number of amplification cycles for PCR was determined to be 14 based on quantification of the amount of post-ligation product with a KAPA Quant Kit for Illumina Sequencing (KAPA Biosystems). The purified amplified libraries were visualized on Agilent DNA 1000 chips. Libraries were quantified using the KAPA Quant Kit for Illumina Sequencing (KAPA Biosystems) and normalized to 2 nM. The samples were pooled based on parasitaemias, denatured and diluted to 11 pM for cluster generation and paired-end 100 cycle sequencing on a HiSeq 2500 Rapid flow cell (Illumina) producing ~13 million reads per sample. Raw reads were trimmed of adapter sequence and low-quality bases and filtered for low quality reads using the FASTX-Toolkit. Remaining reads were mapped to the *P. falciparum* genome, build ASM276v1 using Hisat2[67]. Reads mapping to genes were counted using htseq-count[68]. For each sample, parasite age (hours post-invasion, hpi) was estimated based on gene expression using a previously described maximum likelihood method[28]. Differential expression analysis was performed using the Bioconductor package DESeq2[69], with adjusted *P*-values (*P*adj) < 0.05 considered significant. Differentially expressed genes (DEGs) were analysed for enrichment in gene ontology categories using DAVID[70]. RNA-Seq data (normalized counts data and raw sequencing reads) is available on NCBI GEO (project ID no. GSE148125). Validating RT-qPCR was performed on the 24 above-mentioned samples and on an extra set of 18 samples, 6 dry season and 12 clinical cases during the wet season. VILO cDNAs were synthesized using the SuperScript VILO cDNA synthesis kit (Invitrogen) and purified according to QIAquick 96-well protocol (Qiagen) with a modified centrifugation protocol[71]. Expression levels of 8 transcripts (sir2, rex3, Pfsec23, PFB0100c/KARHP, PF07_0006/STARP antigen, PFB0900c/PHISTc

GEX20, PF08_0020/UBE4B, MIF) were determined by RT-qPCR using Invitrogen Express qPCR SuperMix with premixed ROX reference dye (Invitrogen) in 20 µL reactions. All gene specific oligo sequences were designed using Beacon Designer software (Premier Biosoft) and purchased from LGC Biosearch technologies with double quencher BHQnova fluorescent probes due to AT-rich *P. falciparum* sequences (Supplementary Table 7). In a multiplex format we used reference gene glycine-tRNA ligase%2C putative (PF14_0198) and a standard made from pooled SPIA cDNA. RT-qPCR reactions were carried out at 95ºC for 2 min, and 55 cycles of 95ºC for 15 secs and 60ºC for 1 min. Data was analysed using the 7900HT version 2.4 sequence detection system software per the manufacturer's recommendations.

Metabolite profiling

Plasma metabolomics was performed using both targeted and untargeted approaches, across several LC-MS platforms, for small molecules and lipids, in order to obtain full metabolite coverage. Each plasma sample was split into two independent samples for metabolite extraction. For hydrophilic metabolites, 50 µL of plasma was extracted by the addition of 9X volumes of ice-cold methanol. Samples were briefly vortexed before centrifuging for 10 min to remove precipitated protein. The clarified supernatants were dried under N_2 gas and resuspended in 100 µL (1:2 dilution). Sample groups were pooled to create a group QA and all samples were pooled to create a batch QC, which were injected periodically throughout each run. The hydrophilic extracts were randomized and analysed using reversed-phase high-performance LC-MS by injecting 10 µL onto an ABSciex 5600 (QTOF) TripleTOF in positive ESI mode prior to injection on a Thermo Exactive Plus Orbitrap in negative ESI mode. Samples were separated on the ABSciex 5600 by reverse phase HPLC using a Prominence 20 UFLCXR system (Shimadzu) with a Waters (Milford) BEH C18 column (100 mm x 2.1 mm 1.7 µm particle size) maintained at 55°C and a 20 min aqueous acetonitrile gradient, at a flow rate of 250 µl/min. Solvent A was HPLC grade water with 0.1% formic acid and Solvent B was HPLC grade acetonitrile with 0.1% formic acid. The initial condition were 97% A and 3 % B, increasing to 45% B at 10 min, 75% B at 12 min where it was held at 75% B until 17.5 min before returning to the initial conditions. The eluate was delivered into a 5600 TripleTOF using a Duospray ion source (all AB Sciex). The capillary voltage was set at 4.5 kV in negative ion mode, with a declustering potential of 80 V. The mass spectrometer was operated in Information Dependent Acquisition mode with a 100 ms survey scan from 100 to 1200 m/z, and up to 20 MS/MS product ion scans (100 ms) per duty cycle using a collision energy of 50 V with a 20 V spread. Metabolite separation was performed on the Thermo Exactive Plus Orbitrap as previously described[72] using a Waters XSelect HSS T3 column (2.1 x

100 mm; 2.5 µm). For hydrophobic metabolites, 25 µL of plasma was extracted by the addition of 3X volumes of isopropanol. Samples were briefly vortexed and allowed to sit at room temperature for 10 min. Samples were then placed at -20°C to precipitate overnight. Precipitated samples were centrifuged for 20 min and the clarified supernatant was diluted to 50% water in a glass LCMS sample vial (1:6 dilution). Sample groups were pooled to create a group QA and all samples were pooled to create a batch QC, which were injected periodically throughout each run. The hydrophobic extracts were randomized and analysed using reversed-phase high-performance LC-MS by injecting 10 µL of sample onto an ABSciex 5600 TripleTOF in positive and negative ESI modes. Metabolite separation was performed as previously[73] using a Waters Acquity UPLC CSH C18 column (100 × 2.1 mm; 1.7 µm). Ammonium formate and formic acid were added to the positive ESI solvents and ammonium acetate was used for negative ESI. Targeted analysis of the Orbitrap data was performed as previously described[74]. Untargeted analysis from the 5600 TripleTOF was performed using the default settings in MS-DIAL[75]. The built-in databases were used for putative identification of metabolites at the MS/MS level. QA/QC samples were evaluated to minimize systematic/ technical issues. All data were normalized to the TIC and blank subtracted, to remove background noise, prior to statistical analysis.

P. falciparum field isolates short term culture

RBC pellets isolated from CPT tubes of RDT^+ samples in the dry season and of malaria cases' samples in the transmission season were cultures in fresh human O_{Rh+} erythrocytes at 7% haematocrit in complete RPMI supplemented with 0.25% Albumax II (Gibco) at 37°C in a candle jar for 36 or 48 h. Malaria cases' samples were cultured undiluted and diluted 1:10, 1:25 and 1:50 with non-infected blood, to assure that initial parasitaemia was low (0.5 - 1%) and that all cultures parasites could grow to their maximum potential. Parasitaemia and parasite development were assessed at 0, 16, 24, 30, 36 and 48 h in culture by thin blood smears and flow cytometry. Parasitaemia fold change was determined for each sample (ratio of %iRBCs at each timepoint over its preceding one). The time of highest increase of parasitaemia was the timepoint at which the ratio of %iRBCs at given timepoint over its preceding one was the highest for each sample. Progeny number was determined dividing SybrGreen fluorescence of multinucleated schizonts prior or at the time of the highest increase in parasitaemia in vitro, by the fluorescence of the smallest ring-stage population that sample presented. Fiji software was used to measure *P. falciparum* area.

Microsphiltration of _P. falciparum_ iRBCs

RBC pellets isolated from CPT tubes of RDT+ samples in the dry season and of malaria cases' samples in the transmission season were leucocyte depleted using EasySep CD45 depletion kit (STEMcell Technologies), according to manufacturer instructions. iRBCs were cultured in complete RPMI medium supplemented with Albumax, and microsphiltration was performed in triplicates at 0, 6, 18 and 30 h in culture as previously described[29]. Briefly, calibrated microspheres of 5-15 µm and 15-25 µm in diameter (Sn96.5% tin, 3% silver, 0.5% copper, Industrie des Poudres Sphériques) were mixed at 4 g each in 12 mL complete medium. Filter tips (ref 732-0534, VWR) were cut diagonally on the tip and wet by pushing 200 µL of complete medium through the filter. The bead suspension was vortexed and 400 µL were loaded onto the filter tips, yielding a 1.5 mm layer of microsphere beads. The tips were then filled up with medium and connected to a three-way stopcock. Microsphiltration tips were used within 12 h of preparation. At each timepoint, 600 µL of the 2% haematocrit culture was loaded onto the microbead layer and perfused with 5 mL complete medium at 1 mL/min using a syringe pump (AL-4000, World Precision Instruments). The upstream and downstream samples were collected at the different timepoints and stained for *P. falciparum* quantification by flow cytometry. Samples which parasitaemia increased (fold change > 1) between 0 and 30 h (May) or 0 and 48 h (MAL) were included in the analysis.

Simulation of *P. falciparum* cytoadhesion and splenic clearance

We developed a discrete-time within-host infection model to monitor parasite replication, cytoadhesion and splenic clearance in the absence of host immune responses. The parasite's 48 h life-cycle was divided into eight 6 h time steps and we assumed that the parasite population was fully synchronised. The dynamics of circulating, B_i, and cytoadhering parasites, V_i, are described through the following iterative scheme:

$$B_0^{t+1} = \gamma(B_8^t + V_8^t)$$

$$B_1^{t+1} = (1-\sigma_1)(1-\eta_1)B_0^{t+1}$$

$$V_1^{t+1} = \eta_1 B_0^{t+1}$$

$$B_i^{t+1} = (1-\sigma_i)(1-\eta_i)B_{i-1}^{t+1}, \quad \forall i \in [2,3,\dots,8]$$

$$V_i^{t+1} = \eta_i B_{i-1}^{t+1} + V_{i-1}^{t+1}, \quad \forall i \in [2,3,\dots,8],$$

where B_i^t and V_i^t are the numbers of circulating and cytoadhering parasites of age *i* and at time *t*, respectively. γ is the intrinsic parasite growth rate, i.e. the average number of newly infected red blood cells arising from a single infected cell. As seen from the above equations, only cytoadhering and freely circulating iRBC replicate and contribute to parasite population growth,

whereas the spleen is assumed to remove retained parasites. Removal of infected red blood cells from circulation by means of cytoadhesion, η_i, and splenic clearance, σ_i, is assumed to be dependent on the age of the parasite, *i*, where the rate of removal increases as the parasite starts to express cytoadhering variant surface antigens, PfEMP1, shortly after invasion, and where RBC modification by the parasite gradually increases the cell's rigidity and hence splenic retention. Both removal functions are given by the following sigmoidal forms

$$\sigma_i = \sigma(\mathrm{i}) = \frac{\sigma_{max}}{1 + e^{p_\sigma \times (T_\sigma - i)}}$$

$$\eta_i = \eta(i) = \kappa \frac{\eta_{max}}{1 + e^{p_\eta \times (T_\eta - i)}}$$

and are visualised in Extended Data Fig. 6. σ_{max} and η_{max} are the maximum removal rates by the spleen and cytoadhesion, respectively. $p_{\sigma,\eta}$ and $T_{\sigma,\eta}$ are the shape and location parameters of the sigmoidal functions, were T determines the age at which 50% of the parasites are removed. The factor $\kappa \in [0,1]$ is included to investigate the effect of cytoadhesion on the within-host growth dynamics. All parameters and values used are listed in Supplementary Table 12.

PfEMP1 genes expression

To exclude human reads, all reads were mapped against the human genome (hg19), using bwa mem[76] (-k 32). Reads and their pair that did not map the human genome were used further. Reads were correct with quorum[77], parameter -k 35. Adapters were trimmed with cutadapt [78], using the TruSeq LT adapter sequences. To assemble the *var* genes, the RNA-Seq sequencing reads (fastq files) were first assembled with the pipeline recently published in Otto *et al* [31]. Due to the variable coverage of the sequence reads, the results were not satisfactory. Therefore, an older approach was used to assemble all the non-human sequencing reads with velvet[79], following parameters: Kmer 41, exp_cov 999999999, ins_length 420, cov_cutoff 5, ins_length_sd 30, min_pair_count 5. Different k-mer were tested and k-mer of 41 returned the best results. The obtained contigs were annotated and the domains were called as previously described[31]. For each *var* genes domains and subdomains were annotated as defined by Rask *et al* (vardom [80]). The expression per *var* gene was calculated with two methods. In both methods the reads back with bwa mem were mapped against the assemblies. In the first method, the number of mapped reads was counted on *var* genes larger than 3.5k and normalised by the length of the *var* genes and the number of reads mapped against all contigs, similar to RPKM. In the second method the coverage over the middle of the LARSFADIG motifs

(samtools depth) was addressed. These values were divided by the number of reads mapped on each assembly and multiplied with 10 million. As a complementary validation, a mapping approach was used: the sequencing reads were mapped using bwa mem, parameter -k 31 -a (to allow multiple hits), against a combined database of *var* genes from Otto *et al*[81] (varDB.fulldataset.1kb.nt.fasta.gz) and the *var* genes from Otto et al[82], limited to *var* genes of the length of at least 3kb. Next, the number of reads mapped with an AS score of at least 95 against the *var* genes from this combined database were counted.

Statistical analysis

Mann-Witney or Kruskal-Wallis were used to test for differences in between two or more groups respectively. Differences between No. of clones, and clones' sizes were tested by Mood's median test. PfEMP1 slopes between the beginning and the end of the dry season of subclinical carriers and non-infected individuals were compared using a linear non -interaction model. A spearman rank correlation between linear RT-qPCR normalized data and linear RNA-Seq normalized data of each gene was obtained along with p-values using GraphPad Prism 8.0 software. Metabolites significant differences were determined by a 2-way ANOVA corrected for multiple comparison controlling for an FDR of 0.05%. Statistical significance was defined as a 2-tailed *P*-value of ≤ 0.05. All analyses were performed with GraphPad Prism versions 6.0 or 8.0, JMP 14.0.1, or R.

Data availability

RNA-Seq data (normalized counts data and raw sequencing reads) have been deposited in NCBI's Gene Expression Omnibus and are accessible through GEO Series accession number GSE148125 (https://www.ncbi.nlm.nih.gov/geo/query/acc.cgi?acc=GSE148125

All processed metabolomics spectral data and analytical metadata from this study have been deposited into the international repository for metabolomics data and metadata NIH Metabolomics Workbench (Study number from Metabolomics Workbench: ST001384).

The data file of assembled *var* gene fragments of all isolates are available at: https://github.com/ThomasDOtto/varDB/tree/master/Otherdatasets/Andrade_DryWet2020

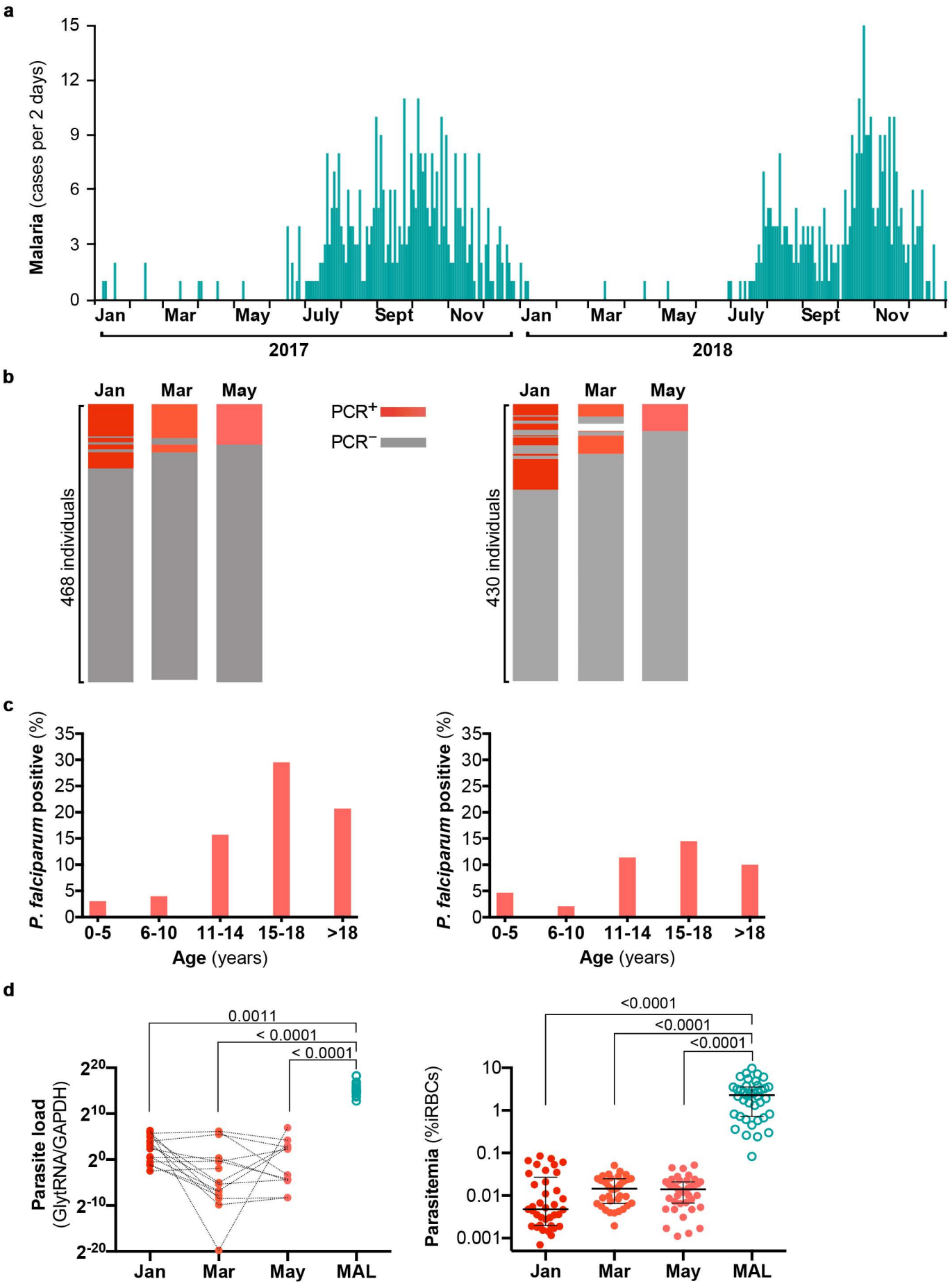
a
Malaria (cases per 2 days)
15
12
9
6
3
0
Jan
Mar
May
July
Sept
Nov
Jan
Mar
May
July
Sept
Nov
2017
2018
b
Jan
Mar
May
PCR+
PCR−
468 individuals
Jan
Mar
May
430 individuals
c
P. falciparum positive (%)
35
30
25
20
15
10
5
0
0-5
6-10
11-14
15-18
>18
Age (years)
P. falciparum positive (%)
35
30
25
20
15
10
5
0
0-5
6-10
11-14
15-18
>18
Age (years)
d
Parasite load
(GlytRNA/GAPDH)
2^20
2^10
2^0
2^-10
2^-20
0.0011
< 0.0001
< 0.0001
Jan
Mar
May
MAL
Parasitemia (%iRBCs)
10
1
0.1
0.01
0.001
<0.0001
<0.0001
<0.0001
Jan
Mar
May
MAL

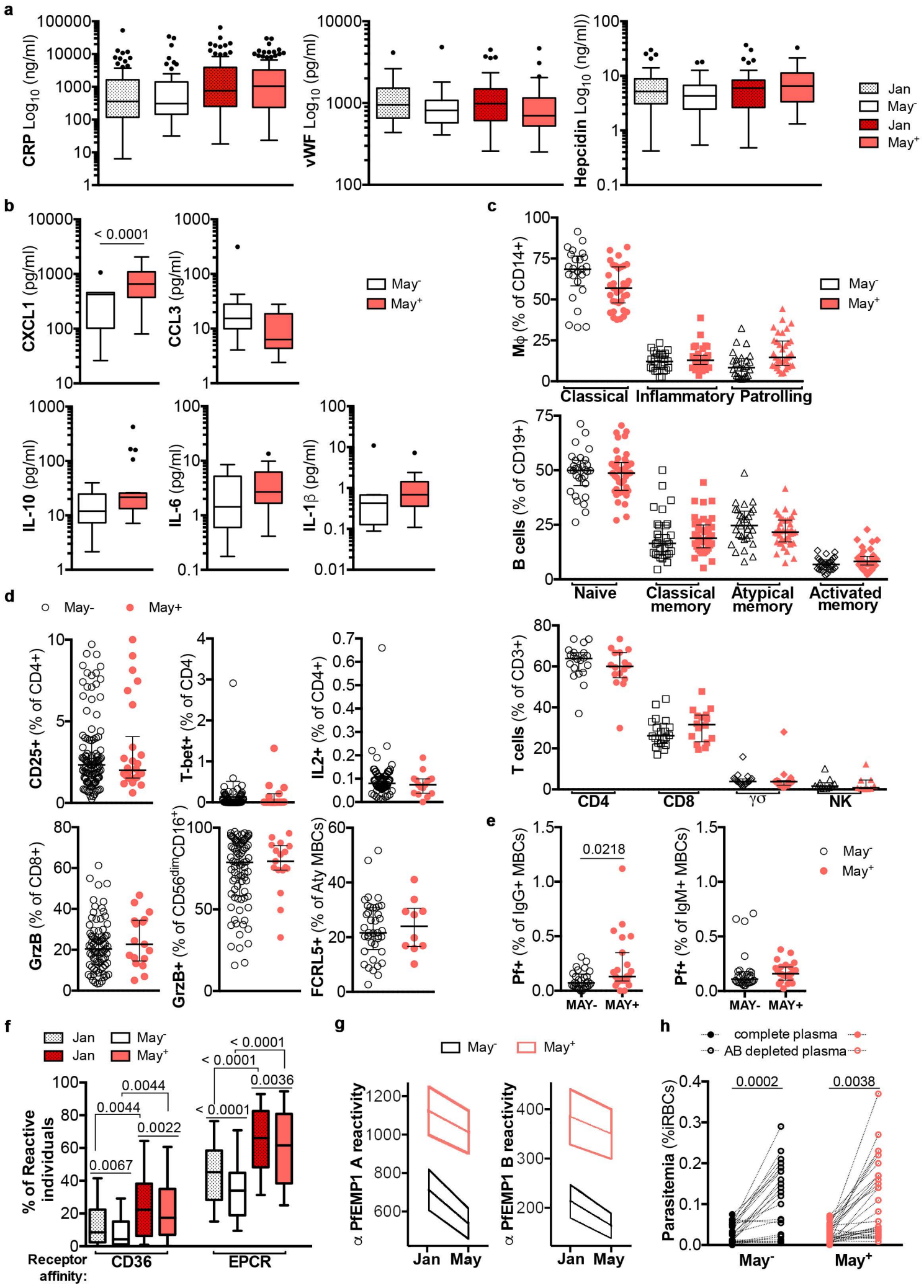
a
CRP Log10 (ng/ml)
vWF Log10 (pg/ml)
Hepcidin Log10 (ng/ml))
Jan
May-
Jan
May+
b
CXCL1 (pg/ml)
< 0.0001
CCL3 (pg/ml)
IL-10 (pg/ml)
IL-6 (pg/ml)
IL-1β (pg/ml)
May-
May+
c
Mϕ (% of CD14+)
Classical
Inflammatory
Patrolling
B cells (% of CD19+)
Naive
Classical memory
Atypical memory
Activated memory
d
May-
May+
CD25+ (% of CD4+)
T-bet+ (% of CD4)
IL2+ (% of CD4+)
T cells (% of CD3+)
CD4
CD8
γσ
NK
GrzB (% of CD8+)
GrzB+ (% of CD56dimCD16+)
FCRL5+ (% of Aty MBCs)
e
Pf+ (% of IgG+ MBCs)
0.0218
Pf+ (% of IgM+ MBCs)
MAY-
MAY+
f
Jan
May-
Jan
May+
% of Reactive individuals
0.0044
0.0044
0.0022
0.0067
< 0.0001
< 0.0001
0.0036
< 0.0001
Receptor affinity:
CD36
EPCR
g
May-
May+
α PfEMP1 A reactivity
α PfEMP1 B reactivity
Jan
May
h
complete plasma
AB depleted plasma
Parasitemia (%iRBCs)
0.0002
0.0038
May-
May+

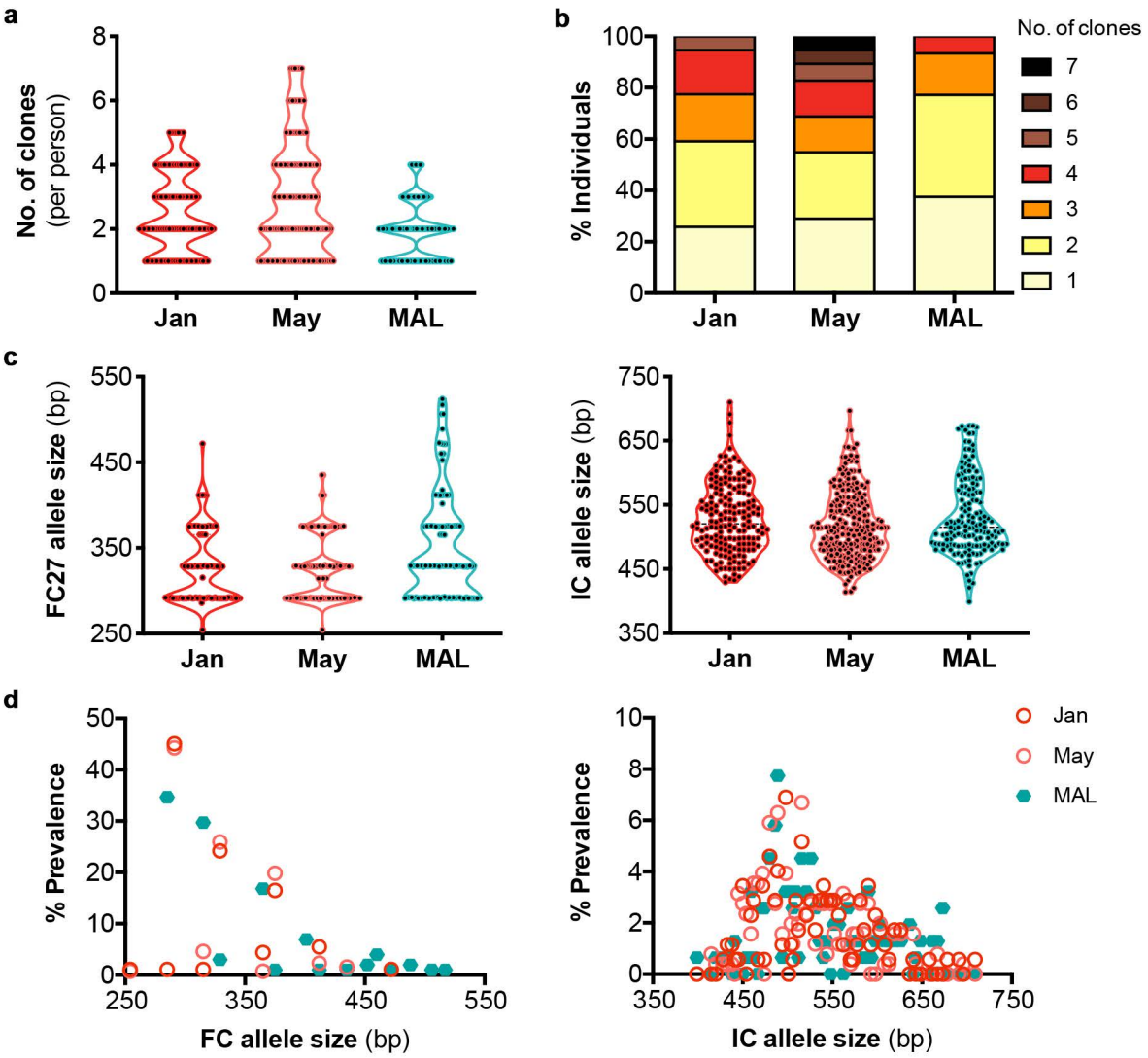
a
No. of clones (per person)
8
6
4
2
0
Jan
May
MAL
b
% Individuals
100
80
60
40
20
0
No. of clones
7
6
5
4
3
2
1
Jan
May
MAL
c
FC27 allele size (bp)
550
450
350
250
Jan
May
MAL
IC allele size (bp)
750
650
550
450
350
Jan
May
MAL
d
% Prevalence
50
40
30
20
10
0
250
350
450
550
FC allele size (bp)
% Prevalence
10
8
6
4
2
0
350
450
550
650
750
IC allele size (bp)
Jan
May
MAL

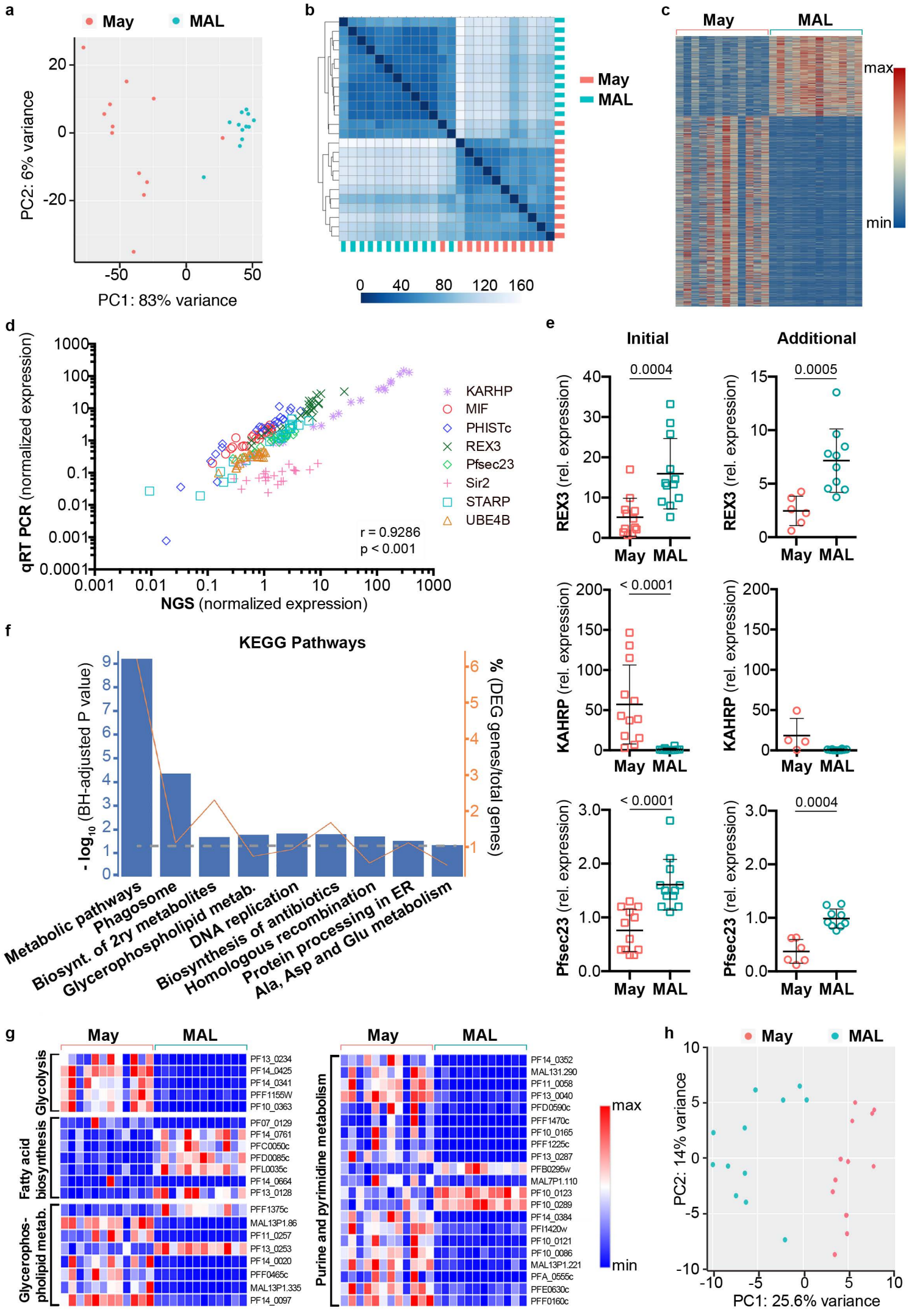
a
May
MAL
PC2: 6% variance
PC1: 83% variance
b
May
MAL
0 40 80 120 160
c
May
MAL
max
min
d
qRT PCR (normalized expression)
NGS (normalized expression)
r = 0.9286
p < 0.001
KARHP
MIF
PHISTc
REX3
Pfsec23
Sir2
STARP
UBE4B
e
Initial
Additional
REX3 (rel. expression)
0.0004
0.0005
KAHRP (rel. expression)
< 0.0001
Pfsec23 (rel. expression)
< 0.0001
0.0004
May MAL
f
KEGG Pathways
- log10 (BH-adjusted P value)
% (DEG genes/total genes)
Metabolic pathways
Phagosome
Biosynt. of 2ry metabolites
Glycerophospholipid metab.
DNA replication
Biosynthesis of antibiotics
Homologous recombination
Protein processing in ER
Ala, Asp and Glu metabolism
g
May
MAL
Glycolysis
PF13_0234
PF14_0425
PF14_0341
PFF1155W
PF10_0363
Fatty acid biosynthesis
PF07_0129
PF14_0761
PFC0050c
PFD0085c
PFL0035c
PF14_0664
PF13_0128
Glycerophos-pholipid metab.
PFF1375c
MAL13P1.86
PF11_0257
PF13_0253
PF14_0020
PFF0465c
MAL13P1.335
PF14_0097
Purine and pyrimidine metabolism
PF14_0352
MAL131.290
PF11_0058
PF13_0040
PFD0590c
PFF1470c
PF10_0165
PFF1225c
PF13_0287
PFB0295w
MAL7P1.110
PF10_0123
PF10_0289
PF14_0384
PFI1420w
PF10_0121
PF10_0086
MAL13P1.221
PFA_0555c
PFE0630c
PFF0160c
max
min
h
May
MAL
PC2: 14% variance
PC1: 25.6% variance

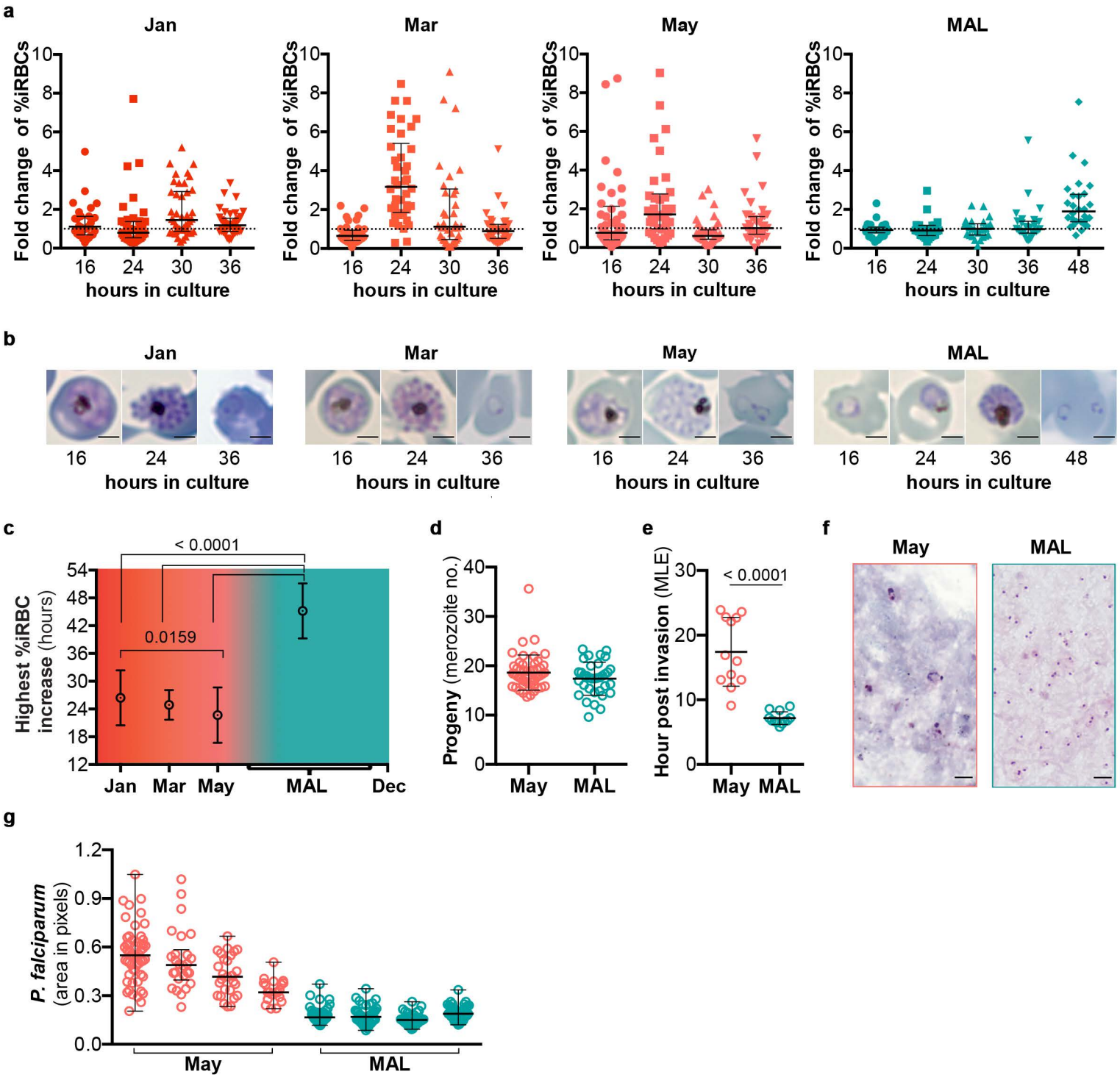
a
Jan
Mar
May
MAL
Fold change of %iRBCs
hours in culture
b
c
Highest %iRBC increase (hours)
< 0.0001
0.0159
Jan
Mar
May
MAL
Dec
d
Progeny (merozoite no.)
e
Hour post invasion (MLE)
< 0.0001
f
g
P. falciparum (area in pixels)

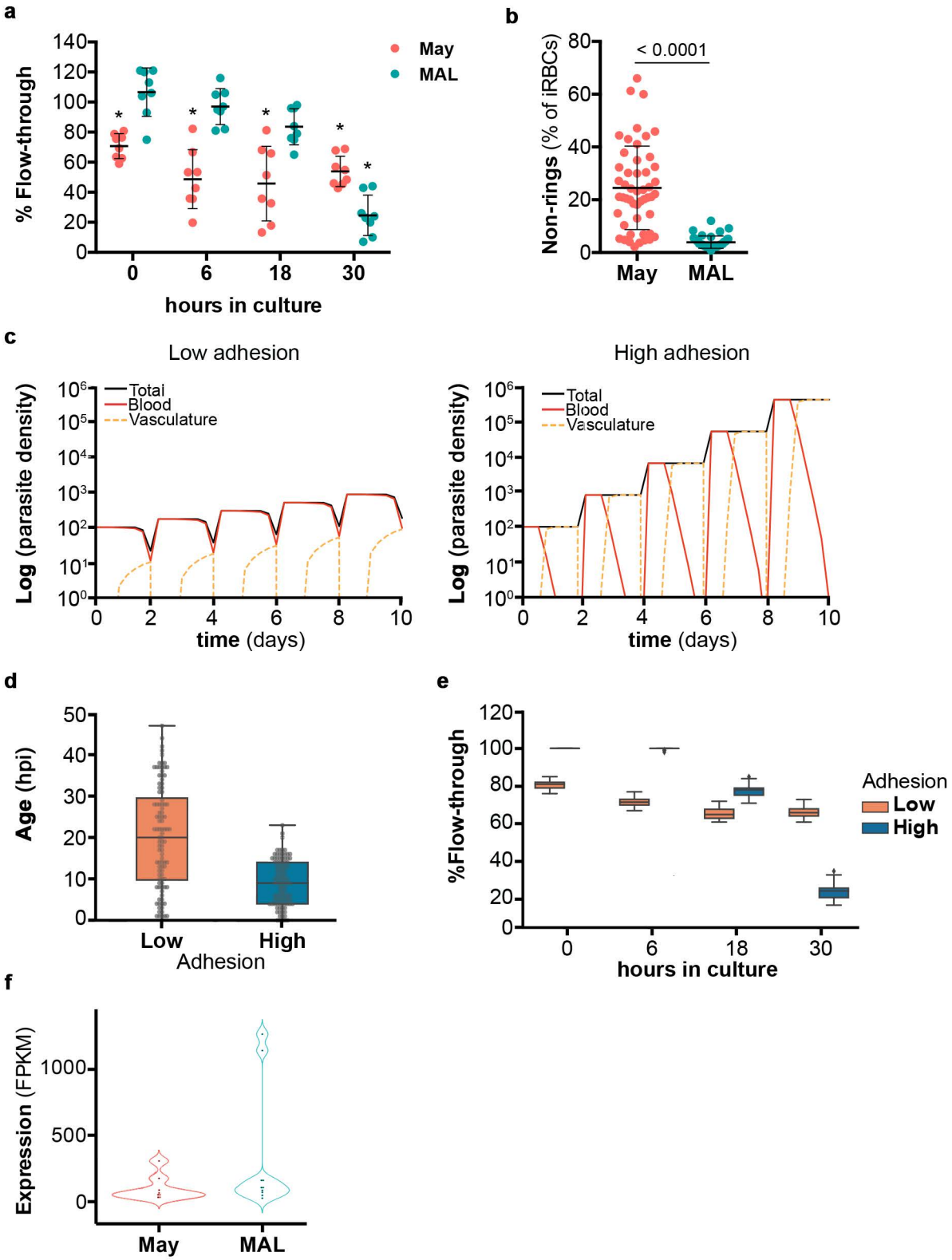
a
% Flow-through
May
MAL
hours in culture
b
Non-rings (% of iRBCs)
< 0.0001
May
MAL
c
Low adhesion
High adhesion
Log (parasite density)
Total
Blood
Vasculature
time (days)
d
Age (hpi)
Low
High
Adhesion
e
%Flow-through
Adhesion
Low
High
hours in culture
f
Expression (FPKM)
May
MAL

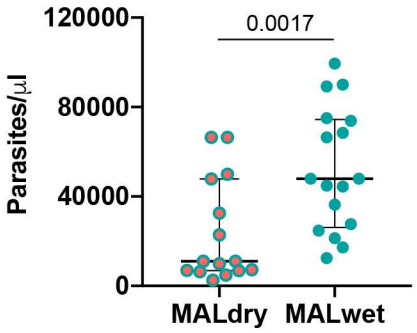
120000
80000
40000
0
Parasites/μl
0.0017
MALdry
MALwet

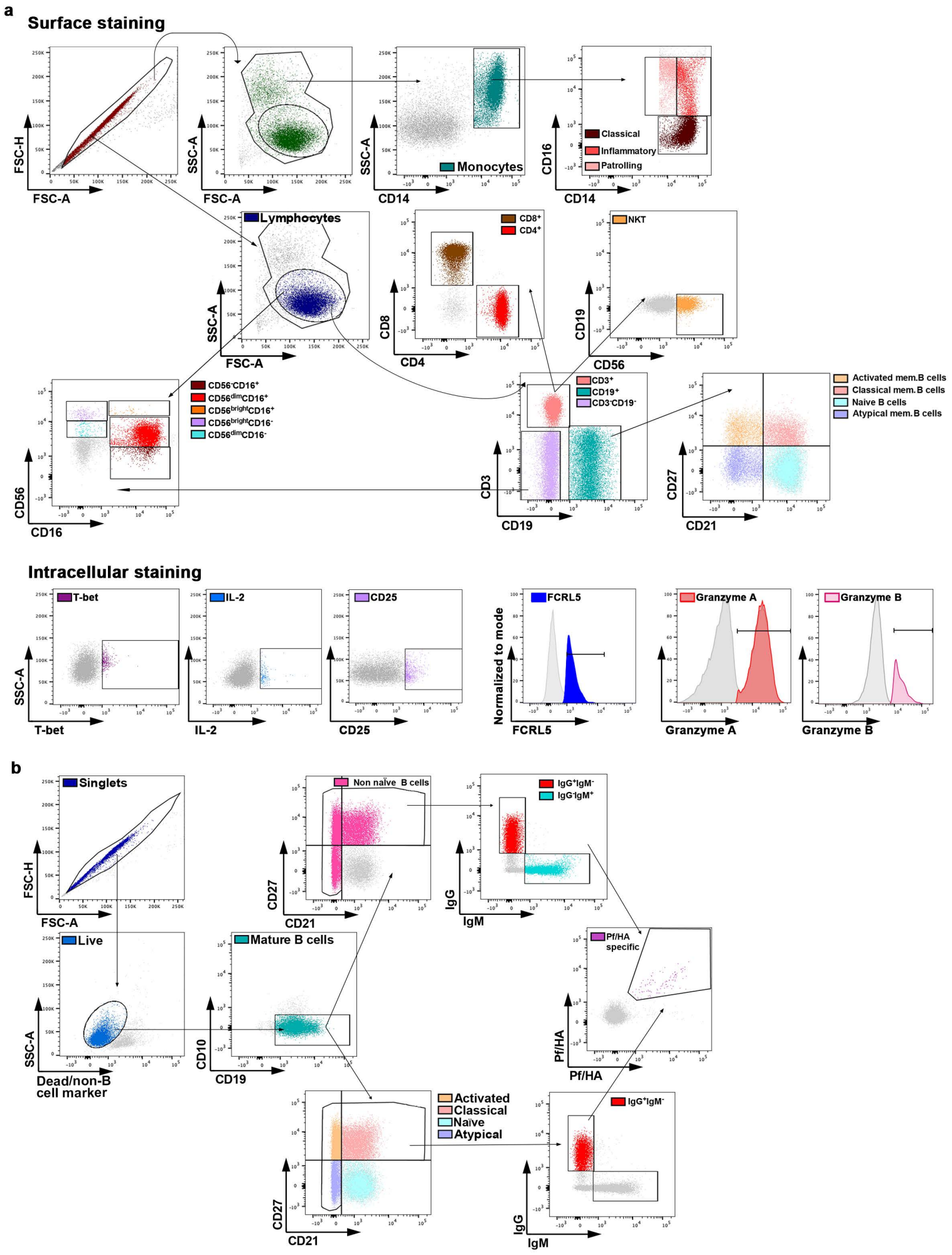
a
Surface staining
FSC-H
FSC-A
SSC-A
FSC-A
SSC-A
CD14
Monocytes
CD16
CD14
Classical
Inflammatory
Patrolling
Lymphocytes
SSC-A
FSC-A
CD8
CD4
CD8+
CD4+
CD19
CD56
NKT
CD56
CD16
CD56-CD16+
CD56dimCD16+
CD56brightCD16+
CD56brightCD16-
CD56dimCD16-
CD3
CD19
CD3+
CD19+
CD3-CD19-
CD27
CD21
Activated mem.B cells
Classical mem.B cells
Naive B cells
Atypical mem.B cells
Intracellular staining
T-bet
SSC-A
T-bet
IL-2
IL-2
CD25
CD25
FCRL5
Normalized to mode
FCRL5
Granzyme A
Granzyme A
Granzyme B
Granzyme B
b
Singlets
FSC-H
FSC-A
Non naïve B cells
CD27
CD21
IgG+IgM-
IgG-IgM+
IgG
IgM
Live
SSC-A
Dead/non-B cell marker
Mature B cells
CD10
CD19
Pf/HA specific
Pf/HA
Pf/HA
Activated
Classical
Naïve
Atypical
CD27
CD21
IgG+IgM-
IgG
IgM

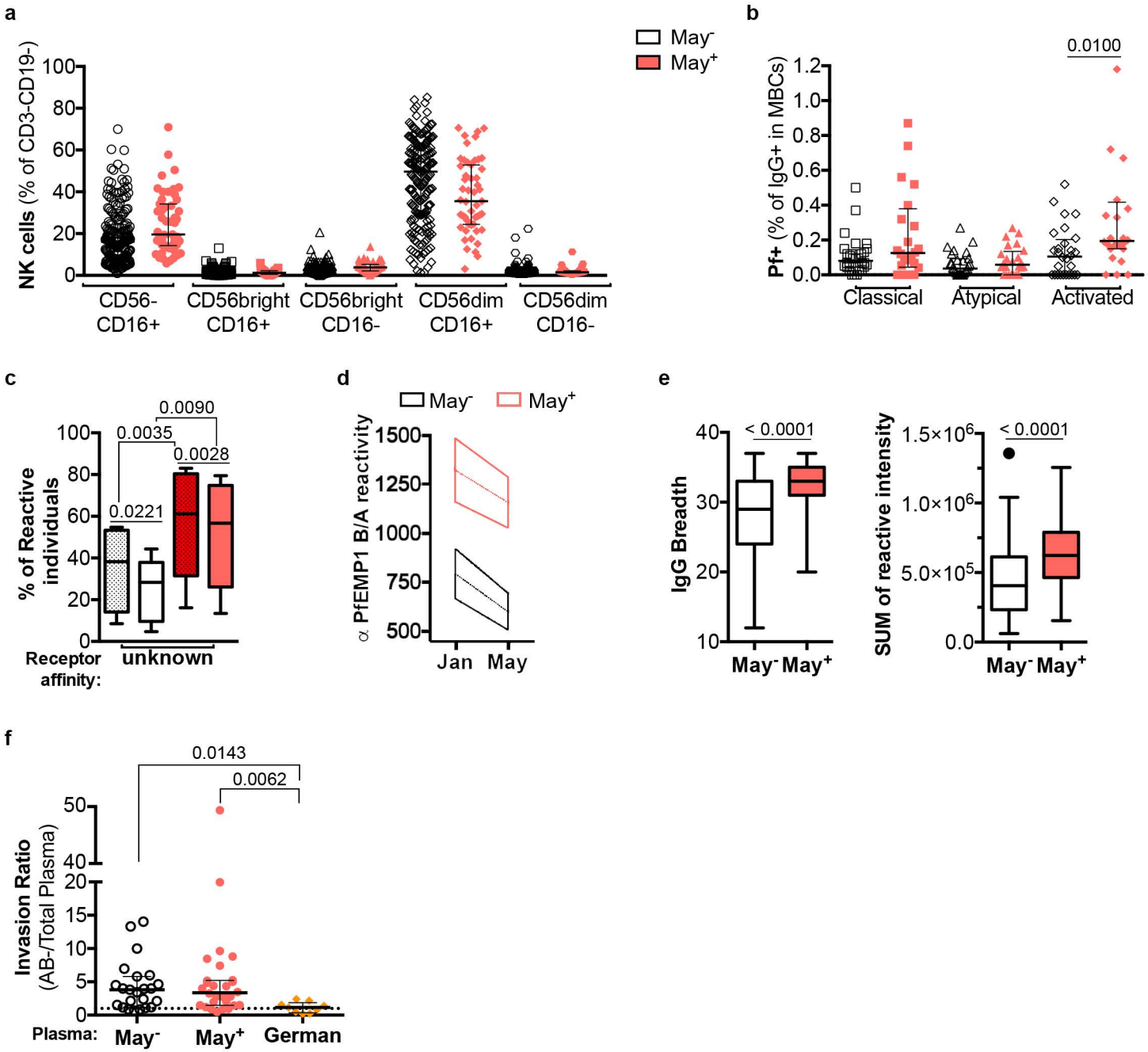
a
May-
May+
NK cells (% of CD3-CD19-)
100
80
60
40
20
0
CD56-
CD16+
CD56bright
CD16+
CD56bright
CD16-
CD56dim
CD16+
CD56dim
CD16-
b
0.0100
Pf+ (% of IgG+ in MBCs)
1.2
1.0
0.8
0.6
0.4
0.2
0.0
Classical
Atypical
Activated
c
0.0090
0.0035
0.0028
0.0221
% of Reactive individuals
100
80
60
40
20
0
Receptor affinity:
unknown
d
May-
May+
α PfEMP1 B/A reactivity
1500
1250
1000
750
500
Jan
May
e
< 0.0001
IgG Breadth
40
30
20
10
May-
May+
< 0.0001
SUM of reactive intensity
1.5×10^6
1.0×10^6
5.0×10^5
0.0
May-
May+
f
0.0143
0.0062
Invasion Ratio (AB-/Total Plasma)
50
40
20
15
10
5
0
Plasma:
May-
May+
German

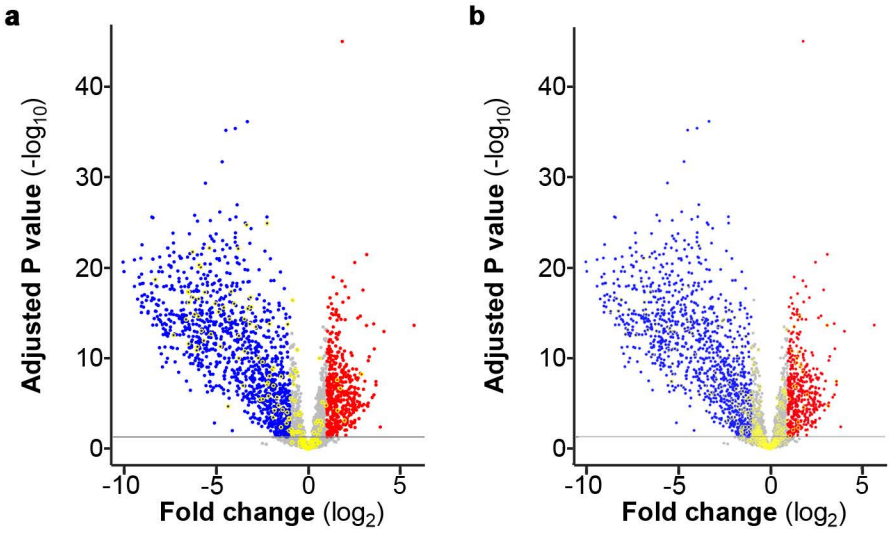
a
b
Adjusted P value (-log10)
Fold change (log2)
40
30
20
10
0
-10
-5
0
5

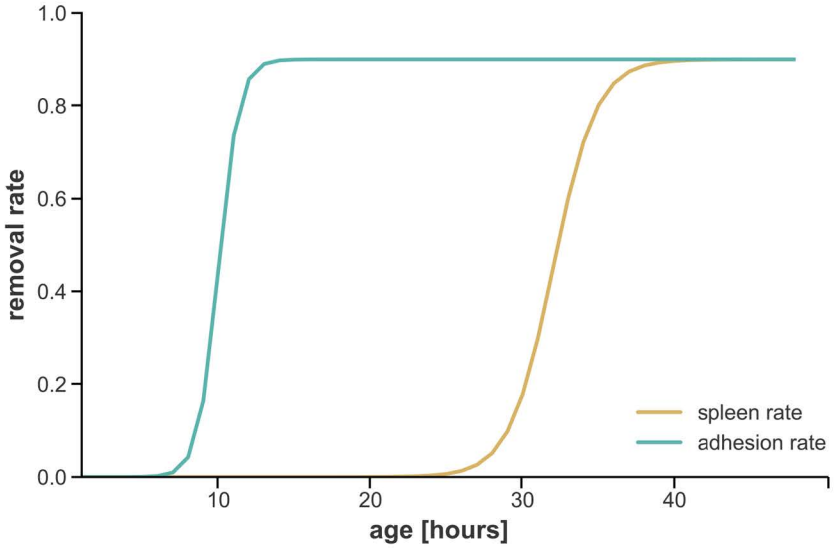
1.0
0.8
0.6
0.4
0.2
0.0
removal rate
10
20
30
40
age [hours]
spleen rate
adhesion rate

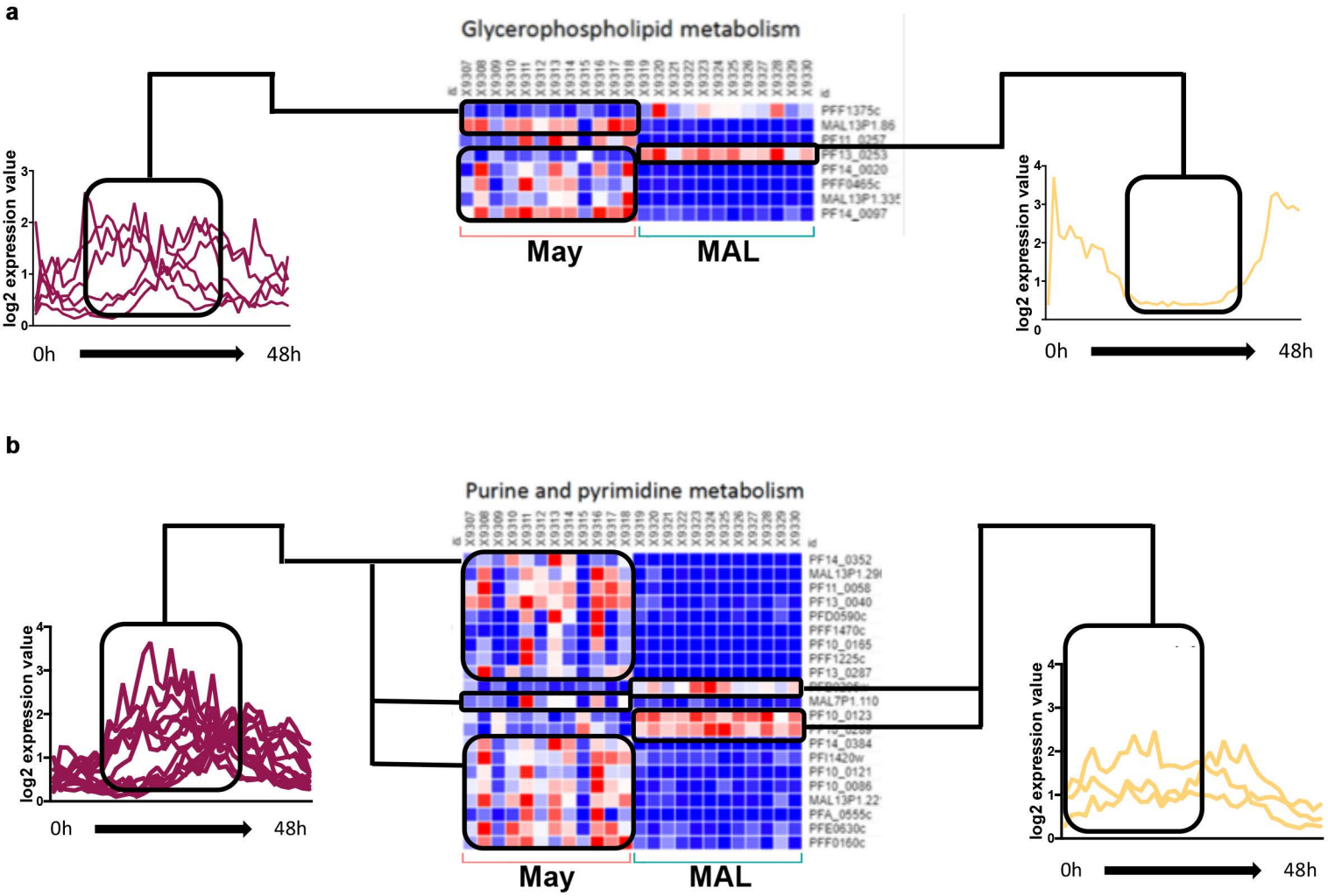
a
Glycerophospholipid metabolism
log2 expression value
0h
48h
May
MAL
PFF1375c
MAL13P1.86
PF13_0253
PF14_0020
PFF0465c
PF14_0097
log2 expression value
0h
48h
b
Purine and pyrimidine metabolism
log2 expression value
0h
48h
May
MAL
PF14_0352
PF11_0058
PF13_0040
PFD0590c
PFF1470c
PF10_0165
PFF1225c
PF13_0287
MAL7P1.110
PF10_0123
PF14_0384
PFI1420w
PF10_0121
PF10_0086
PFA_0555c
PFE0630c
PFF0160c
log2 expression value
0h
48h

Supplementary table 1: Contingency tables with PCR data from beginning and end of the dry season of 2017 and 2018 used to calculate the odds ratio of maintaining the same infection status through the entire dry season

	Neg May17	Pos May17	
Neg Jan17	365	7	372
Pos Jan17	35	61	96
	400	68	468

Odds ratio 2017: 90.88 (CI: 38.63;213.82)

	Neg May18	Pos May18	
Neg Jan18	331	6	337
Pos Jan18	52	41	93
	383	47	430

Odds ratio 2018: 43.5 (CI: 17.46 , 107.54)

Supplementary Table 2. Multiplex bead array quantification of cytokines and chemokines in the plasma children with (May+) or without (May-) persisting *P. falciparum* at the end of the dry season. (n=12 May- and n=21 May+).

Cytokine	**May-** Median (Interquartile range)	May+ Median (Interquartile range)	Adjusted P Value
CXCL1 (GRO)	421.4 (102.2 - 455.8)	656.3 (374.8 - 1095)	**< 0,0001**
CXCL10 (IP10)	202.4 (71.52 - 245.2)	137.3 (107.4 - 383.8)	0,2705
CCL2 (MCP1)	134.1 (103.1 - 280.8)	252.4 (154.1 - 356.8)	0,9973
CCL22 (MDC)	465.6 (220.9 - 817.7)	400.1 (288.5 - 624.5)	0,9991
sCD40L	166.9 (91.06 - 439.7)	181.3 (77.97 - 514.1)	0,9997
CCL3 (MIPa)	15.41 (9.91 - 28)	6.33 (4.35 - 18.69)	> 0.9999
CCL4 (MIP1b)	14.37 (11.49 - 25.77)	16.47 (14.08 - 25.65)	> 0.9999
CCL7 (MCP3)	3.86 (2.45 - 6.95)	2.65 (1.98 - 3.91)	> 0.9999
EGF	7.72 (3.26 - 18.96)	11.35 (3.99 - 21.3)	> 0.9999
Eotaxin	12.59 (11.63 - 15.99)	15.45 (11.9 - 26.76)	> 0.9999
FGFa	7.82 (4.53 - 10.26)	2.74 (1.99 - 4.24)	> 0.9999
Fractaline	5.09 (4.10 - 7.78)	5.58 (4.75 - 12.16)	> 0.9999
GCFS	178.9 (42.32 - 755.2)	185.9 (65.12 - 542.7)	> 0.9999
GMCSF	0.53 (0.34 - 1.26)	1.5 (0.73 - 2.65)	> 0.9999
IFNa2	2.72 (0.91 - 6.64)	5.73 (3.80 - 14.1)	> 0.9999
IFNy	0.84 (0.51 - 2.84)	2.07 (0.64 - 3.21)	> 0.9999
IL1a	10.26 (6.18 - 30.8)	18.16 (5.39 - 34.62)	> 0.9999
IL1b	0.43 (0.13 - 0.68)	0.69 (0.36 - 1.43)	> 0.9999
IL-2	1.86 (1.32 - 2.60)	1.92 (1.53 - 2.59)	> 0.9999
IL-3	0.36 (0.23 - 0.45)	0.41 (0.25 - 0.69)	> 0.9999
IL-6	1.66 (0.81 - 15.63)	2.68 (1.67 - 6.24)	> 0.9999
IL-7	2.42 (1.18 - 49.67)	3.47 (1.25 - 8.30)	> 0.9999
IL-8	18.7 (14.5 - 76.06)	44.99 (22.13 - 122.6)	> 0.9999
IL-9	2.64 (0.73 - 7.38)	2.80 (0.97 - 11.84)	> 0.9999
IL12P40	5.32 (0.40 - 15.76)	9.972 (3.62 - 17.51)	> 0.9999
IL13	1.11 (0.17 - 9.57)	0.57 (0.23 - 97)	> 0.9999
IL15	1.61 (1.33 - 4.87)	1.76 (1.47 - 2.57)	> 0.9999
IL-10	10.23 (7.23 - 24.33)	21.53 (13.28 - 25.77)	> 0.9999
IL-17	1.59 (1.57 - 1.62)	1.61 (1.58 - 1.76)	> 0.9999
IL1RA	1.02 (0.58 - 6.65)	2.52 (1.05 - 8.07)	> 0.9999
TGFb	1.18 (0.86 - 1.66)	1.58 (1.23 - 3.09)	> 0.9999
VEGF	3.46 (1.29 - 8.54)	3.46 (1.20 - 13.14)	> 0.9999

(shown are Adjusted P values calculated through Sidak's multiple comparisons test)

Supplementary Table 3. Expression of surface and intracellular markers of freshly collected PBMCs from children that carried *P. falciparum* parasites (May+) or remained uninfected (May-) during the dry season.

Parameter	n	n May-	May- Mean (SD)	n May+	May+ Mean (SD)	p value	Significant?	test
CD3 (% of Lymphocytes)	252	201	71.72 (8.54)	51	73.75 (7.61)	0,074	No	Mann-Whitney
CD4 (% of CD3 T cells)	235	188	61.9 (6.54)	47	63.63 (5.62)	>0,9999	No	Kruskal-Wallis
CD8 (% of CD3 T cells)	252	201	29.52 (5.61)	51	28.68 (5.4)	>0,9999	No	Kruskal-Wallis
NKT cells (% of CD3 T cells)	252	201	2.659 (1.81)	51	2.15 (1.21)	>0,9999	No	Kruskal-Wallis
Granzyme B (% of CD8 T cells)	97	80	22.2 (12.66)	17	24.51 (12.69)	>0,9999	No	Kruskal-Wallis
Granzyme B (% of NKT cells)	97	80	43.02 (21.75)	17	44.92 (22.59)	>0,9999	No	Kruskal-Wallis
Granzyme B (Geo Mean of CD8 T cells)	97	80	3399 (3169)	17	3294 (2149)	>0,9999	No	Kruskal-Wallis
Granzyme B (Geo Mean of NKT cells)	97	80	18733 (19005)	17	13471 (14620)	>0,9999	No	Kruskal-Wallis
T-bet (% of CD4 T cells)	76	61	0.13 (0.38)	15	0.1656 (0.3477)	>0,9999	No	Kruskal-Wallis
T-bet (% of CD8 T cells)	80	62	3.13 (4.64)	18	2.31 (3.795)	>0,9999	No	Kruskal-Wallis
T-bet (% of NKT cells)	80	62	4.86 (7.85)	18	3.65 (6.19)	>0,9999	No	Kruskal-Wallis
T-bet (Geo Mean of CD4 T cells)	74	59	2577 (6708)	15	1879 (1293)	>0,9999	No	Kruskal-Wallis
T-bet (Geo Mean of CD8 T cells)	77	59	1327 (212.6)	18	1571 (677.4)	0,141	No	Kruskal-Wallis
T-bet (Geo Mean of NKT cells)	74	57	1424 (327.4)	17	1533 (411.2)	0,453	No	Kruskal-Wallis
IL2 (% of CD4 T cells)	84	68	0.094(0.084)	16	0.076 (0.047)	>0,9999	No	Kruskal-Wallis
IL2 (% of CD8 T cells)	92	72	0.081(0.067)	20	0.082 (0.061)	>0,9999	No	Kruskal-Wallis
IL2 (% of NKT cells)	92	72	3.01(3.58)	20	3.03 (5.40)	>0,9999	No	Kruskal-Wallis
CD25 (% of CD4 T cells)	133	107	3.0 (2.30)	26	3.27 (2.74)	>0,9999	No	Kruskal-Wallis
CD25 (% of CD8 T cells)	144	114	0.03 (0.034)	30	0.026 (0.020)	>0,9999	No	Kruskal-Wallis
CD25 (% of NKT cells)	144	114	0.52 (0.51)	30	0.48 (0.44)	>0,9999	No	Kruskal-Wallis
CD25 (Geo Mean of CD4 T cells)	133	107	2846 (424.2)	26	2769 (438.6)	>0,9999	No	Kruskal-Wallis
CD25 (Geo Mean of CD8 T cells)	119	94	3615 (6454)	25	2981 (1753)	0,604	No	Kruskal-Wallis
CD25 (Geo Mean of NKT cells)	137	109	4710 (4167)	28	4378 (2489)	>0,9999	No	Kruskal-Wallis
IL2 (Geo Mean of CD4 T cells)	82	67	5534 (1913)	15	5374 (1551)	>0,9999	No	Kruskal-Wallis
IL2 (Geo Mean of CD8 T cells)	91	71	5262 (1705)	20	5118 (1355)	>0,9999	No	Kruskal-Wallis
IL2 (Geo Mean of NKT cells)	91	72	6113 (5387)	19	5407 (2237)	>0,9999	No	Kruskal-Wallis
CD19 (% of Lymphocytes)	249	198	15.85 (3.98)	51	16.84 (4.45)	0,241	No	Mann-Whitney
Activated MBCs (% of CD19 B cells)	225	177	3.52 (2.0)	48	4.86 (2.87)	0,704	No	Kruskal-Wallis
Classical MBCs (% of CD19 B cells)	225	177	14.47 (6.09)	48	12.92 (5.11)	>0,9999	No	Kruskal-Wallis
Naive (% of CD19 B cells)	225	177	70.7 (9.2)	48	68.1 (9.8)	>0,9999	No	Kruskal-Wallis
Atypical MBCs (% of CD19 B cells)	225	177	11.34 (5.51)	48	14.1 (6.41)	0,423	No	Kruskal-Wallis
FCRL5 (% of Activated MBCs)	50	40	19.32 (8.31)	10	22.36 (10.62)	>0,9999	No	Kruskal-Wallis
FCRL5 (% of Classical MBCs)	50	40	2.06 (1.45)	10	2.61 (2.29)	>0,9999	No	Kruskal-Wallis
FCRL5 (% of Naive MBCs)	50	40	0.46 (0.61)	10	0.63 (0.57)	>0,9999	No	Kruskal-Wallis
FCRL5 (% of Atypical MBCs)	50	40	22.94 (10.59)	10	24.17(9.66)	>0,9999	No	Kruskal-Wallis
Granzyme B (% of Activated MBCs)	97	80	24.05 (20.02)	17	22.79 (19.61)	>0,9999	No	Kruskal-Wallis
Granzyme B (% of Classical MBCs)	97	80	6.13 (10.71)	17	9.4 (14.57)	>0,9999	No	Kruskal-Wallis
Granzyme B (% of Naive MBCs)	97	80	2.43 (5.52)	17	3.73 (8.18)	>0,9999	No	Kruskal-Wallis
Granzyme B (% of Atypical MBCs)	97	80	6.84 (11.36)	17	7.62 (11.67)	>0,9999	No	Kruskal-Wallis
IL2 (Geo Mean ofActivated MBCs)	91	72	841.4 (281)	19	954 (281.6)	0,649	No	Kruskal-Wallis
IL2 (Geo Mean ofClassical MBCs)	91	72	754.6 (249.7)	19	864 (243.3)	0,348	No	Kruskal-Wallis
IL2 (Geo Mean ofNaive MBCs)	91	72	557.8 (175.5)	19	632.5 (174.4)	0,580	No	Kruskal-Wallis
IL2 (Geo Mean ofAtypical MBCs)	91	72	648.7 (202.6)	19	775.2 (230.9)	0,148	No	Kruskal-Wallis
Granzyme B (Geo Mean of Activated MBCs)	96	80	4121 (3791)	16	3773 (3121)	>0,9999	No	Kruskal-Wallis
Granzyme B (Geo Mean of Classical MBCs)	97	80	2359 (2015)	17	2564 (2019)	>0,9999	No	Kruskal-Wallis
Granzyme B (Geo Mean of Naive MBCs)	97	80	1851 (1500)	17	1899 (1565)	>0,9999	No	Kruskal-Wallis
Granzyme B (Geo Mean of Atypical MBCs)	97	80	2231 (2087)	17	2207 (1771)	>0,9999	No	Kruskal-Wallis
CD25 (Geo Mean of Activated MBCs)	91	72	88.82 (34.49)	19	100.6 (25.79)	>0,9999	No	Kruskal-Wallis
CD25 (Geo Mean of Classical MBCs)	91	72	163.4 (29.63)	19	168.5 (21.83)	>0,9999	No	Kruskal-Wallis
CD25 (Geo Mean of Naive MBCs)	91	72	57.71 (16.91)	19	50.82 (10.1)	>0,9999	No	Kruskal-Wallis
CD25 (Geo Mean of Atypical MBCs)	91	72	38.51 (10.56)	19	42.23 (10.08)	>0,9999	No	Kruskal-Wallis
CD56-CD16+ (% of CD3-CD19-	249	198	18.83 (13.22)	51	24.77 (14.38)	>0,9999	No	Kruskal-Wallis
CD56dimCD16- (% of CD3-CD19-)	249	198	1.95 (2.24)	51	1.99 (1.72)	>0,9999	No	Kruskal-Wallis
CD56dimCD16+ (% of CD3-CD19-	249	198	45.73 (19.98)	51	37.86 (17.53)	>0,9999	No	Kruskal-Wallis
CD56brightCD16- (% of CD3-CD19-)	249	198	3.03 (2.26)	51	4.00 (2.47)	0,766	No	Kruskal-Wallis
CD56brightCD16+ (% of CD3-CD19-	249	198	1.4 (1.55)	51	1.52 (1.14)	>0,9999	No	Kruskal-Wallis
Granzyme A (% of CD56-CD16+)	50	40	32.05 (28.37)	10	12.63 (12.04)	0,256	No	Kruskal-Wallis
Granzyme A (% of CD56dimCD16-)	50	40	17.02 (15.51)	10	8.92 (5.98)	>0,9999	No	Kruskal-Wallis
Granzyme A (% of CD56dimCD16+)	50	40	35.02 (25.13)	10	18.71 (17.21)	0,780	No	Kruskal-Wallis
Granzyme A (% of CD56brightCD16-)	50	40	7.71 (9.69)	10	3.61 (5.98)	>0,9999	No	Kruskal-Wallis
Granzyme A (% of CD56brightCD16+)	50	40	19.05 (18.66)	10	10.6 (15.33)	0,444	No	Kruskal-Wallis
Granzyme B (% of CD56-CD16+)	97	80	54.99 (21.82)	17	54.35 (21.6)	>0,9999	No	Kruskal-Wallis
Granzyme B (% of CD56dimCD16-)	97	80	16.45 (11.94)	17	15.72 (11.77)	>0,9999	No	Kruskal-Wallis
Granzyme B (% of CD56dimCD16+)	97	80	72.86 (21.37)	17	77.09 (16.52)	>0,9999	No	Kruskal-Wallis
Granzyme B (% of CD56brightCD16-)	97	80	6.038 (7.042)	17	7.82 (7.589)	>0,9999	No	Kruskal-Wallis
Granzyme B (% of CD56brightCD16+)	97	80	24.72 (25.01)	17	20.92 (16.2)	>0,9999	No	Kruskal-Wallis
MΦ(CD14 +) (% of PBMCs)	234	187	6.356(4.591)	47	5.68 (3.97)	0,464	No	Mann-Whitney
Classical MΦ (% CD14 +)	234	187	73.92(13.3)	47	69 (19.78)	>0,9999	No	Kruskal-Wallis
Inflammatory MΦ (% of CD14 +)	234	187	12.83 (7.75)	47	13.15 (9.171)	>0,9999	No	Kruskal-Wallis
Patrolling MΦ (% of (CD14 +)	234	187	12.21 (8.95)	47	17.01 (14.87)	0,763	No	Kruskal-Wallis
Activated (% of B cells)	52	28	3.827 (2.126)	24	8.807 (6.443)	0,1209	No	Kruskal-Wallis
Classical (% of B cells)	52	28	19.5 (6.028)	24	17.75 (4.915)	>0,9999	No	Kruskal-Wallis
Atypical (% of B cells)	52	28	9.866 (3.702)	24	14.4 (6.849)	0,5455	No	Kruskal-Wallis
Naive (% of B cells)	52	28	66.8 (7.496)	24	59.05 (14.19)	>0,9999	No	Kruskal-Wallis
Pf specific (IgM+ of non-naive mature B cells)	52	28	0.1765 (0.1833)	24	0.1753 (0.09002)	0,1046	No	Mann-Whitney
HA specific (IgM+ of non-naive mature B cells	52	28	0.05646 (0.05032)	24	0.04124 (0.02893)	0,5074	No	Mann-Whitney
Pf specific (IgG+ of non-naive mature B cells)	52	28	0.1005 (0.08167)	24	0.237 (0.2624)	0,0218	Yes	Mann-Whitney
HA specific (IgG+ of non-naive mature B cells	52	28	0.163 (0.1773)	24	0.09068 (0.06453)	0,1151	No	Mann-Whitney
Pf specific (% IgG+ of Classical)	52	28	0.1098 (0.1107)	24	0.2724 (0.3818)	0,6448	No	Kruskal-Wallis
Pf specific (% IgG+ of Atypical)	52	28	0.0615 (0.06772)	24	0.08229 (0.08235)	>0,9999	No	Kruskal-Wallis
Pf specific (% IgG+ of Activated)	52	28	0.1297 (0.1439)	24	0.3593 (0.3929)	0,01	Yes	Kruskal-Wallis
HA specific (% IgG+ of Classical)	52	28	0.1306 (0.1008)	24	0.0773 (0.0575)	0,3174	No	Kruskal-Wallis
HA specific (% IgG+ of Activated)	52	28	0.313 (0.779)	24	0.08079 (0.09381)	>0,9999	No	Kruskal-Wallis
HA specific (% IgG+ of Atypical)	52	28	0.1906 (0.1914)	24	0.1117 (0.12)	0,3054	No	Kruskal-Wallis

Supplementay Table 4. Different domain types of the VSA multigene family var, which were grouped according to their endothelial-receptor affinity (CD36, EPCR or unknown receptor) and PfEMP1 UPS type (A, B or B/A) and non-VSA controls.

Protein name	CIDR domain class	PfEMP1 group	Binding phenotype	Genome/ Isolate	PfEMP1
CIDRα6_IT4var12_IT4	α6	B	CD36	IT4	IT4var12
CIDRα5_IT4var14_IT4	α5	B	CD36	IT4	IT4var14
CIDRα2.2_IT4var24_IT4	α2.2	B	CD36	IT4	IT4var24
CIDRα3.3_IT4var26_IT4	α3.3	B	CD36	IT4	IT4var26
CIDRα2.10_IT4var30_IT4	α2.10	B	CD36	IT4	IT4var30
CIDRα2.4_IT4var33_IT4	α2.4	B	CD36	IT4	IT4var33
CIDRα2.9_IT4var45_IT4	α2.9	B	CD36	IT4	IT4var45
CIDRα2.7_IT4var61_IT4	α2.7	B	CD36	IT4	IT4var61
CIDRα3.1_DD2var01_DD2	α3.1	B	CD36	DD2	DD2var01
CIDRα3.1_HB3var27_HB3	α3.1	B	CD36	HB3	HB3var27
CIDRα3.1_IT4var21_IT4	α3.1	B	CD36	IT4	IT4var21
CIDRα3.5_IT4var15_IT4	α3.5	B	CD36	IT4	IT4var15
CIDRα1.4_HB3var03_HB3	α1.4	A	EPCR	HB3	HB3var03
CIDRα1.1_IT4var20_IT4	α1.1	B/A	EPCR	IT4	IT4var20
CIDRα1.4_IT4var7_IT4	α1.4	A	EPCR	IT4	IT4var7
CIDRα1.1_igh_var19_IGH	α1.1	B/A	EPCR	IGH	igh_var19
CIDRα1.1_raj116_var8_raj116	α1.1	B/A	EPCR	raj116	raj116_var8
CIDRα1.5a_1965_2_1965	α1.5a	A	EPCR	1965	1965_2
CIDRα1.5a_GA013_ERS010323	α1.5a	A	EPCR	ERS010323	GA013
CIDRα1.5a_GA014_ERS010022	α1.5a	A	EPCR	ERS010022	GA014
CIDRα1.5b_1918_5_1918	α1.5b	A	unknown	1918	1918_5
CIDRα1.5b_1983_13_1983	α1.5b	A	unknown	1983	1983_13
CIDRα1.6a_HB3var02_HB3	α1.6a	A	EPCR	HB3	HB3var02
CIDRα1.6b_GA018_ERS010570	α1.6b	A	EPCR	ERS010570	GA018
CIDRα1.6b_GA019_ERS010031	α1.6b	A	EPCR	ERS010031	GA019
CIDRα1.7_1965_8_1965	α1.7	A	EPCR	1965	1965_8
CIDRα1.7_1918_3_1918	α1.7	A	EPCR	1918	1918_3
CIDRα1.7_GA024_ERS010438	α1.7	A	EPCR	ERS010438	GA024
CIDRα1.8a_Ga026_ERS010178	α1.8a	B/A	EPCR	ERS010178	Ga026
CIDRα1.8b_Ga027_2053	α1.8b	B/A	EPCR	2053	Ga027
CIDRα1.8b_Ga029_ERS010532	α1.8b	B/A	EPCR	ERS010532	Ga029
CIDRδ_HB3var05_HB3	δ	A	unknown	HB3	HB3var05
CIDRδ_HB3var35_HB3	δ	A	unknown	HB3	HB3var35
CIDRδ_IT4var02_IT4	δ	A	unknown	IT4	IT4var02
CIDRγ_IT4var08_IT4	γ	A	unknown	IT4	IT4var08
CSP-1	N/A	N/A	N/A	N/A	N/A
AMA-1	N/A	N/A	N/A	N/A	N/A
MSP-1	N/A	N/A	N/A	N/A	N/A
TET TOX	N/A	N/A	N/A	N/A	N/A
BSA	N/A	N/A	N/A	N/A	N/A

Supplementary Table 5. RNAseq of RDT+ individuals at the end of the dry season (May) and first clinical malaria cases (MAL).

	n	*P. falciparum* smear+ (n)	*P. malariae* PCR+ (n)	age mean (95% CI)	parasites/ul mean (95% CI)	Million reads mapped mean (95% CI)	Million reads mapped to genes mean (95% CI)
May	12	12	3	7.8 (7.5 - 8.2)	1067 (542 - 1591)	0.67 (0.46 - .75)	0.35 (0.22 - 0.48)
MAL	12	12	0	7.9 (7.2 - 8.6)	104231 (62193 - 146270)	2.21 (1.66 - 2.75)	1.34 (1.00 - 167)

Supplementary Table 6. *P. falciparum ex vivo* genes expression compared between 12 RDT+ subclinical individuals at the end of the dry season (May) and 12 first clinical malaria episodes in the ensuing wet season (MAL). log2 Fold Change >1 or <-1 and adjusted P value < 0.05 was considered DEG. (due to the length of the table we present only the first page on this submited version of Andrade et al.)

gene name	locus_tag	ncbi ID	PlasmoDB ID	description	log2FoldChange May vs MAL	pvalue	padj	DEG
PF07_0061	PF07_0061	XP_001349055.1	PF3D7_0715200	conserved Plasmodium protein, unknown function	10,07	5,00E-23	2,35E-21	up May
PFI1210w	PFI1210w	XP_001352117.1	PF3D7_0924600	conserved Plasmodium protein, unknown function	10,02	7,25E-22	2,63E-20	up May
nek-3	PFL0080c	XP_001350425.1	PF3D7_1201600	NIMA related kinase 3	9,45	4,88E-20	1,15E-18	up May
PFB0730w	PFB0730w	XP_001349665.1	PF3D7_0216000	DEAD/DEAH box helicase, putative	9,45	2,66E-23	1,32E-21	up May
PFI1465w	PFI1465w	XP_001352168.1	PF3D7_0930000	procollagen lysine 5-dioxygenase, putative	9,28	1,72E-18	2,94E-17	up May
PFI0205w	PFI0205w	XP_001351916.1	PF3D7_0904200	conserved Plasmodium protein, unknown function	9,20	3,52E-21	1,10E-19	up May
PFL2320w	PFL2320w	XP_001350868.1	PF3D7_1248400	conserved Plasmodium protein, unknown function	9,15	2,44E-20	6,30E-19	up May
PF10_0195	PF10_0195	XP_001347480.2	PF3D7_1020200	conserved Plasmodium protein, unknown function	9,10	1,56E-23	8,75E-22	up May
PFI0185w	PFI0185w	XP_001351912.1	PF3D7_0903800	LCCL domain-containing protein	9,07	1,23E-17	1,80E-16	up May
PF14_0684	PF14_0684	XP_001348858.1	PF3D7_1471700	conserved Plasmodium protein, unknown function	9,07	7,02E-17	8,78E-16	up May
PFC0185w	PFC0185w	XP_001351116.1	PF3D7_0304100	inner membrane complex protein 1e, putative	9,06	1,53E-21	5,07E-20	up May
MESA	PFE0040c	XP_001351567.1	PF3D7_0500800	mature parasite-infected erythrocyte surface antigen	9,04	2,89E-25	2,85E-23	up May
PF08_0017	PF08_0017	XP_001349254.1	PF3D7_0827200	conserved Plasmodium protein, unknown function	9,04	6,81E-19	1,28E-17	up May
PF14_0683	PF14_0683	XP_001348857.1	PF3D7_1471600	conserved Plasmodium protein, unknown function	9,04	4,46E-18	7,02E-17	up May
PFL2420w	PFL2420w	XP_001350888.1	PF3D7_1250400	conserved Plasmodium protein, unknown function	9,02	2,07E-20	5,44E-19	up May
PF08_0126	PF08_0126	XP_001349480.1	PF3D7_0803400	DNA repair and recombination protein RAD54,putative	8,98	1,96E-20	5,22E-19	up May
PF14_0337	PF14_0337	XP_001348511.1	PF3D7_1435600	conserved Plasmodium protein, unknown function	8,95	1,54E-17	2,22E-16	up May
PFF0380w	PFF0380w	XP_966067.1	PF3D7_0607700	conserved Plasmodium protein, unknown function	8,90	4,91E-19	9,32E-18	up May
PF11_0481	PF11_0481	XP_001348148.1	PF3D7_1147200	tubulin--tyrosine ligase, putative	8,80	2,39E-18	3,99E-17	up May
PFB0177c	PFB0177c	XP_001349550.2	PF3D7_0203800	conserved Plasmodium protein, unknown function	8,74	8,26E-19	1,53E-17	up May
PFL2290w	PFL2290w	XP_001350862.2	PF3D7_1247800	dipeptidyl aminopeptidase 2	8,71	8,30E-17	1,03E-15	up May
MAL8P1.76	MAL8P1.76	XP_001349356.2	PF3D7_0816800	meiotic recombination protein DMC1, putative	8,70	5,34E-17	6,83E-16	up May
MAL13P1.312	MAL13P1.312	XP_001350337.1	PF3D7_1362600	conserved Plasmodium protein, unknown function	8,53	2,23E-20	5,80E-19	up May
PF07_0104	PF07_0104	XP_001349152.1	PF3D7_0724900	kinesin-19, putative	8,53	7,33E-22	2,64E-20	up May
PFL1030w	PFL1030w	XP_001350612.1	PF3D7_1221400	inner membrane complex protein 1h, putative	8,53	2,57E-18	4,26E-17	up May
PF14_0522	PF14_0522	XP_001348696.1	PF3D7_1454900	conserved Plasmodium protein, unknown function	8,51	3,06E-19	5,95E-18	up May
MAL8P1.161	MAL8P1.161	XP_001349507.1	PF3D7_0800800	Plasmodium exported protein (hyp7), unknown function	8,50	8,73E-29	2,46E-26	up May
PFL1010c	PFL1010c	XP_001350608.1	PF3D7_1221000	histone-lysine N-methyltransferase, H3 lysine-4 specific	8,46	1,22E-18	2,16E-17	up May
PFC0895w	PFC0895w	XP_002808631.1	PF3D7_0320200	CPW-WPC family protein	8,45	2,55E-15	2,17E-14	up May
PFI1355w	PFI1355w	XP_001352146.1	PF3D7_0927600	conserved Plasmodium protein, unknown function	8,45	2,07E-23	1,06E-21	up May
MAL8P1.206	MAL8P1.206	XP_002808894.1	PF3D7_0831400	Plasmodium exported protein, unknown function	8,44	1,14E-28	2,96E-26	up May
PFI0180w	PFI0180w	XP_001351911.1	PF3D7_0903700	alpha tubulin 1	8,44	2,24E-23	1,13E-21	up May
PF10_0303	PF10_0303	XP_001347587.1	PF3D7_1031000	25 kDa ookinete surface antigen precursor	8,39	1,63E-18	2,79E-17	up May
MAL8P1.25	MAL8P1.25	XP_002808879.1	PF3D7_0825800	conserved Plasmodium protein, unknown function	8,39	1,53E-18	2,66E-17	up May
PF13_0299	PF13_0299	XP_001350272.1	PF3D7_1356100	conserved Plasmodium protein, unknown function	8,38	3,89E-16	4,07E-15	up May
PFF0510w	PFF0510w	XP_966093.1	PF3D7_0610400	histone H3	8,32	6,66E-21	1,99E-19	up May
MAL13P1.195	MAL13P1.195	XP_002809057.1	PF3D7_1338800	CPW-WPC family protein	8,31	4,84E-17	6,24E-16	up May
PF11_0431	PF11_0431	XP_001348100.1	PF3D7_1141900	inner membrane complex protein 1b, putative	8,27	5,02E-17	6,45E-16	up May
PF08_0118	PF08_0118	XP_001349464.1	PF3D7_0805300	conserved Plasmodium protein, unknown function	8,26	4,23E-20	1,01E-18	up May
PF08_0024	PF08_0024	XP_001349268.1	PF3D7_0825700	conserved Plasmodium protein, unknown function	8,25	7,24E-18	1,09E-16	up May
PFD0385w	PFD0385w	XP_001351392.1	PF3D7_0407800	conserved Plasmodium protein, unknown function	8,25	2,47E-15	2,11E-14	up May
MAL13P1.316	MAL13P1.316	XP_001350341.1	PF3D7_1362900	conserved Plasmodium protein, unknown function	8,22	5,22E-20	1,20E-18	up May
PFL0655w	PFL0655w	XP_001350540.1	PF3D7_1213500	integral membrane protein GPR180, putative	8,21	2,25E-16	2,46E-15	up May
PF13_0168	PF13_0168	XP_001350046.1	PF3D7_1331400	CPW-WPC family protein	8,16	9,84E-18	1,46E-16	up May
Stevor	MAL7P1.227	XP_002808742.1	PF3D7_0832000	stevor	8,12	5,09E-16	5,12E-15	up May
PFA_0535c	PFA_0535c	XP_001351039.1	None	kinesin%2C putative	8,12	7,20E-22	2,63E-20	up May
PfMC-2TM	MAL7P1.5	XP_001348951.1	PF3D7_0701600	Pfmc-2TM Maurer's cleft two transmembrane protein	8,12	2,20E-18	3,70E-17	up May
PFL0325w	PFL0325w	XP_001350474.1	PF3D7_1206500	Tat binding protein 1(TBP-1)-interacting protein, putative	8,09	1,18E-12	6,75E-12	up May
ApiAP2	PF11_0442	XP_001348111.1	PF3D7_1143100	transcription factor with AP2 domain(s)	8,08	1,03E-23	6,33E-22	up May
PFD0090c	PFD0090c	XP_001351334.1	PF3D7_0402000	Plasmodium exported protein (PHISTa), unknown function	8,06	6,18E-16	6,08E-15	up May
PF11_0214	PF11_0214	XP_001347885.1	PF3D7_1120700	conserved Plasmodium protein, unknown function	8,04	2,13E-22	8,68E-21	up May
PfMC-2TM	PFA_0680c	XP_002808615.1	PF3D7_0114100	Pfmc-2TM Maurer's cleft two transmembrane protein	8,03	1,44E-16	1,64E-15	up May
PF14_0685	PF14_0685	XP_001348859.1	PF3D7_1471800	conserved Plasmodium protein, unknown function	8,01	1,03E-15	9,55E-15	up May
PFE0770w	PFE0770w	XP_002808691.1	PF3D7_0515400	conserved Plasmodium protein, unknown function	7,99	6,25E-12	3,27E-11	up May
PF10_0374	PF10_0374	XP_001347658.2	PF3D7_1038400	gametocyte-specific protein	7,94	7,90E-22	2,78E-20	up May
PFL0650c	PFL0650c	XP_001350539.1	PF3D7_1213400	conserved Plasmodium protein, unknown function	7,93	2,27E-15	1,96E-14	up May
PFE0220w	PFE0220w	XP_001351603.1	PF3D7_0504500	conserved Plasmodium protein, unknown function	7,93	2,11E-10	9,09E-10	up May
PF11_0325	PF11_0325	XP_001347996.1	PF3D7_1131500	conserved Plasmodium protein, unknown function	7,89	3,45E-14	2,41E-13	up May
PF14_0667	PF14_0667	XP_001348841.1	PF3D7_1469900	conserved Plasmodium protein, unknown function	7,88	4,74E-18	7,41E-17	up May
PFF0915w	PFF0915w	XP_966174.2	PF3D7_0618900.	phosphatidylinositol N-acetylglucosaminyltransferase subu	7,88	6,47E-15	5,17E-14	up May
ApiAP2	PFL1900w	XP_001350786.1	PF3D7_1239200	transcription factor with AP2 domain(s)	7,86	5,33E-20	1,22E-18	up May
PFC0176c	PFC0176c	XP_001351114.1	PF3D7_0303900	phosphatidylethanolamine-binding protein,putative	7,81	1,57E-15	1,40E-14	up May
Pf38	PFE0395c	XP_001351638.1	PF3D7_0508000	6-cysteine protein	7,79	9,68E-13	5,65E-12	up May
PFF1170w	PFF1170w	XP_966225.2	PF3D7_0624300	conserved Plasmodium protein, unknown function	7,77	9,84E-15	7,63E-14	up May
PFE0115c	PFE0115c	XP_001351582.1	PF3D7_0502300	conserved Plasmodium protein, unknown function	7,76	3,41E-14	2,39E-13	up May
PFF0595c	PFF0595c	XP_966110.1	PF3D7_0612200	leucine-rich repeat protein	7,75	2,08E-14	1,52E-13	up May
PFE0940c	PFE0940c	XP_002808700.1	PF3D7_0518800	secreted ookinete protein, putative	7,74	1,50E-16	1,70E-15	up May
PF11_0307	PF11_0307	XP_001347978.1	PF3D7_1129600	phosphatidylinositol-4-phosphate 5-kinase,putative	7,73	3,14E-17	4,29E-16	up May
PFD1100c	PFD1100c	XP_001351536.1	PF3D7_0423300	conserved Plasmodium protein, unknown function	7,72	5,97E-11	2,75E-10	up May
MAL13P1.308	MAL13P1.308	XP_002809096.1	None	conserved Plasmodium protein%2C unknown function	7,72	4,23E-20	1,01E-18	up May
PF11_0342	PF11_0342	XP_001348013.1	PF3D7_1133200	conserved Plasmodium protein, unknown function	7,72	2,30E-15	1,97E-14	up May
PFL1450c	PFL1450c	XP_001350696.1	PF3D7_1230100	thioredoxin-like associated protein 1, putative	7,71	2,08E-14	1,52E-13	up May
PF14_0210	PF14_0210	XP_001348384.1	PF3D7_1421800	conserved Plasmodium protein, unknown function	7,69	3,25E-17	4,41E-16	up May
PFI0775w	PFI0775w	XP_001352030.1	PF3D7_0915800	glycolipid transfer protein, putative	7,65	2,10E-11	1,02E-10	up May
PF14_0227	PF14_0227	XP_001348401.2	PF3D7_1423600	calcium-dependent protein kinase, putative	7,65	7,73E-25	6,61E-23	up May
PF10_0006	PF10_0006	XP_001347293.1	PF3D7_1000600	rifin	7,64	5,23E-14	3,58E-13	up May
PF13_0146	PF13_0146	XP_001349996.1	PF3D7_1325800	conserved Plasmodium protein, unknown function	7,63	7,33E-25	6,52E-23	up May
PF14_0333	PF14_0333	XP_001348507.1	PF3D7_1435200	conserved Plasmodium protein, unknown function	7,60	2,58E-14	1,85E-13	up May
PFF1455c	PFF1455c	XP_966282.2	PF3D7_0630000	CPW-WPC family protein, putative	7,58	5,04E-16	5,10E-15	up May
PF14_0737	PF14_0737	XP_001348911.1	PF3D7_1476700	lysophospholipase, putative	7,57	1,18E-22	5,04E-21	up May
PFC0950c	PFC0950c	XP_001351285.1	PF3D7_0321500	peptidase, putative	7,54	7,15E-24	4,65E-22	up May
PF10_0306	PF10_0306	XP_001347590.2	PF3D7_1031200	MORN repeat-containing protein 1	7,53	1,06E-16	1,26E-15	up May
GyrB	PFL1915w	XP_001350789.1	PF3D7_1239500	DNA gyrase subunit B	7,53	2,81E-21	8,97E-20	up May
PF07_0019	PF07_0019	XP_001348981.1	PF3D7_0704800	conserved Plasmodium protein, unknown function	7,50	1,08E-19	2,37E-18	up May
MAL7P1.93	MAL7P1.93	XP_001349086.1	PF3D7_0718400	mitochondrial ribosomal protein S8 precursor,putative	7,50	1,03E-14	8,00E-14	up May
PFA_0545c	PFA_0545c	XP_001351041.1	PF3D7_0111300	replication factor c protein, putative	7,49	4,31E-15	3,54E-14	up May
PF11_0482	PF11_0482	XP_001348149.1	PF3D7_1147300	conserved Plasmodium protein, unknown function	7,47	8,27E-16	7,90E-15	up May
PF13_0031	PF13_0031	XP_001349786.1	PF3D7_1305900	conserved Plasmodium protein, unknown function	7,46	2,19E-22	8,82E-21	up May
PF10_0368	PF10_0368	XP_001347652.1	PF3D7_1037500	dynamin-like protein	7,46	1,59E-22	6,65E-21	up May
PFC0170c	PFC0170c	XP_001351112.1	PF3D7_0303700	lipoamide acyltransferase component of branched-chain al	7,46	1,10E-16	1,31E-15	up May
MAL13P1.129	MAL13P1.129	XP_002809029.1	PF3D7_1322900	conserved Plasmodium protein, unknown function	7,45	1,07E-12	6,19E-12	up May
PFD0850c	PFD0850c	XP_002808659.1	PF3D7_0417500.	memo-like protein	7,42	4,76E-17	6,16E-16	up May
PFE0090w	PFE0090w	XP_001351577.1	PF3D7_0501800	chromosome assembly factor 1	7,41	3,84E-20	9,40E-19	up May
PFL1875w	PFL1875w	XP_001350781.2	None	conserved Plasmodium protein	7,40	7,88E-20	1,75E-18	up May

Supplementary Table 7. Oligo sequences and probes for RTq-PCR expression data of eight selected and one housekeeping *P. falciparum* transcripts.

Gene	GeneBank#	Oligo	5'-3' sequence
GlyRS	XM_001348335.2	FOR	TGAGTGATATGGATAATATAAAGGAACAAA
		REV	GGATGATATTTCACAAACGTATCTTTCT
		CalFluorGold540_BHQNova	TAAGCTCTTCCAAACTACCACATCCATCATTCTCT
REX3	XM_001352191.1	FOR	TTTCCTTTGCTTATATCTTAATACGTTCAACT
		REV	CTTGTGAAGTTGTTGCTTCTATATGTGAT
		6FAM_BHQNova	ACCACCTCATACGAAGGGAGCAGTTTC
MIF	XM_001350654.1	FOR	GGTAGCAACGAAGCTTATTGTTTTGTA
		REV	CAAGTTGCTTACAAGGAGTTTCGTTAT
		6FAM_BHQNova	ATCAGCAAGAGCAGAATTATTTGACCTATTAATTCCTCCA
Pfsec23	XM_001349263.1	FOR	CGGTGTAGCATTGAGTGTTGCT
		REV	CTTAAAGGCGTATCTACAATTTTACCAG
		6FAM_BHQNova	TGCTCCACCTATAAACATCATAACACGACCACTTAATT
Sir2	XM_001349975.1	FOR	AAGAGATATATCATCCGATTATGAAATAGAAAT
		REV	AATCCATCTACATTTTGTGTTACTACTGATT
		6FAM_BHQNova	CCAAACTTTCTAAAGTTGATAAAGCTACATGACCATTGTT
UBE4B	XM_002808834.1	FOR	TATGCCTGTAAATACGACCGATTC
		REV	TTGCATTATTATTATTAGAGTTGGTGGTTG
		6FAM_BHQNova	CCTCTTGTGGAACATCATTATTACCATTGCTGT
PHISTc	XM_001349662.1	FOR	TTTGGTTATGGTTATACGAACAAGG
		REV	TTTTCTACATTATTCAAGATTTTCTTTCCT
		6FAM_BHQNova	ATCCTCATACAGATTAATTTCAAGTTGAATCAAAACGT
KAHRP	XM_001349498.2	FOR	GTGAGAACCATCGTGTGCACTT
		REV	TGTGGACCTGCCGCTATAGATT
		6FAM_BHQNova	TGTTCCAGCAGATGCACCAAATGGCT
STARP	XM_001348922.1	FOR	CCGTGGTTGTTGTAATATTATTATTGTCT
		REV	TAAATACAAAACCCATTGATAATAATAACACA
		6FAM_BHQNova	TGTCTGTGTTCTTATTATCTGTTTCCTTTGTGCCTG

Supplementary Table 8. Metabolite corrected peak areas measured by LC-MS in the plasma of 12 subclinical individuals at the end of the dry season (May) and 12 first clinical malaria episodes in the ensuing wet season (MAL).
(due to the length of the table we present only the first page on this submited version of Andrade et al.)

Targetted metab | Aqueous positive metab | Lipid positive metab | Lipid negative metab

parasitaemia Pf/µl	725	1150	500	15050	750	750	675	600	675	1050	1950	3375	*8175*
season	May	May	May	May	May	May	May	May	May	May	May	May	MAL
IDs	May244	May308	May320	May325	May326	May334	May351	May355	May357	May373	May388	May448	MAL161
pyruvate	1,47E+09	1,41E+09	2,71E+09	1,06E+09	1,66E+09	1,02E+09	1,88E+09	1,24E+09	1,27E+09	1,52E+09	2,35E+09	8,95E+08	1,14E+09
alanine/sarcosine	7,94E+07	8,53E+07	1,05E+08	5,36E+07	8,50E+07	5,82E+07	9,52E+07	9,15E+07	5,85E+07	1,03E+08	1,03E+08	7,19E+07	5,27E+07
lactate	2,07E+09	1,99E+09	3,11E+09	1,61E+09	2,36E+09	1,44E+09	2,23E+09	1,80E+09	1,58E+09	1,98E+09	3,53E+09	1,27E+09	1,32E+09
acetoacetate	3,44E+08	4,14E+07	1,09E+08	3,41E+08	5,07E+08	7,50E+08	6,92E+07	3,76E+07	3,83E+08	1,77E+08	7,88E+07	6,74E+07	1,14E+09
4-aminobutyrate	5,38E+06	8,75E+06	8,34E+06	4,59E+06	6,64E+06	5,44E+06	5,75E+06	7,14E+06	5,85E+06	3,95E+06	6,97E+06	9,96E+06	4,21E+06
serine	7,04E+07	7,18E+07	6,55E+07	5,17E+07	7,75E+07	6,99E+07	6,75E+07	7,12E+07	6,57E+07	9,15E+07	9,15E+07	8,30E+07	4,92E+07
glycerate	1,81E+08	8,78E+07	1,50E+08	1,39E+08	1,33E+08	8,35E+07	2,49E+08	1,19E+08	8,00E+07	1,22E+08	1,54E+08	9,20E+07	7,28E+07
proline	2,90E+08	3,38E+08	3,94E+08	4,58E+08	4,21E+08	3,34E+08	2,87E+08	4,23E+08	6,38E+08	4,30E+08	3,09E+08	3,45E+08	3,30E+08
fumarate	1,17E+07	1,30E+07	1,55E+07	1,13E+07	1,16E+07	1,46E+07	8,02E+06	1,26E+07	8,55E+06	8,18E+06	1,52E+07	6,24E+06	1,25E+07
2-keto-isovalerate	3,47E+07	4,41E+07	3,01E+07	2,36E+07	5,14E+07	3,24E+07	2,99E+07	2,80E+07	4,32E+07	2,62E+07	3,54E+07	3,05E+07	6,55E+07
Acetyl-glycine	6,11E+07	2,99E+07	4,92E+07	6,35E+07	6,93E+07	6,82E+07	4,73E+07	3,76E+07	6,12E+07	5,99E+07	5,38E+07	3,46E+07	6,73E+07
indole	2,47E+06	1,52E+06	2,34E+06	1,98E+06	2,35E+06	1,13E+06	1,94E+06	2,12E+06	2,14E+06	2,80E+06	2,20E+06	2,32E+06	1,71E+06
valine	9,75E+08	7,57E+08	7,10E+08	6,12E+08	1,20E+09	5,93E+08	7,57E+08	7,33E+08	8,85E+08	9,81E+08	8,12E+08	6,86E+08	1,46E+09
succinate/Methylmalonic	1,12E+08	5,88E+07	1,03E+08	1,20E+08	1,31E+08	1,21E+08	8,90E+07	7,08E+07	8,75E+07	7,33E+07	1,29E+08	6,36E+07	1,02E+08
threonine/homoserine	2,14E+08	1,35E+08	2,62E+08	1,30E+08	2,80E+08	1,51E+08	1,83E+08	1,62E+08	2,64E+08	3,18E+08	2,10E+08	2,66E+08	1,59E+08
3-S-methylthiopropionate	1,33E+04	1,88E+04	1,15E+05	7,42E+04	9,09E+04	1,14E+05	2,08E+04	5,55E+03	2,51E+04	2,33E+05	1,25E+05	1,02E+05	1,20E+05
cysteine	9,26E+05	8,06E+05	1,19E+06	6,39E+05	2,05E+06	1,31E+06	3,50E+05	1,48E+06	1,30E+06	1,13E+06	5,04E+05	1,58E+06	3,50E+05
taurine	7,05E+08	4,91E+08	7,69E+08	6,17E+08	7,67E+08	5,81E+08	8,98E+08	5,13E+08	4,79E+08	3,75E+08	7,50E+08	6,57E+08	4,11E+08
Pyroglutamic ac.	4,40E+08	2,79E+08	4,36E+08	5,16E+08	6,11E+08	3,40E+08	4,12E+08	3,82E+08	3,83E+08	4,49E+08	4,87E+08	3,37E+08	4,40E+08
DL-Pipecolic ac.	6,32E+07	4,49E+07	4,64E+07	6,16E+07	7,97E+07	3,42E+07	3,68E+07	5,74E+07	5,27E+07	5,43E+07	5,38E+07	4,44E+07	3,69E+07
Citraconic ac.	2,20E+07	3,43E+07	2,72E+07	2,01E+07	2,96E+07	3,13E+07	2,21E+07	2,93E+07	2,82E+07	3,25E+07	3,28E+07	2,57E+07	2,57E+07
Ketoleucine	9,60E+08	7,04E+08	9,07E+08	5,72E+08	6,49E+08	8,79E+08	5,35E+08	9,23E+08	9,68E+08	1,02E+09	9,36E+08	6,75E+08	1,23E+09
N-Acetyl-L-alanine	5,76E+07	2,21E+07	6,89E+07	4,62E+07	6,39E+07	4,81E+07	5,15E+07	2,86E+07	4,55E+07	3,56E+07	6,54E+07	3,43E+07	5,97E+07
hydroxyproline/Aminolev	1,57E+07	1,02E+07	2,53E+07	1,51E+07	2,83E+07	1,88E+07	1,12E+07	1,84E+07	1,96E+07	1,45E+07	2,20E+07	1,31E+07	1,39E+07
leucine	1,01E+09	7,50E+08	8,38E+08	8,69E+08	1,04E+09	9,27E+08	8,50E+08	1,16E+09	1,08E+09	1,30E+09	1,27E+09	8,89E+08	1,72E+09
isoleucine	5,11E+08	3,01E+08	3,92E+08	2,47E+08	5,59E+08	3,30E+08	4,09E+08	4,15E+08	4,80E+08	5,81E+08	3,60E+08	3,64E+08	5,74E+08
oxaloacetate	3,86E+05	1,72E+04	2,04E+05	2,55E+05	2,93E+05	1,57E+05	1,78E+05	3,97E+04	1,06E+05	2,34E+05	3,87E+05	3,06E+04	8,80E+04
asparagine	2,46E+07	2,39E+07	3,25E+07	2,23E+07	3,41E+07	3,04E+07	2,60E+07	3,35E+07	2,81E+07	6,60E+07	3,48E+07	3,50E+07	1,66E+07
Hydroxyisocaproic ac.	4,88E+07	2,36E+07	2,88E+07	3,22E+07	4,03E+07	2,77E+07	3,26E+07	4,46E+07	3,97E+07	3,93E+07	5,40E+07	4,38E+07	7,78E+07
ornithine	1,70E+07	1,50E+07	1,95E+07	1,41E+07	2,30E+07	1,65E+07	1,72E+07	1,62E+07	1,98E+07	2,49E+07	1,92E+07	2,14E+07	8,67E+06
aspartate	1,92E+09	1,28E+09	1,92E+09	1,79E+09	1,69E+09	1,83E+09	1,85E+09	1,81E+09	1,72E+09	1,95E+09	2,06E+09	1,46E+09	1,95E+09
malate	6,67E+07	5,47E+07	8,29E+07	5,95E+07	6,14E+07	6,73E+07	4,43E+07	5,69E+07	4,13E+07	3,97E+07	8,05E+07	2,97E+07	6,33E+07
Methylcysteine	6,79E+06	3,34E+06	3,64E+06	3,74E+06	6,43E+06	6,63E+06	5,46E+06	5,26E+06	3,49E+06	1,30E+07	4,48E+06	8,45E+06	3,41E+07
p-aminobenzoate	3,97E+04	1,95E+04	3,88E+04	2,98E+04	7,01E+02	1,11E+04	2,30E+04	3,68E+04	2,42E+03	3,68E+04	3,68E+04	2,10E+03	2,74E+04
p-hydroxybenzoate	1,82E+05	1,95E+05	1,65E+05	2,55E+05	1,99E+05	1,94E+05	5,57E+05	3,10E+05	4,73E+05	1,31E+05	1,93E+05	1,27E+05	5,32E+04
a-ketoglutarate	1,66E+08	1,33E+08	2,23E+08	1,59E+08	1,67E+08	1,76E+08	1,21E+08	1,23E+08	1,57E+08	1,25E+08	2,42E+08	8,54E+07	1,13E+08
glutamine	1,36E+09	1,09E+09	1,20E+09	1,16E+09	1,47E+09	1,33E+09	1,09E+09	1,26E+09	1,23E+09	1,30E+09	1,49E+09	1,30E+09	8,04E+08
lysine	1,43E+07	1,31E+07	1,24E+07	1,12E+07	1,75E+07	9,31E+06	2,05E+07	8,15E+06	1,40E+07	1,42E+07	9,76E+06	1,13E+07	9,42E+06
glutamate	1,28E+09	1,56E+09	1,82E+09	1,05E+09	1,52E+09	1,20E+09	1,30E+09	1,22E+09	1,24E+09	8,81E+08	1,59E+09	1,72E+09	1,02E+09
2-oxo-4-methylthiobutanc	2,76E+04	6,41E+04	1,76E+04	4,48E+04	8,25E+04	8,25E+03	4,86E+04	1,48E+04	1,00E+05	8,68E+04	3,64E+04	3,98E+04	0,00E+00
2-Hydroxy-2-methylbutar	5,41E+07	1,99E+07	2,83E+07	2,77E+07	3,45E+07	3,59E+07	4,25E+07	2,79E+07	2,38E+07	2,34E+07	3,86E+07	2,64E+07	5,42E+07
methionine	2,55E+08	1,30E+08	2,82E+08	1,48E+08	2,36E+08	1,46E+08	2,40E+08	1,57E+08	1,84E+08	2,19E+08	2,75E+08	1,57E+08	1,15E+08
ribose	7,50E+07	8,20E+07	7,31E+07	5,59E+07	7,15E+07	6,48E+07	6,61E+07	6,58E+07	5,61E+07	7,39E+07	7,55E+07	7,01E+07	6,25E+07
xanthine	4,13E+07	2,83E+07	3,41E+07	2,91E+07	3,21E+07	3,67E+07	2,94E+07	2,36E+07	3,72E+07	7,46E+06	2,34E+07	2,89E+07	4,37E+07
Hydroxyphenylacetic ac.	1,08E+05	9,47E+04	6,82E+04	7,00E+04	1,23E+05	6,41E+04	7,51E+04	1,67E+05	3,67E+06	1,90E+03	7,89E+04	4,85E+04	5,37E+04
Dithioerythritol	3,57E+04	2,90E+04	2,54E+04	3,56E+04	3,32E+04	1,61E+04	1,91E+04	6,66E+03	1,27E+04	2,57E+04	1,77E+04	2,04E+04	8,18E+03
histidine	4,60E+07	4,89E+07	5,55E+07	4,38E+07	5,03E+07	4,84E+07	4,35E+07	5,21E+07	4,97E+07	6,01E+07	5,76E+07	6,06E+07	3,43E+07
orotate	2,53E+06	3,30E+06	4,36E+06	5,93E+06	5,37E+06	4,02E+06	5,64E+06	4,72E+06	4,21E+06	3,92E+06	5,63E+06	4,08E+06	4,71E+06
allantoin	7,81E+06	5,94E+06	6,54E+06	7,65E+06	8,51E+06	6,29E+06	9,78E+06	1,08E+07	5,72E+06	1,74E+07	7,09E+06	1,09E+07	6,48E+06
Indole-3-carboxylic ac.	1,73E+05	1,19E+05	2,41E+05	1,89E+05	2,45E+05	1,58E+05	1,82E+05	2,03E+05	1,96E+05	2,95E+05	4,73E+05	2,55E+05	1,68E+05
Aminoadipic ac.	1,26E+07	7,00E+06	9,27E+06	5,94E+06	1,42E+07	5,52E+06	6,80E+06	4,08E+06	9,38E+06	5,70E+06	5,45E+06	5,11E+06	3,01E+07
phenylpyruvate	1,87E+06	8,28E+06	4,49E+06	2,86E+06	2,42E+06	1,54E+06	4,74E+06	2,79E+06	2,09E+06	6,00E+06	7,25E+06	3,64E+06	4,74E+06
phenylalanine	1,85E+09	1,78E+09	1,97E+09	1,72E+09	1,96E+09	1,68E+09	1,65E+09	2,08E+09	1,91E+09	2,96E+09	2,18E+09	1,96E+09	3,91E+09
Phenyllactic ac.	8,71E+06	2,14E+07	1,04E+07	1,14E+07	7,69E+06	6,39E+06	1,44E+07	1,19E+07	7,76E+06	1,34E+07	2,02E+07	1,56E+07	3,07E+07
quinolinate	1,39E+06	1,14E+06	2,26E+06	1,53E+06	2,13E+06	7,74E+05	2,27E+06	1,03E+06	1,64E+06	1,44E+06	1,46E+06	2,68E+06	1,72E+06
phosphoenolpyruvate	1,28E+06	1,61E+06	2,11E+06	1,64E+06	1,46E+06	8,85E+05	1,26E+06	1,28E+06	1,21E+06	1,27E+06	1,91E+06	9,98E+05	3,87E+05
Uric ac.	1,81E+09	1,78E+09	2,10E+09	1,64E+09	2,56E+09	1,51E+09	2,16E+09	1,85E+09	1,41E+09	1,40E+09	1,53E+09	1,56E+09	2,10E+09
pyridoxine	4,39E+03	7,54E+03	4,42E+02	7,54E+03	7,54E+03	5,29E+03	7,54E+03	7,54E+03	7,54E+03	2,02E+01	4,50E+03	7,78E+03	7,54E+03
dihydroxy-acetone-phosp	2,16E+07	2,62E+07	2,25E+07	6,10E+07	4,59E+07	3,20E+07	6,64E+07	1,92E+07	3,95E+07	1,50E+07	4,56E+07	2,74E+07	3,30E+06
sn-glycerol-3-phosphate	4,44E+06	5,62E+06	2,57E+06	3,03E+06	4,85E+06	5,04E+06	1,55E+06	4,17E+06	5,44E+06	5,44E+06	3,16E+06	3,89E+06	5,23E+05
aconitate	1,76E+08	2,15E+08	2,02E+08	1,57E+08	2,27E+08	2,56E+08	1,57E+08	1,74E+08	2,28E+08	2,51E+08	2,47E+08	1,68E+08	2,06E+08
N-acetyl-L-ornithine	7,41E+06	2,41E+06	1,23E+07	1,01E+07	8,65E+06	1,29E+07	1,09E+07	1,01E+07	1,03E+07	1,40E+07	1,09E+07	1,08E+07	2,06E+07
arginine	1,02E+07	3,05E+06	1,04E+07	5,59E+06	1,18E+07	6,08E+06	6,72E+06	5,69E+06	1,10E+07	1,58E+07	8,44E+06	8,84E+06	3,11E+06
acetyl-aspartate	6,62E+07	3,52E+07	6,81E+07	5,90E+07	5,69E+07	5,85E+07	5,56E+07	5,31E+07	5,47E+07	6,10E+07	7,47E+07	3,97E+07	6,17E+07
citrulline	7,22E+07	7,31E+07	8,16E+07	6,58E+07	1,02E+08	8,24E+07	8,06E+07	7,80E+07	8,63E+07	9,85E+07	8,17E+07	9,97E+07	4,58E+07
N-carbamoyl-L-aspartate	3,75E+05	5,94E+05	8,77E+05	5,64E+05	6,46E+05	6,40E+05	5,94E+05	1,02E+06	9,55E+05	6,72E+05	8,22E+05	6,03E+05	8,67E+05
allantoate	1,49E+06	6,63E+05	1,66E+06	2,17E+06	1,97E+06	3,56E+06	1,48E+06	1,80E+06	1,46E+06	1,13E+07	2,40E+06	2,08E+06	1,33E+06
2-Isopropylmalic ac.	4,09E+05	1,34E+06	4,16E+05	7,48E+05	5,11E+05	5,06E+05	1,06E+06	1,22E+06	5,29E+05	2,59E+06	6,80E+05	9,60E+05	2,42E+05
Pyrophosphate	1,09E+06	2,10E+05	1,08E+06	6,16E+05	5,63E+05	4,01E+05	1,38E+06	4,71E+05	5,03E+05	2,47E+05	8,46E+05	1,93E+05	5,04E+05
myo-inositol	1,20E+06	1,50E+06	1,75E+06	1,61E+06	1,58E+06	2,58E+06	7,55E+05	5,61E+05	2,08E+06	1,08E+06	4,01E+06	3,10E+06	1,66E+06
Hexose	3,63E+09	3,89E+09	3,54E+09	2,81E+09	3,61E+09	3,18E+09	3,35E+09	3,26E+09	2,83E+09	3,81E+09	3,74E+09	3,36E+09	3,02E+09
tyrosine	6,59E+08	7,16E+08	9,65E+08	6,43E+08	1,01E+09	5,60E+08	6,16E+08	7,70E+08	8,51E+08	7,42E+08	7,89E+08	7,06E+08	6,50E+08
4-hydroxyphenyllactate	9,66E+06	2,11E+07	1,44E+07	1,10E+07	1,09E+07	9,99E+06	1,33E+07	1,27E+07	1,87E+07	1,21E+07	2,35E+07	1,33E+07	1,83E+07
homocysteic ac.	7,85E+05	5,71E+05	5,88E+05	5,86E+05	7,36E+05	6,16E+05	1,23E+06	7,31E+05	4,43E+05	5,86E+05	7,61E+05	5,43E+05	3,67E+05
4-Pyridoxic ac.	2,33E+06	1,02E+06	3,96E+06	2,84E+06	3,01E+06	1,49E+06	2,88E+06	1,97E+06	1,81E+06	1,86E+06	1,79E+06	1,90E+06	7,37E+05
3-phosphoglycerate	9,91E+06	8,48E+06	1,33E+07	9,08E+06	1,16E+07	5,39E+06	1,14E+07	5,43E+06	4,73E+06	3,99E+06	1,04E+07	6,96E+06	2,49E+06
N-acetyl-glutamine	4,91E+06	2,61E+06	4,13E+06	4,09E+06	4,50E+06	3,42E+06	4,09E+06	3,16E+06	4,38E+06	4,59E+06	5,02E+06	3,77E+06	4,63E+06
Acetyllysine	3,44E+06	1,70E+06	3,62E+06	2,88E+06	3,80E+06	2,08E+06	3,25E+06	2,65E+06	2,13E+06	2,19E+06	3,34E+06	2,72E+06	3,78E+06
Kynurenic ac.	3,80E+05	2,21E+05	4,77E+05	4,87E+05	4,18E+05	5,64E+05	3,90E+05	3,18E+05	6,54E+05	1,10E+06	6,49E+05	3,41E+05	2,61E+06
N-acetyl-glutamate	2,49E+06	1,51E+06	3,08E+06	1,63E+06	2,76E+06	2,17E+06	2,15E+06	2,00E+06	1,80E+06	2,39E+06	3,94E+06	1,43E+06	3,86E+06
citrate/isocitrate	4,45E+09	2,73E+09	3,66E+09	3,41E+09	3,93E+09	4,38E+09	3,08E+09	2,82E+09	3,71E+09	4,11E+09	4,37E+09	2,61E+09	3,99E+09
2-dehydro-D-gluconate	7,49E+07	6,94E+07	6,94E+07	6,78E+07	1,94E+08	8,16E+07	7,77E+07	5,83E+07	5,97E+07	5,95E+07	7,88E+07	6,25E+07	1,39E+08
D-gluconate	1,24E+08	1,13E+08	1,65E+08	1,10E+08	1,36E+08	8,53E+07	1,27E+08	1,05E+08	9,58E+07	1,28E+08	1,37E+08	1,29E+08	1,18E+08
D-erythrose-4-phosphate	4,92E+06	8,18E+05	1,64E+06	5,33E+06	6,53E+06	3,43E+06	1,27E+06	7,30E+05	6,33E+06	3,81E+06	1,47E+06	1,46E+06	3,28E+06
Acetylcarnitine	1,18E+06	1,12E+05	4,78E+05	2,15E+06	9,36E+05	5,10E+05	7,86E+05	2,06E+05	7,02E+05	3,35E+06	1,15E+05	3,73E+05	1,13E+06
tryptophan	4,14E+08	2,32E+08	4,28E+08	3,62E+08	4,23E+08	2,22E+08	3,42E+08	2,86E+08	3,80E+08	4,56E+08	3,94E+08	3,34E+08	3,07E+08
Xanthurenic ac.	2,57E+05	2,30E+05	2,94E+05	2,43E+05	3,21E+05	2,62E+05	3,23E+05	3,00E+05	2,96E+05	4,01E+05	4,23E+05	3,31E+05	5,03E+05
Kynurenine	2,46E+07	3,00E+07	3,49E+07	2,52E+07	4,23E+07	2,29E+07	3,30E+07	2,50E+07	3,13E+07	3,51E+07	3,09E+07	3,50E+07	3,15E+07
D-glucarate	1,62E+08	9,97E+07	1,25E+08	1,12E+08	6,85E+07	9,00E+07	1,34E+08	8,85E+07	5,05E+07	1,00E+08	1,35E+08	8,40E+07	2,77E+07
deoxyribose-phosphate	2,03E+05	1,57E+05	3,13E+05	2,61E+05	2,37E+05	1,48E+05	2,23E+05	2,23E+05	1,88E+05	1,57E+05	2,91E+05	7,24E+04	2,78E+05
pantothenate	9,30E+06	5,14E+06	1,24E+07	8,54E+06	1,24E+07	1,33E+07	7,25E+06	9,66E+06	9,21E+06	9,83E+06	8,43E+06	8,93E+06	4,67E+06

Supplementary Table 9. Metabolites significantly different by LC-MS with a FDR 0.05% in the plasma of 12 subclinical individuals at the end of the dry season (May) and 12 first clinical malaria episodes in the ensuing wet season (MAL), and their correlation with parasitaemia (X) at the time of blood draw.

	Mean Diff. MAL-May	Discovery?	q value	Individual P Value	Spearman r x parasitaemia	95% confidence interval	P (two-tailed)	P value summary	Significant? (alpha = 0.05)
X vs. acetoacetate	269575000	Yes	<0.0001	<0.0001	0,2475	-0.1854 to 0.6000	0,2436	ns	No
X vs. aspartate	411666667	Yes	<0.0001	<0.0001	0,5635	0.1950 to 0.7925	0,0041	**	Yes
X vs. EtherPC 38:4e; PC(14:0e/24:4); [M+H]+	-2248333	Yes	<0.0001	<0.0001	-0,4566	-0.7321 to -0.05259	0,0249	*	Yes
X vs. EtherPE 38:5e; PE(16:1e/22:4); [M-H]-	-3989167	Yes	<0.0001	<0.0001	-0,4446	-0.7251 to -0.03764	0,0295	*	Yes
X vs. FA 16:0; [M-H]-	14593333	Yes	<0.0001	<0.0001	0,2962	-0.1342 to 0.6326	0,1599	ns	No
X vs. FA 18:1; [M-H]-	33825833	Yes	<0.0001	<0.0001	0,2784	-0.1532 to 0.6208	0,1878	ns	No
X vs. FA 18:2; [M-H]-	13220833	Yes	<0.0001	<0.0001	0,2418	-0.1912 to 0.5961	0,2549	ns	No
X vs. glutamate	-381666667	Yes	<0.0001	<0.0001	-0,4923	-0.7528 to -0.09840	0,0145	*	Yes
X vs. glutamine	-380416667	Yes	<0.0001	<0.0001	-0,6804	-0.8538 to -0.3709	0,0003	***	Yes
X vs. Hexose	876666667	Yes	<0.0001	<0.0001	0,6042	0.2537 to 0.8144	0,0018	**	Yes
X vs. Ketoleucine	244416667	Yes	0,0001	<0.0001	0,2358	-0.1974 to 0.5919	0,2674	ns	No
X vs. leucine	184666667	Yes	0,0102	0,0006	0,2663	-0.1660 to 0.6127	0,2085	ns	No
X vs. LysoPC 16:0; [M+H]+	-33613333	Yes	<0.0001	<0.0001	-0,7564	-0.8913 to -0.4986	<0.0001	****	Yes
X vs. LysoPC 18:1; [M+H]+	-8505250	Yes	<0.0001	<0.0001	-0,789	-0.9068 to -0.5570	<0.0001	****	Yes
7	-10976750	Yes	<0.0001	<0.0001	-0,7705	-0.8980 to -0.5236	<0.0001	****	Yes
X vs. LysoPC 20:4; [M+H]+	-3494750	Yes	<0.0001	<0.0001	-0,777	-0.9011 to -0.5353	<0.0001	****	Yes
X vs. phenylalanine	1399166667	Yes	<0.0001	<0.0001	0,6976	0.3989 to 0.8625	0,0002	***	Yes
X vs. pyruvate	159333333	Yes	0,0462	0,0032	-0,06092	-0.4632 to 0.3621	0,7773	ns	No
X vs. TG 50:3; TG(16:0/16:1/18:2); [M+NH4]+	-1688167	Yes	0,005	<0.0001	-0,2201	-0.5811 to 0.2133	0,3014	ns	No
X vs. TG 52:2; TG(16:0/18:1/18:1); [M+NH4]+	3079167	Yes	<0.0001	<0.0001	0,3654	-0.05718 to 0.6769	0,0791	ns	No
X vs. TG 52:3; TG(16:0/18:1/18:2); [M+NH4]+	4867500	Yes	<0.0001	<0.0001	0,5766	0.2137 to 0.7997	0,0032	**	Yes
X vs. Unknown 190.0861	-501567	Yes	0,0445	0,001	-0,6751	-0.8512 to -0.3624	0,0003	***	Yes
X vs. Unknown 203.0527	504167	Yes	0,0433	0,001	0,4747	0.07558 to 0.7427	0,0191	*	Yes
X vs. Unknown 218.1301	6368459	Yes	<0.0001	<0.0001	0,4591	0.05580 to 0.7336	0,024	*	Yes
X vs. Unknown 230.0128	3706116	Yes	0,0001	<0.0001	0,4655	0.06389 to 0.7374	0,0219	*	Yes
X vs. Unknown 240.1101	1569890	Yes	0,0131	0,0003	0,3743	-0.04688 to 0.6825	0,0715	ns	No
X vs. Unknown 263.2371	1022750	Yes	<0.0001	<0.0001	0,2845	-0.1467 to 0.6249	0,1778	ns	No
X vs. Unknown 281.2479	563000	Yes	0,0114	0,0002	0,3019	-0.1281 to 0.6363	0,1517	ns	No
X vs. Unknown 291.0827	-4316667	Yes	<0.0001	<0.0001	-0,3272	-0.6527 to 0.1003	0,1186	ns	No
X vs. Unknown 293.0988	1783333	Yes	<0.0001	<0.0001	-0,04986	-0.4544 to 0.3717	0,817	ns	No
X vs. Unknown 299.1394	1484000	Yes	0,0254	0,0006	0,4176	0.004405 to 0.7090	0,0423	*	Yes
X vs. Unknown 315.0831	2277758	Yes	<0.0001	<0.0001	0,3045	-0.1252 to 0.6380	0,1479	ns	No
X vs. Unknown 337.1052	-1773333	Yes	0,0023	<0.0001	-0,5024	-0.7586 to -0.1117	0,0124	*	Yes
X vs. Unknown 369.3516	-15250000	Yes	<0.0001	<0.0001	-0,4899	-0.7514 to -0.09528	0,0151	*	Yes
X vs. Unknown 369.352	-1483333	Yes	0,0254	0,0006	0,122	-0.3074 to 0.5102	0,57	ns	No
X vs. Unknown 376.2602	2654167	Yes	<0.0001	<0.0001	0,2712	-0.1608 to 0.6160	0,1999	ns	No
X vs. Unknown 381.299	1118083	Yes	<0.0001	<0.0001	0,3065	-0.1231 to 0.6393	0,1453	ns	No
X vs. Unknown 412.285	830175	Yes	<0.0001	<0.0001	0,3933	-0.02464 to 0.6942	0,0573	ns	No
X vs. Unknown 414.2155	-551167	Yes	0,0148	0,0003	-0,2921	-0.6299 to 0.1386	0,1661	ns	No
X vs. Unknown 414.3008	1659250	Yes	<0.0001	<0.0001	0,2127	-0.2207 to 0.5759	0,3183	ns	No
X vs. Unknown 415.2119	9286167	Yes	<0.0001	<0.0001	0,3661	-0.05637 to 0.6774	0,0785	ns	No
X vs. Unknown 415.2123	601667	Yes	0,0042	<0.0001	0,2515	-0.1813 to 0.6027	0,2358	ns	No
X vs. Unknown 416.317	668059	Yes	0,0008	<0.0001	0,2636	-0.1687 to 0.6109	0,2133	ns	No
X vs. Unknown 460.27	-2532917	Yes	<0.0001	<0.0001	-0,2052	-0.5706 to 0.2281	0,3362	ns	No
X vs. Unknown 480.3077	-4261500	Yes	<0.0001	<0.0001	-0,7451	-0.8858 to -0.4789	<0.0001	****	Yes
X vs. Unknown 494.3241	-1262000	Yes	<0.0001	<0.0001	-0,7068	-0.8671 to -0.4140	0,0001	***	Yes
X vs. Unknown 496.3408	-1594583	Yes	<0.0001	<0.0001	-0,7031	-0.8652 to -0.4078	0,0001	***	Yes
X vs. Unknown 496.3409	-12285833	Yes	<0.0001	<0.0001	-0,7209	-0.8740 to -0.4375	<0.0001	****	Yes
X vs. Unknown 518.322	-2000833	Yes	0,0002	<0.0001	-0,7255	-0.8763 to -0.4453	<0.0001	****	Yes
X vs. Unknown 520.341	-4395000	Yes	<0.0001	<0.0001	-0,5476	-0.7839 to -0.1729	0,0056	**	Yes
X vs. Unknown 522.3561	-5231667	Yes	<0.0001	<0.0001	-0,6056	-0.8152 to -0.2558	0,0017	**	Yes
X vs. Unknown 524.3711	-927333	Yes	<0.0001	<0.0001	-0,5523	-0.7864 to -0.1794	0,0051	**	Yes
X vs. Unknown 524.3712	-15630250	Yes	<0.0001	<0.0001	-0,7776	-0.9014 to -0.5363	<0.0001	****	Yes
X vs. Unknown 524.3714	-1526358	Yes	0,0186	0,0004	-0,7656	-0.8957 to -0.5147	<0.0001	****	Yes
X vs. Unknown 524.3723	-8718333	Yes	<0.0001	<0.0001	-0,6221	-0.8239 to -0.2803	0,0012	**	Yes
X vs. Unknown 542.3224	-1412500	Yes	0,0448	0,001	-0,7648	-0.8953 to -0.5134	<0.0001	****	Yes
X vs. Unknown 544.3409	-2318692	Yes	<0.0001	<0.0001	-0,4941	-0.7539 to -0.1008	0,0141	*	Yes
X vs. Unknown 546.3528	-907083	Yes	<0.0001	<0.0001	-0,7566	-0.8914 to -0.4989	<0.0001	****	Yes
X vs. Unknown 546.3536	-1720333	Yes	0,0038	<0.0001	-0,7825	-0.9037 to -0.5452	<0.0001	****	Yes
X vs. Unknown 546.356	-827917	Yes	<0.0001	<0.0001	-0,563	-0.7923 to -0.1943	0,0042	**	Yes
X vs. Unknown 549.4878	-1617417	Yes	0,0091	0,0002	-0,1931	-0.5621 to 0.2400	0,3659	ns	No
X vs. Unknown 549.4885	-3514100	Yes	<0.0001	<0.0001	-0,3046	-0.6381 to 0.1251	0,1478	ns	No
X vs. Unknown 554.3441	-6504750	Yes	<0.0001	<0.0001	-0,702	-0.8647 to -0.4061	0,0001	***	Yes
X vs. Unknown 562.3274	-620917	Yes	0,0028	<0.0001	-0,6456	-0.8361 to -0.3162	0,0007	***	Yes
X vs. Unknown 562.3284	-1586583	Yes	0,0116	0,0002	-0,7982	-0.9111 to -0.5738	<0.0001	****	Yes
X vs. Unknown 577.5192	6582500	Yes	<0.0001	<0.0001	0,3976	-0.01959 to 0.6968	0,0544	ns	No
X vs. Unknown 585.2725	1576957	Yes	<0.0001	<0.0001	0,6664	0.3486 to 0.8467	0,0004	***	Yes
X vs. Unknown 603.5349	1811667	Yes	0,0017	<0.0001	0,1953	-0.2379 to 0.5637	0,3604	ns	No
X vs. Unknown 605.5502	2558317	Yes	<0.0001	<0.0001	0,4367	0.02781 to 0.7204	0,0329	*	Yes
X vs. Unknown 637.3054	506083	Yes	0,0429	0,0009	0,2488	-0.1841 to 0.6009	0,2411	ns	No
X vs. Unknown 732.5544	2539542	Yes	<0.0001	<0.0001	0,5007	0.1094 to 0.7576	0,0127	*	Yes
X vs. Unknown 79.0212	-1381500	Yes	<0.0001	<0.0001	-0,2392	-0.5943 to 0.1939	0,2603	ns	No
X vs. Unknown 812.6735	-2508450	Yes	<0.0001	<0.0001	-0,428	-0.7152 to -0.01712	0,0369	*	Yes
X vs. Unknown 813.6857	-2590833	Yes	<0.0001	<0.0001	0,07482	-0.3500 to 0.4741	0,7283	ns	No
X vs. Unknown 814.6336	-1678500	Yes	0,0053	<0.0001	-0,3933	-0.6942 to 0.02464	0,0573	ns	No
X vs. Unknown 818.5896	4249417	Yes	<0.0001	<0.0001	0,5457	0.1702 to 0.7828	0,0058	**	Yes
X vs. Unknown 885.3681	620333	Yes	0,0028	<0.0001	0,4317	0.02163 to 0.7174	0,0352	*	Yes
X vs. Unknown 922.7857	-1874104	Yes	0,0009	<0.0001	-0,03567	-0.4431 to 0.3839	0,8686	ns	No
X vs. Unknown 991.6738	-1587592	Yes	<0.0001	<0.0001	-0,6929	-0.8601 to -0.3912	0,0002	***	Yes
X vs. w/o MS2:LysoPE 19:0; [M+H]+	231750000	Yes	0,0003	<0.0001	-0,7242	-0.8757 to -0.4431	<0.0001	****	Yes
X vs. w/o MS2:MLS001165756-01!fexofenadine M+	-2934667	Yes	<0.0001	<0.0001	-0,7525	-0.8894 to -0.4917	<0.0001	****	Yes
X vs. valine	-606531	Yes	0,0039	<0.0001	0,4152	0.001531 to 0.7075	0,0436	*	Yes

Supplementary Table 10. var gene overview of 12 subclinical individuals at the end of the dry season (May) and 12 first clinical malaria episodes in the ensuing wet season (MAL).

	LARS FADIG contain contigs			All fragments			500 bp contigs									Mapped base approach			
Sample ID	total length	#	longest	total length	#	longest	total length	#	longest	length in bp of assembly of RNA-Seq	ratio var / genes	#reads non human	mapped reads	% back onto whole transcriptome assembly	ratio # var versus mapped	# hits against varDB	# reads mapped (multi hits possible)	Id of highest hit	Domain structure of highest hit
9307	2492	1	6763	18920	10	6763	18301	8	6763	742606	2,5	15975868,0	8895625	55,7	7,03	2693	197714	PF0159-C.g637	NTS-DBLa-CIDRa-DBLb-DBLg-DBLd-CIDRb-DBLb-DBLg-
9308	5533	1	5348	9624	5	5348	9465	4	5348	1445482	0,7	11848168,0	6148180	51,9	687,43	14	628	PF0145-C.g513	NTS-DBLa-CIDRa-DBLd-CIDRb-
9309	0	0	670	1296	2	670	1296	2	670	1046246	0,1	11998236,0	6183146	51,5	99,69	13	246	PF0084-C.g173	NTS-DBLa-CIDRa-DBLd-CIDRb-
9310	14655	3	6227	18769	10	6227	17668	6	6227	1341324	1,4	13326412,0	7123920	53,5	86,89	216	8458	PF0043-C.g402	DBLd-CIDRb-
9311	0	0	2292	2292	1	2292	2292	1	2292	611982	0,4	14767424,0	8843839	59,9	163,71	14	266	PT0294-C.g1327	DBLa-CIDRa-DBLb-DBLg-DBLd-CIDRb-DBLb-DBLg-
9312	2706	1	3170	20556	18	3170	18992	12	3170	2975794	0,7	20051744,0	11653423	58,1	321,19	64	2097	PF0051-C.g887	DBLa-CIDRa-DBLd-CIDRb-
9313	0	0	2292	4721	8	2292	3948	3	2292	752927	0,6	8928980,0	4343024	48,6	786,83	6	125	PT0122-C.g1412	NTS-DBLa-CIDRa-DBLb-DBLz-DBLe-
9314	10604	2	9011	39049	28	9011	35930	16	9011	2114337	1,8	14321116,0	7415290	51,8	157,46	248	6516	PF0262-C.g611	DBLb-DBLb-DBLd-CIDRg-
9315	6708	0	4176	5824	3	4176	5685	2	4176	2541773	0,2	26000276,0	13663141	52,5	30,18	193	12370	PF0062-C.g430	NTS-DBLa-CIDRa-DBLd-CIDRb-
9316	0	0	3400	9185	13	3400	6840	5	3400	1478168	0,6	14287136,0	7202926	50,4	75,91	121	2046	PA0182-C.g826	NTS-DBLa-CIDRa-
9317	12594	1	5234	19689	20	5234	17610	10	5234	2407641	0,8	14286292,0	6838626	47,9	21,52	915	31564	PM0098-C.g1086	NTS-DBLa-CIDRa-DBLd-CIDRg-
9318	6244	1	6004	10131	10	6004	9313	3	6004	2235506	0,5	17725064,0	8526775	48,1	198,65	51	2534	PF0417-C.g422	NTS-DBLa-CIDRa-DBLd-CIDRb-
9319	78542	23	10423	173674	133	10423	158685	68	10423	3537833	4,9	7132196,0	3328961	46,7	133,70	1299	39212	PA0146-C.g1029	DBLd-CIDRb-
9320	0	0	2208	8666	20	2208	4740	4	2208	3381312	0,3	9539044,0	4380531	45,9	131,30	66	1224	PA0224-C.g312	DBLa-CIDRa-DBLd-CIDRb-
9321	20294	2	9564	23668	12	9564	22883	5	9564	3822936	0,6	9449748,0	4344423	46,0	20,60	1149	79918	PF0097-C.g294	NTS-DBLa-CIDRa-DBLb-DBLg-DBLd-CIDRb-
9322	55784	16	10046	138491	170	10046	107548	47	10046	3729370	3,7	14093972,0	7193001	51,0	163,70	846	33778	PA0092-C.g461	DBLd-CIDRg-DBLg-DBLz-
9323	7436	5	3571	35909	43	3571	30853	23	3571	3066791	1,2	11050240,0	5527362	50,0	348,63	103	2823	PA0253-C.g804	NTS-DBLa-CIDRa-DBLd-CIDRb-
9324	4363	5	4626	43517	56	4626	36282	28	4626	3237633	1,3	10679044,0	5404733	50,6	319,98	136	3264	PF0189-C.g397	DBLd-CIDRb-
9325	0	0	3849	3849	1	3849	3849	1	3849	2549304	0,2	10567928,0	5285348	50,0	9,84	391	9861	PF0801-C.g1202	DBLg-DBLz-DBLe-DBLe-
9326	76081	16	8812	113437	87	8812	101455	36	8812	3959051	2,9	16438892,0	8495227	51,7	144,51	785	23150	QG0212-C.g1592	NTS-DBLa-CIDRa-DBLd-CIDRb-
9327	5170	2	4225	11330	14	4225	8242	4	4225	2543923	0,4	5085208,0	2190678	43,1	138,17	82	1893	PA0237-C.g706	NTS-DBLa-CIDRa-DBLd-CIDRb-
9328	2752	1	2688	12501	16	2688	10623	6	2688	2862046	0,4	8045316,0	3659940	45,5	198,43	63	2197	PF0228-C.g1045	CIDRa-DBLd-CIDRb-
9329	49030	17	9161	122076	120	9161	105911	48	9161	4088463	3,0	13708444,0	6617359	48,3	94,78	1288	64690	PA0167-C.g886	NTS-DBLa-CIDRa-DBLd-CIDRg-
9330	52218	13	11752	106347	87	11752	98474	49	11752	3878236	2,7	15329884,0	7832231	51,1	253,21	420	14671	PT0211-C.g738	NTS-DBLa-CIDRa-DBLb-DBLd-CIDRb-

PM - Mali, PF - Ghana, PT - Malawi, PA - The Gambia/Guinea, QG - Congo

Supplementary Table 11. List of *P. falciparum* invasion-specific proteins included in the analysis of the protein microarray.

Previous ID	ID	Name	Description
MAL13P1.174	PF3D7_1334800	MSRP2	MSP7-like protein (MSRP2)
MAL13P1.176	PF3D7_1335300	RH2B	reticulocyte binding protein 2 homologue b (RH2b)
MAL7P1.176	PF3D7_0731500	EBA175	erythrocyte binding antigen-175 (EBA175)
PF10_0281	PF3D7_1028700	MTRAP	merozoite TRAP-like protein (MTRAP)
PF10_0348	PF3D7_1035700	DBLMSP	duffy binding-like merozoite surface protein (DBLMSP)
PF10_0351	PF3D7_1035900	M566	probable protein, unknown function
PF10_0352	PF3D7_1036000	MSP11	merozoite surface protein (MSP11)
PF10_0355	PF3D7_1036300	DBLMSP2	merozoite surface protein (MSP3.8)
PF11_0344	PF3D7_1133400	AMA1	apical membrane antigen 1 (AMA1)
PF11_0381	PF3D7_1136900	SUB2	subtilisin-like protease 2 (SUB2)
PF13_0197	PF3D7_1335100	MSP7	merozoite surface protein 7 (MSP7)
PF14_0201	PF3D7_1420700	P113	surface protein, Pf113 (Pf113)
PF14_0495	PF3D7_1452000	RON2	rhoptry neck protein 2 (RON2)
PFA0125c	PF3D7_0102500	EBA181	erythrocyte binding antigen-181 (EBA181)
PFB0300c	PF3D7_0206800	MSP2	merozoite surface protein 2 (MSP2)
PFB0305c	PF3D7_0206900	MSP5	merozoite surface protein 5 (MSP5)
PFB0310c	PF3D7_0207000	MSP4	merozoite surface protein 4 (MSP4)
PFB0335c	PF3D7_0207500	SERA6	serine repeat antigen 6 (SERA6)
PFB0340c	PF3D7_0207600	SERA5	serine repeat antigen 5 (SERA5)
PFB0345c	PF3D7_0207700	SERA4	serine repeat antigen 4 (SERA4)
PFB0350c	PF3D7_0207800	SERA3	serine repeat antigen 3 (SERA3)
PFD1145c	PF3D7_0424100	RH5	reticulocyte binding protein homologue 5 (RH5)
PFE0340c	PF3D7_0506900	ROM4	rhomboid protease ROM4 (ROM4)
PFF0995c	PF3D7_0620400	MSP10	merozoite surface protein 10 (MSP10)
PFI1475w	PF3D7_0930300	MSP1	merozoite surface protein 1 (MSP1)
PFL1385c	PF3D7_1228600	MSP9	merozoite surface protein 9 (MSP9)
PFL2505c	PF3D7_1252100	RON3	rhoptry neck protein 3 (RON3)

Supplementary Table 12. Model parameters and values.

Parameter	Description	Value
γ	parasite growth rate	8
σ	maximal proportion of parasites removed by spleen [6h-1]	0,9
η	maximal proportion of parasites removed through cytoadhesion [6h-1]	0,9
p_σ	shape parameter, spleen	0,7
p_η	shape parameter, cytoadhesion	1,5
T_σ	location parameter, spleen	32
T_η	location parameter, cytoadhesion	10
κ	scale parameter (relative cytoadhesion)	[0,1]